A comprehensive review on TiO2-based heterogeneous photocatalytic technologies for emerging pollutants removal from water and wastewater: From engineering aspects to modeling approaches

Yassine Jari, Noura Najid, Mohamed Chaker Necibi, Bouchaib Gourich, Christophe Vial, Alaâeddine Elhalil, Parminder Kaur, Idriss Mohdeb, Yuri Park, Yuhoon Hwang, et al.

A comprehensive review on TiO_2-based heterogeneous photocatalytic technologies for emerging pollutants removal from water and wastewater: From engineering aspects to Modeling approaches

Yassine Jari[1], Noura Najid[2], Mohamed Chaker Necibi[1], Bouchaib Gourich[1,2], Christophe Vial[3], Alaâeddine Elhalil[2], Parminder Kaur[4], Idriss Mohdeb[5], Yuri Park[5], Yuhoon Hwang[5], Alejandro Ruiz Garcia[6], Nicolas Roche[1,7], Azzeddine El Midaoui[1]

[1] International Water Research Institute (IWRI), Mohammed VI Polytechnic University, Ben Guerir, Morocco.

[2] Laboratory of Process and Environmental Engineering, Higher School of Technology, Hassan II University of Casablanca, Morocco

[3] Université Clermont Auvergne, CNRS, SIGMA Clermont, Institut Pascal, F-63000 Clermont–Ferrand, France

[4] Geological Survey of Finland, P.O. Box 96, FI-02151, Espoo, Finland

[5] Department of Environmental Engineering, Seoul National University of Science and Technology, Seoul 01811, Republic of Korea

[6] Department of Electronic Engineering and Automation, University of Las Palmas de Gran Canaria, Edificio de Ingenierías, Campus Universitario de Tafira, 35017 Las Palmas de Gran Canaria, Spain

[7] Aix-Marseille University, CNRS, IRD, INRAE, Coll France, CEREGE, CEDEX, 13454 Aix-en-Provence, France

**Corresponding authors: Bouchaib Gourich (gourichb@gmail.com), Mohamed Chaker Necibi (chaker.necibi@um6p.ma)*

Abstract

The increasing presence of emerging pollutants (EPs) in water poses significant environmental and health risks, necessitating effective treatment solutions. Originating from industrial, agricultural, and domestic sources, these contaminants threaten ecological and public health, underscoring the urgent need for innovative and efficient treatment methods. TiO_2-based

semiconductor photocatalysts have emerged as a promising approach for the degradation of EPs, leveraging their unique band structures and heterojunction schemes. However, few studies have examined the synergistic effects of operating conditions on these contaminants, representing a key knowledge gap in the field. This review addresses this gap by exploring recent trends in TiO_2-driven heterogeneous photocatalysis for water and wastewater treatment, with an emphasis on photoreactor setups and configurations. Challenges in scaling up these photoreactors are also discussed. Furthermore, Machine Learning (ML) models play a crucial role in developing predictive frameworks for complex processes, highlighting intricate temporal dynamics essential for understanding EPs behavior. This capability integrates seamlessly with Computational Fluid Dynamics (CFD) modeling, which is also addressed in this review. Together, these approaches illustrate how CFD can simulate the degradation of EPs by effectively coupling chemical kinetics, radiative transfer, and hydrodynamics in both suspended and immobilized photocatalysts. By elucidating the synergy between ML and CFD models, this study offers new insights into overcoming traditional limitations in photocatalytic process design and optimizing operating conditions. Finally, this review presents recommendations for future directions and insights on optimizing and modeling photocatalytic processes.

Keywords: Emerging pollutants; TiO_2-based photocatalysis; Degradation; Photocatalytic reactor designs; Machine learning; CFD Modeling

1. Introduction

Within the last few years, unparalleled growth in both industrialization and urbanization has driven the release into the environment of numerous unregulated chemical and biological substances, known globally as EPs (Zhao et al., 2024). The United States Environmental Protection Agency defines EPs as chemicals or materials from recent sources or new pathways that lack published health standards and pose potential or real threats to human health or the environment (Richardson and Ternes, 2014). They emanate from a diverse range of sources, including the industrial, agricultural, pharmaceutical, mineral processing, construction, and urban sectors (*i.e.*, agricultural runoff, industrial discharges, wastewater effluents, and improper disposal of consumer products) (Deblonde et al., 2011; Khan et al., 2022). Indeed, These activities expose the environment to trillions of tons of chemicals, with humans creating over 140,000 compounds, most of which were previously unknown, for the spread of geogenic substances (Mishra et al., 2023). Overall, there are more than 20 classes of compounds considered to be EPs, including persistent organic pollutants (POPs), pharmaceuticals and personal care products (PPCPs), veterinary drugs such as antibiotics, endocrine disruptors (EDCs) and nanomaterials such as micro/nano plastics, whose environmental fate or impacts are poorly understood (Eggen et al., 2010; Taheran et al., 2018; Vasilachi et al., 2021; Zhao et al., 2024). The speciation of EPs is fundamental to understanding their behavior and effects on the environment. EPs can mutate through a variety of physical, chemical, and biological processes, resulting in the formation of transformation products. Thus, these end products frequently possess significant differences in terms of toxicity, persistence, and bioavailability compared to their original compounds, which complicate risk assessment and remediation measures.

EPs have been found in various environments (Askari et al., 2025; Jari et al., 2022), including dust, air, sediments, soils, biota, and even the Arctic, indicating their high persistence and bio-accumulative nature (Yu et al., 2024). Additionally, these contaminants mainly enter aquatic environments (*i.e.*, surface waters) via wastewater streams from laboratories, industries, agriculture, hospitals, households, and hospitals (Eggen et al., 2010; Matamoros et al., 2009; Verlicchi et al., 2010). In particular, some EPs such as antibiotics, azole antifungals, non-steroid anti-inflammatory drugs, lipid regulators, parabens, antiseptics, and bisphenol A can infiltrate groundwater through landfill leachate (García-Galán et al., 2010; Ma et al., 2012; Peng et al., 2014). For instance, Peng et al. (2014) reported that various antibiotic compounds (*i.e.*, sulfamethoxazole, lincomycin, and erythromycin) were found in groundwater in Europe and North America, reaching maximum concentrations of 5.7 ‒ 103 $ng.L^{-1}$. Indeed, several studies have shown that when concentrations of EPs in water bodies exceed natural levels ($ng.L^{-1}$ to $\mu g.L^{-1}$), they pose significant risks to ecological security, clean water, and food supplies, thus threatening human health (Li et al., 2023; Nguyen et al., 2023) (Fig. 1).

EPs in water pollution harm aquatic life and human health, causing toxic effects, endocrine disruption, developmental flaws, acute and chronic toxicity, and antibiotic resistance in microorganisms (Khan et al., 2024). Certain EPs can severely impact aquatic organisms, leading to biodiversity loss and ecosystem destabilization (Geissen et al., 2015; Yu et al., 2024). In this context, strategies and legislative efforts are underway to monitor and remove EPs, addressing their increasing threats. Initiatives like the European Union's Water Framework Directive (European Commission, 2024), the U.S. Environmental Protection Agency's Candidate List (Jones-Lepp and Alvarez, 2010; US EPA, 2014), and World Health Organization (WHO) (WHO, 2011) aimed to identify, control, and regulate EPs in wastewater, drinking water, surface water

and groundwater. Parallelly, scientific research focused on developing effective EPs removal technologies and enhancing detection methods.

To date, various treatment methods have been explored for removing EPs from water and wastewater, including membrane filtration, adsorption, coagulation/flocculation, activated sludge processes, ion-exchange, electrochemical oxidation, biological treatments, catalytic ozonation, and photocatalytic degradation processes (Bilal et al., 2019; Kumari et al., 2022; Montenegro-Ayo et al., 2023; Rathi and Kumar, 2021; Sahay et al., 2023; Wang et al., 2021). The biological treatment of pharmaceutical pollutants such as ibuprofen in the effluents of wastewater treatment plants only results in partial elimination; moreover, its primary metabolites (carboxy and/or hydroxyl ibuprofen) persist as toxic by-products (Méndez-Arriaga et al., 2009). The adsorption technique presents benefits such as low energy consumption, easy operation, and the absence of byproducts. It does not, however, remove EPs; instead, it just facilitates pollution transition. The main drawbacks include expensive sorbent production, reduced sorption capacity over multiple treatment cycles, and significant expenses for regenerating and disposing of used adsorbents (Zhao et al., 2018). Due to their high solubility, pharmaceutical EPs like nonsteroidal anti-inflammatory drugs are challenging to extract using separation techniques such as filtration, flotation, and coagulation. For example, employing coagulants resulted in a separation efficiency of 50% - 70% for diclofenac (Méndez-Arriaga et al., 2009). Electrochemical oxidation efficiently removes EPs from water and wastewater without external chemicals. However, its widespread adoption is limited by expensive electrode materials, poor mass transfer rates, low current efficiency, high energy consumption, and the generation of byproducts (Bampos et al., 2021; Yang et al., 2023). Photolysis/photocatalysis and ozonation have potential disadvantages

that include the production of toxic byproducts, high energy consumption, operational issues, and matrix interactions (Abromaitis et al., 2024; Zhang et al., 2022).

Advanced Oxidation Processes (AOPs) effectively eliminate EPs instead of just transferring them between phases, as traditional treatment systems often do. Contrary to other AOPs, which frequently involve the addition of chemical oxidants, photocatalysis utilizes light to produce reactive oxygen species, in particular hydroxyl radicals ($OH^{\bullet}$) (Aoudj et al., 2019), which are highly reactive and can non-selectively oxidize persistent EPs into innocuous final products. This makes photocatalysis an interesting option for EPs treatment due to its low operational cost, its ability to exploit natural sunlight and the fact that it avoids the use of chemical reagents (Deblonde et al., 2011). In addition, photocatalysis minimizes the formation of secondary pollutants, which can be a serious problem in other treatment processes, such as ozonation or Fenton-type processes, which generate residual sludge or toxic by-products (Lee et al., 2017). Despite their usage in water and wastewater treatment, AOPs have various limitations, including the necessity for sophisticated equipment, ozone's short half-life, UV radiation absorption, partial mineralization of pollutants, and expensive prices. Furthermore, many AOPs need the use of additional chemicals for oxidants and energy, exacerbating the energy issue. Most AOPs, aside from semiconductor-based photocatalysis, face practical limitations such as the transport and storage of H_2O_2, expensive oxidant synthesis, and sludge production (Sewnet et al., 2022). In this context, semiconductor-based photocatalysis is increasingly preferred over chemical-based AOPs due to its potential efficiency and the availability of cost-effective photocatalysts (Jorfi et al., 2016). Photocatalysis is a potential wastewater treatment process that utilizes sunlight to remove EPs and hazardous microorganisms (Mishra and Sundaram, 2023). Its efficiency is affected by the type of photocatalysts and the irradiation light source. Higher irradiation

intensities often result in more efficient photolysis degradation processes (Fageria et al., 2014). The ability to harness renewable solar energy makes photocatalysis more sustainable and cost-effective in the long term, particularly in regions with abundant sunlight, compared to traditional thermal catalysis and other conventional treatment technologies such as adsorption, membrane separation, and biological processes (Ahmad et al., 2023). The main photocatalysts include metal oxides/sulfides (TiO_2, ZnO, WO_3, Fe_2O_3, Co_3O_4, Nb_2O_5, Cu_2O, CdS, ZnS, etc.), a combination of them, or more recently metal oxides/sulfides combined with graphene oxide (GO) or carbon nanotube (Abromaitis et al., 2024; Zhao et al., 2018). Among the several photocatalysts, TiO_2 is a prominent one due to its chemical stability, high surface area, non-toxicity, and inexpensive cost (Abd Rahman et al., 2023; Chen et al., 2020). However, due to its broad energy band gap (3-3.2 eV), it can only be activated by UV light (λ < 400 nm), yielding less than 5% of the irradiation solar energy (Tong et al., 2012). Furthermore, the rapid recombination rate of electron-hole pairs severely limits further development of its photocatalytic activity. Previously developed visible light response semiconductors, such as BiOX (X = I or Br), have a lower energy band gap (<3 eV) (An et al., 2008). However, they still suffer from serious photo-corrosion problems in aqueous media due to redox reactions and fast recombination of electron-hole pairs during the reaction process. As a result, it is extremely important to establish an effective technique to improve the performance of semiconductor photocatalysts.

Generally, photocatalyst performance is primarily evaluated based on charge recombination rates, energy band gaps, and surface redox potentials. Pure semiconductors often necessitate high-intensity light to generate charge carriers, a requirement that hampers their commercial viability. To address these challenges, several strategies have been developed recently, including surface morphology engineering, metal/non-metal doping, composite formation, and the creation

of heterostructures or Z-heterostructures (He et al., 2021). These approaches aim to produce photocatalysts with narrower band gaps, decreased charge recombination rates, and enhanced reactivity under visible light, specifically tailored to the unique physicochemical properties of the materials utilized (Zhao et al., 2020). The development of composite materials, particularly semiconductor photocatalysts, has shown significant performance improvements due to the synergistic effects of their substances. This methodology is applied in designing these materials, which are synthesized through various techniques such as heteroatom doping or forming heterojunctions. Fig. 2 illustrates a comprehensive review of recent advancements in the design and fabrication of composite photocatalysts, highlighting their enhanced effectiveness in wastewater treatment. This review provides an in-depth analysis of the current progress in creating these advanced materials, underscoring their potential in practical applications.

In the field of semiconductor photocatalysts and composite materials, modeling methods such as Artificial Neural Networks (ANN) and CFD play crucial roles in advancing research and development. ANN models are employed to predict the behavior and performance of photocatalysts based on complex interactions between their components, aiding in the optimization of material composition and synthesis parameters. These models utilize historical data to simulate the synergistic effects of various materials and improve the efficiency of photocatalytic processes. On the other hand, CFD simulations are instrumental in studying fluid dynamics and mass transport phenomena within photocatalytic reactors. They help optimize reactor design, understand flow patterns, and predict the distribution of contaminants and reaction products. Integrating ANN for predictive modeling and CFD for process optimization provides a comprehensive approach to enhancing the performance and efficiency of semiconductor photocatalysts in environmental and wastewater treatment applications.

The objective of this review is to provide a comprehensive overview of recent advancements in heterogeneous photocatalytic technologies for removing EPs from water and wastewater. While significant progress has been made in photocatalysis, challenges persist in optimizing photoreactor configurations, addressing operational issues, and accurately predicting system performance. Many studies currently face limitations due to a lack of scalable solutions, an incomplete understanding of reaction mechanisms, and inadequate integration of modeling techniques. The review delves into key engineering aspects, including the design and optimization of photocatalytic systems, the development of novel photocatalysts, and the scaling challenges these technologies encounter in practical applications. By consistently addressing the gaps in existing research, this study underlines the necessity of advancing photocatalytic materials that not only enhance degradation efficiency, but also are amenable to real-world applicability. Additionally, the review examines the potential of CFD and ML models to predict and simulate heterogeneous photochemical processes applied to water and wastewater treatment. These models integrate various phenomena-chemical, radiative, and hydrodynamic-across similar time and spatial scales, enabling a deeper understanding of complex interactions within photocatalytic systems. The incorporation of ML techniques also provides a novel approach to analyze large datasets generated in photocatalytic experiments, facilitating the discovery of hidden patterns and optimizing processes more effectively. Future perspectives on the optimization of heterogeneous photochemical processes are thoroughly discussed, emphasizing the potential of these methodologies to propel advancements in the field and contribute to sustainable water treatment solutions.

2. Mechanism and semiconductors photocatalyst

Recent advances in water and wastewater treatment processes have led to the development in oxidative destruction procedures for EPs. AOPs have been employed as an alternative to conventional water treatment processes. AOPs are founded on the in-situ generation of hydroxyl radicals (OH•) that are responsible for the decomposition of emerging organic compounds in aqueous media (Wang et al., 2022). The OH• radicals are reactive, highly powerful, and non-selective oxidizing agents that react very rapidly with organic contaminants. Among the AOPs, heterogeneous photocatalytic processes have long been considered an attractive and sustainable strategy to simultaneously solve energy and environmental problems (Reddy et al., 2016; Rueda-Marquez et al., 2020).

When a semiconductor absorbs photons of light with an energy equal to or greater than its gap energy, electrons (e^-) are excited from the valence band (VB) into the semiconductor conduction band (CB), leaving behind a hole (h^+) of positive charges in the valence band. Then they participate in oxidation and reduction reactions respectively. In general, the photocatalytic degradation process includes the following steps: (1) irradiation of the catalyst (Byrne et al., 2018), (2) separation and production of photoinduced electron-hole pairs, (3) recombination processes of photoexcited electron-hole pairs, and (4) the occurrence of oxidation and reduction reactions driven by photogenerated electron-hole pairs on the surface of the catalyst (Byrne et al., 2018), as shown in Fig. .

Up to now, considerable attention has been applied to oxide semiconductors like photocatalysts, such as TiO_2 (Lavudya et al., 2023), ZnO (Weerathunga et al., 2022), WO_3 (Hkiri et al., 2024), CuO (George et al., 2020) and Bi_2O_3 (Gupta et al., 2022). The photocatalysts most widely owing to their high photocatalytic activity and stability are TiO_2 and ZnO. While these catalysts have major drawbacks, including rapid recombination of electron-hole pairs and a large

band gap that only works in the UV domain. Generating ultraviolet light is expensive and poses greater risks to human health than visible light. Furthermore, only about 5 percent of sunlight is UV, while the proportion of visible light is > 43% (Ahuja et al., 2023). For this reason, photocatalysts active in visible light are currently the subject of intense research, which may offer great potential to harness sunlight for photocatalytic wastewater treatment.

3. Modification strategies of TiO_2 for environmental photocatalytic applications

A wide variety of modification methods have been developed to reduce the e^-/h^+ recombination rate and improve the utilization of visible light for wide-bandgap semiconductors. Among strategies for improving the photocatalytic activity of semiconductors are metal doping, non-metal doping, and coupling semiconductors.

3.1. *Metal doping*

Huge efforts in recent years have been devoted to improving the photocatalytic performance of TiO_2, and to use solar energy as an irradiation source. Doping with metallic elements has been widely employed to enhance photoactivity, in which these elements are inserted into the bulk of the TiO_2 or are widely dispersed at the TiO_2 interface. In the study of Bibi et al. (2023), when using only the TiO_2 catalyst, photocatalytic degradation of Congo red dye was about 61 %, which increased to around 99% in the presence of TiO_2 with 3 w% Cu-doping after 50 min of irradiation. In addition, Ratshiedana et al. (2021) indicated that the photocatalyst doped with 0.21% silver ion showed the highest photocatalytic efficiency, with 87% of the tartrazine removed in 180 min under visible light. Moreover, Wang et al. (2020) successfully synthesized visible light-active Fe-doped TiO_2 nanomaterials using a one-step hydrothermal deposition method. The photocatalytic degradation performance of these nomaterials was evaluated against

bisphenol A under a visible light source. The Fe-doped TiO_2 demonstrated exceptional degradation efficiency, achieving an overall removal efficiency of 99.99%.

The comparison of the photocatalytic activity of Au-doped TiO_2, Ag-doped TiO_2, and pristine TiO_2 for the degradation of organic environmental pollutants under direct sunlight was studied by. Saroha et al. (2023). The efficient photocatalytic degradation reached 90.62% for Au-TiO_2, higher than that of Ag-TiO_2 (82.87%) and TiO_2 (72.79%) photocatalysts. Divya et al. (2023) reported the synthesis of Zr-doped TiO_2 mesoporous nanostructures using a microwave-assisted sol-gel method. The resulting photocatalyst was employed for the photocatalytic degradation of Bismark Brown Red (BBR) dye. Zirconium doping led to a reduction in both band gap energy and particle size, while increasing the surface area of the Zr-TiO_2 nano-catalysts. Under visible light irradiation, the catalyst achieved a degradation rate of 99% for BBR. Notably, the photocatalytic performance remained effective even after four cycles. The photocatalytic reaction was primarily driven by electron-hole pair generation and the formation of hydroxyl radicals ($OH^{\bullet}$).

Noble metals typically have a high work function, Ag ~4.5–4.7 eV and Au ~5.1–5.3 eV than TiO_2 (~4.2 eV) (Sellappan et al., 2013). The formation of Schottky barriers (Sellappan et al., 2013) at the surfaces is obtained by the alignment of Fermi levels, when Au/Ag comes in direct contact with TiO_2, which inhibits the recombination of the photogenerated electrons and holes on the conduction and valence bands.

3.2. Non-metal doping

Recently, researchers have been interested in improving the activity of photocatalysts by adopting a doping process with non-metal doping that can reduce recombination effects. Non-

metal doping can strongly enhance the photocatalytic activity by influencing the electronic properties of a semiconductor. Yang et al. (2023) reported the elaboration of F-TiO_2 by a modified solvothermal process followed by surface fluorination, the potassium fluoride dihydrate was used as a source of fluorine. The photocatalytic efficiency of catalysts was measured through phenol degradation in the presence of visible light irradiation. Based on the reaction rate constant, the photocatalytic performance of F-doped TiO_2 is two times greater than that of pure TiO_2. The enhanced photoactivity of F-TiO_2 is associated with a reduction in the band gap that strengthens the response to visible light and the decrease in the probability of recombination of photogenerated electrons and holes. Chen et al. (2017) developed an S^{6+}-doped TiO_2 nanoparticle catalyst using an ionic liquid method for the photocatalytic degradation of phenol. Under visible light irradiation, the nanocomposite exhibited a degradation efficiency of 84%. Moreover, Khan et al. (2023) evaluated the photocatalytic properties of reference TiO_2 in comparison with synthesized N-TiO_2 nanoparticles catalysts and evaluated their photocatalytic property under visible light illumination by measuring the degradation of 2,4-dichlorophenol contaminant. After 240 min of treatments, the visible/reference TiO_2 sample exhibited low photocatalytic degradation of contaminant (21.5%). While the visible/N-TiO_2 materials elaborated by the modified sol-gel method show a very high photocatalytic activity of about 77.6%.

3.3. Coupling semiconductors

The development of TiO_2-based composites has been shown to significantly enhance photocatalytic efficiency by improving charge separation and expanding light absorption. For instance, Salmanzadeh-Jamadi et al. (2022) reported the synthesis of TiO_2/Bi_3O_4Br by hydrothermal method with various amounts of Bi_3O_4Br (10, 20, 30 and 40%). The

photodegradation of Rhodamine B under visible light in the presence of all photocatalysts is higher than that of pure TiO_2. At the same time, the excellent photocatalytic efficacy in removing Rhodamine B is 99% after 90 min of irradiation, which was obtained with TiO_2/Bi_3O_4Br (30%) composite. This can be attributed to the formation of heterojunction between the Bi_3O_4Br and TiO_2 materials, which facilitates charge transfer at the interface between TiO_2 and Bi_3O_4Br and promotes charge segregation (Salmanzadeh-Jamadi et al., 2022).

Recently, the coupling of WO_3 and pure TiO_2 was studied for the photodegradation of methylene blue (Liu et al., 2022). After only 10 min under sunlight, the 1 mol% monolayer WO_3/TiO_2 composite removed up to 98.05%, which was significantly superior to that of commercial TiO_2 (63.2%). During solar illumination on TiO_2 and WO_3 semiconductors, the electrons in VB absorb photon energy and are excited towards their respective CB, where photogenerated electrons and holes are produced (Liu et al., 2022). Also, Wang et al. (2023) employed novel $BiVO_4/TiO_2$ composites for Rhodamine B removal under solar irradiation. The outcomes show that the $BiVO_4/TiO_2$ heterostructures with 30 wt% of $BiVO_4$ demonstrated the highest photocatalytic degradation ability of 96.7% after irradiation for 60 min. This is associated with high electron-hole pair separation efficiency, strong redox capacity, and wide light response range (Wang et al., 2023).

Khasawneh et al. (2021) synthesized Fe_2O_3/TiO_2 nanocomposites with varying concentrations using the sol-gel synthesis method. The incorporation of 5 wt% Fe_2O_3 significantly reduced particle size, stabilized the anatase phase, increased the specific surface area, enhanced the optical properties, and lowered the bandgap to 1.6 eV. The highest photocatalytic degradation efficiency of acetaminophen was achieved under alkaline conditions (pH 11), with a catalyst loading of 1.25 $g.L^{-1}$ and an initial acetaminophen concentration of 30 $mg.L^{-1}$. Additionally,

Tanos et al. (2024) prepared $TiO_2/CaTiO_3/Cu_2O/Cu$ composites with varying amounts of GO using a solid-state synthesis method. The experimental results showed that the introduction of 0.5 mM peroxymonosulfate, which generates $^{\bullet}SO_4^-$ radicals, significantly enhanced the removal performance of paracetamol. The highest photocatalytic efficiency for paracetamol degradation, 96% after 3 h under visible light, was achieved with the composite containing 3% GO. The performance comparison of TiO_2-based materials for the removal of EPs from water is summarized in Table 1.

3.4.The role of semiconductors in heterogeneous photocatalysts for degrading pollutants

In heterogeneous photocatalysis, while semiconductors like titanium dioxide and zinc oxide are commonly utilized due to their efficient light absorption and redox properties, other materials also play significant roles. TiO_2 is extensively researched for its remarkable photoactivity in both O_2 reduction and surface H_2O/hydroxyl group oxidation, while zinc oxide (ZnO) exhibits similar activity but suffers from poor photostability (Okpara et al., 2023). Metals, metal oxides, metal sulfides, carbon-based materials, and even certain organic compounds have demonstrated photocatalytic activity in various applications. The choice of photocatalyst depends on factors such as reaction type, desired kinetics, stability, and cost-effectiveness (Jabbar et al., 2024). Metals like platinum and gold, metal oxides such as cadmium sulfide, carbon-based materials like graphene, and organic compounds like porphyrins offer unique advantages and challenges, making them attractive options for specific photocatalytic processes. However, semiconductors like cadmium sulfide (CdS), zinc-cadmium sulfide (ZnxCd1-xS), and silver-based ones are discouraged due to toxicity, high cost, and low stability (Okpara et al., 2023). Overall, while semiconductors are prevalent, the diversity of materials used in heterogeneous photocatalysis underscores the versatility and ongoing exploration in this field (Wang et al., 2022).

Semiconductors play a crucial role in heterogeneous photocatalysts used for pollutant degradation. Main steps in the photocatalysis process are summarized in Table 2.

It would be useful to mention that the surface area and morphology of semiconductor catalysts are critical factors influencing their photocatalytic activity and pollutant degradation efficiency. A larger surface area provides more active sites for catalytic reactions, enhancing interactions between the catalyst and pollutant molecules (Rengifo-Herrera and Pulgarin, 2023). This increased interfacial contact leads to more frequent collisions, accelerating the kinetics of the photocatalytic process. Nanostructured semiconductors, such as nanoparticles and nanotubes, exemplify this approach by offering high surface-to-volume ratios, which provide abundant reactive sites for pollutant adsorption and degradation. Additionally, the morphology of these catalysts, including features like crystallinity, surface roughness, and porosity, significantly affects the accessibility of active sites and the diffusion of reactants. Hierarchical structures with complex architectures further enhance surface area and promote pollutant adsorption. By optimizing the morphology of semiconductor catalysts, researchers can effectively tailor their photocatalytic properties for specific applications and environmental conditions (Wu et al., 2020). Regarding the band structure of semiconductors, it is crucial for their efficiency in generating and separating electron-hole pairs, which are essential for photocatalytic processes (Tahir et al., 2020). Ideally, the semiconductor should have a bandgap energy that aligns with the photon energy of the light source (Murali et al., 2020), ensuring optimal light absorption and facilitating the photoexcitation of electrons from the valence to the conduction band (Kumari et al., 2022). The mechanism of electron-hole pair generation and reactions is influenced by the heterojunction configurations between different semiconductor materials, each exhibiting unique band structures (Low et al., 2017): (i) *Type I Heterojunctions* (Qureshi et al., 2024) allow for

efficient charge separation, with electrons migrating from a narrower bandgap semiconductor to a wider bandgap one (Fig. 4) (Lin et al., 2023). This configuration enhances charge transfer processes, enabling efficient hydrogen production through redox reactions (Yuan et al., 2024), (ii) *Type II Heterojunctions* (F. Li et al., 2024) exhibit staggered band alignments, leading to spatial charge separation (Murillo-Sierra et al., 2021). In this type, electrons and holes localize in different regions, as illustrated in the NaLiTi3O7-La_2S_3 system (Fig. 5) (Mohd Nasir et al., 2023). This mechanism enhances carrier lifetimes and improves photocatalytic performance (Zhao et al., 2019)

4. Synergistic approaches with heterogenous photocatalysis

By integrating different treatment technologies, synergistic effects can be harnessed to address various challenges associated with EPs removal from water and wastewater. Heterogeneous photocatalysis coupled with adsorption techniques offers a dual-action approach, where photocatalysts facilitate the degradation of EPs while adsorbents selectively capture contaminants from the aqueous phase (Aoudj et al., 2019). This combined process not only extends the range of EPs that can be effectively treated but also enhances overall removal efficiency by targeting different classes of contaminants simultaneously. Furthermore, membrane filtration technologies integrated with photocatalysis provide an additional barrier for the retention of particles, bacteria, and organic matter, thereby producing treated effluents of higher quality (Molinari et al., 2004; Zhao et al., 2024). Such hybrid processes leverage the strengths of each process while mitigating their respective limitations, leading to more efficient and sustainable water treatment solutions.

In recent times, there has been a notable trend among researchers to explore synergistic approaches in various applications, including wastewater treatment. Chen et al. (2020) utilized a combined approach of electrocoagulation with UV/TiO_2 to reduce COD levels in petroleum refinery wastewater to meet regulatory standards. They integrated a tubular electrocoagulation reactor coupled with multi-point graphite anode discharge alongside a novel photo-reactor setup operating in batch circulation mode. Through optimization using response surface methodology, they achieved a significant COD removal efficiency of 91.26% with electrocoagulation process using UV/TiO_2. An interesting discovery from this research is the considerable improvement in removal efficiency achieved by combining electrocoagulation with UV/TiO_2 process, marking a 23% enhancement over the use of UV/TiO_2 alone. However, this enhancement was accompanied by increased process costs, although with a significant reduction in electrical energy consumption (EEC) per ton of treated wastewater by 55% with electrocoagulation coupled with UV/TiO_2 process. Furthermore, Poblete et al. (2024) explored the efficacy of ultrasound combined with the photo-Fenton process, employing fly ash as a catalyst for treating landfill leachate. In this study, they revealed synergistic effects between ultrasound and UV irradiation, facilitating the degradation of complex organic pollutants with hydroxyl radicals as the predominant active species. Operational costs for landfill leachate treatment under optimized conditions were estimated at 322.6 \$US.m^{-3}. While addressing key factors in landfill leachate purification, pollutant concentrations remain unsatisfactory, suggesting the need for extended treatment times and potential coupling with biological methods to further reduce pollutant levels. Indeed, Fernandes et al. (2020) developed a technology offering two alternative scenarios for implementation: one aiming to maximize degradation effectiveness, while the other focuses on degrading sulfide ions to enable further treatment at corrected pH values. Their study

demonstrated good synergism between TiO_2, UV, and oxidants, although real wastewater matrices negatively impacted volatile organic compound degradation rates compared to model effluents. The addition of TiO_2 reduced operational costs for O_3 and O_3/H_2O_2 technologies, showing promise as pre-treatment stages before further chemical or biological treatment, effectively degrading toxic compounds and avoiding H_2S formation. Additionnaly, Baaloudj et al. (2023) investigated hybrid systems to improve photocatalytic process efficiency, combining $Bi_{12}TiO_{20}$ with polyaniline to enhance cefixime removal. Polyaniline alone demonstrated efficient cefixime removal via adsorption, achieving 76.83% efficiency within 70 min. Their study revealed efficient cefixime removal via adsorption with polyaniline alone and remarkable enhancement with the hybrid system, indicating very high efficiency. Chandrabose et al. (2021) introduced a novel approach to enhance dye pollutant filtration efficiency in textile wastewater treatment, utilizing ultrathin, 2D MoS_2-mediated adsorption sites onto light-active TiO_2 host nanoparticles through a single-step hydrothermal process. The developed nanocomposite holds promise for advancing zero liquid discharge processes. C. Zhang et al. (2021) critically examined the coupling of photocatalytic and biological processes as a promising approach for decontaminating water polluted with recalcitrant chemicals, such as phenolic and aromatic substances. The coupling of photocatalysis and biotransformation, whether supported by porous carriers or not, has shown superior performance in removing refractory contaminants by leveraging the advantages of both processes. This emerging alternative has garnered increased attention and has undergone substantial development in the past five years.

In the case of membrane technology, Li et al. (2024) developed a synergistic membrane catalyst, incorporating a highly active cadmium sulfide/titanium dioxide (CdS/TiO_2) heterojunction and ferroelectric polyvinylidene fluoride, which exhibited significant efficiency in

reducing chloramphenicol and decomposing organic pollutants (methylene blue and bisphenol A) under solar-simulated irradiation. The catalyst maintained durable photoactivity over 20 cycles of recycling, minimizing the risk of secondary pollution. Furthermore, a customized panel wastewater purification system utilizing this membrane catalyst demonstrated high efficiency in chloramphenicol reduction and organic matter degradation, benefiting from the combined effects of light activation and piezoelectric polarization. This research sheds light on the potential of membrane catalyst-assisted panel technology for photocatalytic wastewater purification. Furthermore, Szymański et al. (2024) assessed the performance of a hybrid system, combining a submerged photo membrane reactor with ultrafiltration for ketoprofen-contaminated water treatment. Although the membrane unit cannot reject ketoprofen, the photocatalytic process aids in its removal. After 24 h, ketoprofen removal stabilizes at 93-96% across different water types. TOC removal varies, with faster mineralization in brackish and seawater. The study highlights the potential of this hybrid system for water treatment, emphasizing the need for photocatalytic optimization and the potential separation of the photocatalytic unit for efficiency. Moreover, the synergistic effect of combining external oxidants (O_3, H_2O_2, and their combination) with TiO_2 and UV light (Fernandes et al., 2020), significantly improved the reduction of chemical and biological oxygen demand (COD and BOD_5) as well as degrading volatile organic compounds (VOCs) in the effluents (Wang et al., 2021). Specifically focus on metronidazole (MNZ) and penicillin G (PG), by using the $AgZnFe_2O_4$@Ch catalyst to activate persulfate (PS) under UV light (Rajabi et al., 2024). This study achieved significant degradation rates of 81.5% for MNZ and 82.3% for PG within 50 min under optimal conditions (0.4 $g.L^{-1}$ catalyst, 4 mM PS, 5 $mg.L^{-1}$ antibiotics, pH 5) .

In general, synergistic strategies employing heterogeneous photocatalysis in water and wastewater treatment exhibit potential, but present various drawbacks that necessitate comprehensive analysis and mitigation (Xinchen et al., 2020). Operational parameter optimization remains a challenge, requiring extensive tuning of factors like reaction time, dosage, and environmental conditions. Efficient recycling of adsorbents and control of secondary pollution are crucial, given the large quantities of materials used in coupled processes. Tailoring synergism strategies for diverse water sources is complex due to variations in composition and pollutant concentrations. Developing cost-effective materials suitable for synergistic technologies is essential for scalability and accessibility. Ambiguity in mechanisms and uncertain contributions of photocatalysis hinder its practical application and optimization. Complex assessment techniques are needed to analyze synergies effectively, while a potential shift to single-phase catalysts may simplify assessment but requires further investigation. Hypothetical observations of synergy need empirical validation to advance photocatalysis in wastewater treatment effectively. Integrating synergistic heterogeneous photocatalysts into existing treatment technologies poses challenges, necessitating careful consideration of compatibility, scalability, and cost-effectiveness.

5. Photocatalytic reactor design

5.1.Examination of different types of photocatalytic reactors

The growing demand for scaling up the photocatalytic degradation process has led to a proliferation of various reactor setups and configurations for EPs removal from water and wastewater. Wang et al. (2021) highlighted the complexity of classifying photocatalytic reactors, making it a challenging task. The design of the photocatalytic reactor is directly influenced by several factors, including geometry, light source, and photocatalyst type (Sacco et al., 2020).

Among these, the state of photocatalyst is a particularly significant parameter and has notable influence in the design of photocatalytic reactors in recent years. Thereby, in this review, a simplified approach categorizes photocatalytic reactors based on whether the photocatalyst is suspended (e.g., slurry photoreactor) or immobilized. This simplified approach is due to the variety of photoreactor designs proposed in the literature, which hinders the lack of a general design methodology. This is also the reason why there is a need for new design methodologies such as CFD (see section 6.2), which can simultaneously consider hydrodynamics, light transfer, mass transfer, heat transfer and chemical processes over a wide range of time and space scales. The weakness of CFD is that it is too computationally intensive to be used for process control, for which ML appears to be the most promising strategy (see section 6.1).

5.1.1. Dispersed system

Slurry photocatalytic reactors, utilizing suspended TiO_2 particles are the most ubiquitous photocatalytic reactor configurations used for photocatalytic degradation processes (Manassero et al., 2017a). These reactors involve a uniform mixture of dispersed photocatalyst particles in an aqueous medium (Fig. 6). Due to their large surface area relative to volume and enhanced mass transport capacity, such dispersed-phase reactors are favored for their high photocatalytic efficiency compared to immobilized systems (Manassero et al., 2017a; Visan et al., 2019; Zheng et al., 2020). Since it has excellent photocatalytic performance, slurry photocatalytic reactor are commonly used as a benchmark to compare the photocatalytic performances of different immobilized photocatalytic reactors (El-Kalliny et al., 2014; Zheng et al., 2020). However, the required separation step of photocatalyst from the reaction medium and operation complexity under continuous mode motivate drive the exploration of alternative systems (Visan et al., 2019). One promising solution is the membrane module, which addresses the separation issues in the

slurry photocatalytic reactors and showed promising results as a potential alternative for conventional slurry photocatalytic reactor for water and wastewater treatment (Molinari et al., 2004). In fact, Li et al. (2019) introduced a new photocatalytic reactor concept coupling a submerged ceramic membrane photocatalytic reactor with suspended TiO_2 photocatalyst for the degradation of amoxicillin. This integration of membrane separation technology into slurry photocatalytic reactor exhibited excellent mineralization ability without significant decrease in degradation efficiency after three cycles (Li et al., 2019). However, during the separation process, the accumulation of suspended TiO_2 particles onto the membrane surface could result in blocked membrane pores (*i.e.,* membrane fouling), reducing the long-term efficiency of photocatalytic membrane reactors (H. Zhang et al., 2021).

5.1.2. Immobilized system

It was reported that suspended photocatalytic reactor exhibits superior photocatalytic performances as compared to immobilized photocatalytic reactor (Manassero et al., 2017a). However, in practical applications, reactors with immobilized photocatalysts are preferred. They are suitable for continuous operation without the need for a separation process and offer the potential for reusing the catalyst support for multiple cycles (Manassero et al., 2017b). In immobilized systems, the photocatalyst can be anchored to the walls of the reactor (Ling et al., 2004), or embedded onto/within the membrane surface (Leong et al., 2014; Mozia, 2010). Fig. 7 depicts schematic presentation of photocatalytic membrane reactor with immobilized photocatalyst particles on and within membrane structure. Optical fiber-based photocatalytic reactor with its double function as a light transmitter and support for the photocatalyst, have drawn considerable attention from researchers in the last two decades (Danion et al., 2007; Hofstadler et al., 1994; O'Neal Tugaoen et al., 2018). Moreover, the employing of optical fiber

as a support for the photocatalyst ensures the uniform distribution of light on the surface of photocatalyst, thereby increasing the photoconversion efficiency. Indeed, Fujishima et al. (2008) demonstrated that the immobilization of photocatalyst on a large surface area support increases the photocatalyst efficiency, by increasing the surface-to-volume ratio. In this regard, El-Kalliny et al. (2014) successfully immobilized TiO_2 on stainless steel meshes. This photocatalytic reactor configuration was later investigated for the degradation of humic acid, as one major component of natural organic matter. The immobilization of TiO_2 on mesh structures resulted in a high specific photocatalytic surface area with effective light penetration. Another configuration, the microreactor presents a solution to the critical challenges faced by an immobilized photocatalytic reactor. The concept of microreactor was first introduced in photocatalysis back in 2004 (Gorges et al., 2004). Microreactor is considered a promising reactor system due to its high surface-to-volume ratio and high mass transfer efficiency. However, its low process throughput is considered a serious drawback limiting its application to lab scale studies (Binjhade et al., 2022).

5.1.3. Comparison between different types of photocatalytic reactor systems

Different benchmarks can be used to objectively assess the photocatalytic performance across various reactor setups and configurations. For example, (Manassero et al., 2017a) compared the degradation efficiency of clofibric acid by three photocatalytic configurations of the same reactor setup (*i.e.*, a slurry reactor with suspended TiO_2 particles, fixed film reactor with TiO_2 immobilized onto the reactor walls, and fixed bed reactor with TiO_2-coated glass ring) using quantum and photonic efficiency. The result showed that slurry reactor was the most efficient configuration with quantum and photonic efficiency values equals to 4.59% and 1.68%, respectively (Manassero et al., 2017a). Li et al. (2010) used the ratio between initial reaction rates as a benchmark to compare the photocatalytic performance of suspended and immobilized

systems. The results showed that the efficiency of the suspended system was 2.5-9.2 times more efficient than immobilized system. Leblebici et al. (2015b) reviewed and compared 12 photocatalytic reactor designs using the photocatalytic space-time yield as a new benchmark measure. The results showed that high area-to-geometries such as microreactors integrated with immobilized photocatalyst can become competitive technology to slurry photocatalytic reactors for removal of EPs from wastewater treatment (Leblebici et al., 2015b). In an attempt to give a more objective assessment of the photocatalytic efficiency of different photocatalytic reactor designs, Sundar and Kanmani (2020) reviewed 24 photocatalytic reactor designs and compared them using five benchmarks (*i.e.*, apparent degradation rate, space time yield, photocatalytic space time yield, Specific removal rate, EEC). As it was expected, photocatalytic reactors with higher surface-to-volume ratios such as microreactor and packed bed photocatalytic reactors exhibited the highest space time yield STY (*i.e.*, 1 m^3 capacity of photocatalytic reactor to handle a volume of pollutants (m^3) in a day (m^3 pollutant.m^{-3} photocatalytic reactor.day^{-1}). In the case of packed bed photocatalytic reactor integrated LED illumination technology, the photocatalytic space time yield PSTY (*i.e.*, STY divided by lamp power) was the highest amongst the other photocatalytic reactors. This enhancement in PSTY was ascribed to the increased mass and photon transfer efficiency. More interestingly, a packed bed photocatalytic reactor with its low EEC is highly desirable for practical applications. On the contrary, spinning disc photocatalytic reactors, micro-photocatalytic reactors, and fluidized bed photocatalytic reactors showed the highest energy consumption making them the least desirable on the grounds of lighting cost, which is high (Sundar and Kanmani, 2020).

5.2. Factors affecting the performance of photocatalytic reactors

5.2.1. Geometry

The collection and utilization of emitted light by photocatalyst, which largely affect the photocatalytic activity, is directly influenced by the geometric shape of photocatalytic reactor (Visan et al., 2019). Photocatalytic reactors with cylindrical or rectangular geometric shapes are the most ubiquitous in the literature (Abd Rahman et al., 2023). Typically, light irradiation is supplied to the reaction medium either from the outside or the inside of the photocatalytic reactor using lamps and/or LED strips, as described in Fig. 8. These geometries are linked with the problem of insufficient light absorption by the suspended photocatalyst (Sacco et al., 2020). In this context, the flat plate geometry with its excellent ability to collect effectively sunlight is one of the most used photocatalytic reactor geometries employed in pilot scale-studies (Li Puma et al., 2020). Zhang et al. (2004) compared photocatalytic performance of a flat plate reactor with a newly designed corrugated plate reactor for EPs removal from wastewater. The outcomes showed that the corrugated plate reactor exhibited superior photocatalytic performances compared to the flat plate reactor. The improved photocatalytic performance of the corrugated plate reactor was attributed to the increased illuminated surface area of the photocatalyst per unit volume. However, the large footprint of these systems represents a significant drawback for this reactor type.

Flat plates, annular, and rectangular geometric shapes are widely used in solar photocatalytic reactors (Abdel-Maksoud et al., 2016). The geometric shape of the solar photocatalytic reactor is oftentimes coupled with a solar collector to increase the light intensity reaching the surface of the photocatalyst. Solar photocatalytic reactor can be divided into two categories based on whether it is manufactured with a concentrating collector (*e.g.*, parabolic through collector (PTC)) or a non-concentrating collector (e.g., inclined plate collector (IPC), compound parabolic reactor (CPR)) (Braham and Harris, 2009; Zheng et al., 2020). Among these designs, CPR are very popular solar

photocatalytic reactor that uses a parabolic round mirror, which allows the concentration of sunlight on the surface of the Pyrex tube (Sacco et al., 2019). In a comparative study, Bandala et al. (2004) investigated the photocatalytic efficiency of several tubular solar photocatalytic reactors (i.e., parabolic through concentrator (PTC), tubular collector (TC), CPR, and V-trough collector (VC)) for degradation of EPs. Although the results exhibited no significant difference between the performances of the photocatalytic reactors, CPR exhibited better performances in terms of the amount of energy collected.

5.2.2. Light source

The nature of the light source is one of the main design criteria in photocatalytic reactors. Solar light-supplied reactors are subject to different design specifications compared to those using artificial light as irradiation source. For instance, solar photocatalytic reactors have a large, exposed surface area to absorb more photons. However, the main drawback in solar light-supplied photocatalytic reactors is the ever-changing light intensity and variable weather conditions. More importantly, the overall energy efficiency of converting photons to hydroxyl radicals ($^{\bullet}OH$) for EPs degradation from sunlight was estimated to be less than that of artificial light (0.0005-0.4% using sunlight and 0.0002-2% using UV lamps) (Loeb et al., 2019). It has been due to these shortcomings, a light source of the photocatalytic reactor has seen a shift from sunlight to artificial lighting in the last few years (Sundar and Kanmani, 2020).

Light emitting diodes (LEDs) technology has gained more attention since the first UV LED photocatalytic reactor was first developed for degradation of perchloroethylene in 2005 (Chen et al., 2005). LED lamps showed several advantages over traditional lamps such as robustness, long-life span, environmental friendliness as they do not contain toxic compounds such as

mercury (Jo and Tayade, 2014), and the ability to be adjusted to different geometric shapes due to their excellent flexibility (Sundar and Kanmani, 2020). However, the usage of LEDs as a source of irradiation without a judicious optimization of light distribution throughout the photocatalytic reactor is not a guarantee for higher photocatalytic efficiency as it can result in lighting systems less effective than conventional ones. Martín-Sómer et al. (2017) studied the influence of light distribution on the photocatalytic efficiency of photocatalytic reactor with three different AUV light sources (*i.e.*, mercury fluorescent lamp, 8-LED based system, and 40 LED based system). The result showed that mercury fluorescent exhibited better light distribution and higher photonic efficiency compared to LED based systems. On the other hand, LED lighting systems exhibited higher electricity to photon conversion ability. In addition, the results showed that the increase in the number of LED lamps from 8 to 40 enhanced significantly the light distribution and photonic efficiency. Finally, the relevant study concludes that the photocatalytic efficiency could not be enhanced if the light distribution throughout the photoreactor is not regarded during the design stage (Martín-Sómer et al., 2017).

5.2.3. Photocatalyst

The photocatalyst loading is a key factor influencing the photocatalytic reactor efficiency. The increase in photocatalyst dosage in slurry photocatalytic reactor is correlated with the increase in the overall number of active sites, which leads to generating more $^{\bullet}OH$ radicals and therefore increasing degradation efficiency (Binjhade et al., 2022). However, it was reported that it exists an optimum concentration of photocatalyst beyond which the photocatalytic reactor efficiency decreases (Ehrampoush et al., 2011; Guettaï and Ait Amar, 2005). This happens mainly because of the mass transfer and photon transfer limitation (Mehrotra et al., 2003). To overcome the photon transfer limitations in a slurry photocatalytic reactor, Zhu et al. (2014) proposed a novel

configuration combining a fluidized-bed photocatalytic reactor with an optical-fiber light source. The findings showed that this novel photocatalytic reactor exhibited higher degradation efficiency due to the effective use of photons compared to conventional flat plate fluidized bed photocatalytic reactor. Another configuration that showed promising results regarding handling high concentrations of photocatalyst in slurry photocatalytic reactors was a rotor-stator spinning disk (Chaudhuri et al., 2022). In rotor-stator spinning disk photoreactor the high degree of shear and turbulence generated by the rotating disk significantly decreases mass transfer limitations.

In the immobilized systems, the thickness of the photocatalyst is of great significance and can directly alter the photocatalytic reactor performance. For instance, in the case of photocatalyst coated optical fiber-based photoreactor, photocatalyst thickness should consider the minority carrier's diffusion length, which is the minimum field-free region of electron-hole pairs to recombination (Hodes and Kamat, 2015; O'Neal Tugaoen et al., 2018).

5.2.4. Oxidant agent

Semiconductor-based photocatalysis has proven to be very effective for EPs degradation. However, the low separation and rapid recombination of photogenerated electron-hole pairs significantly affect the photocatalytic efficiency of the photocatalyst (Low et al., 2017). The inclusion of an oxidant agent as an electron scavenger is of great help since this can improve the separation efficiency of photogenerated electron-hole pairs (Tseng et al., 2012). San et al. (2001) investigated the effect of three electron acceptors (i.e., H_2O_2, $K_2S_2O_8$, and $KBrO_3$) on the degradation of 3-aminophenol in a cylindrical photocatalytic reactor. They found that $KBrO_3$ led to superior photocatalytic performances compared to the other additives. This increase in the photocatalytic efficiency was ascribed to the high number of electrons that react with $KBrO_3$ to

generate bromide ions, as shown in Eq. (1) (San et al., 2001). Tseng et al. (2012) have studied the effect of oxygen and H_2O_2 on the photocatalytic degradation of monochlorobenzene in a hollow cylindrical photoreactor. The results showed that oxygen has a higher contribution to the degradation of monochlorobenzene concerning H_2O_2. Typically, aeration (thus the dissolved oxygen) is used as a conveying media of oxygen to the surface of photocatalyst surface presented inside the photocatalytic reactor (Tseng et al., 2012). Xu et al. (2012) investigated the impact of aeration methods (i.e., airlift, bubbling, and stirring methods) on the photocatalytic degradation of methylene blue using a quartz tube photocatalytic reactor with ZnO photocatalyst. The results exhibited that the airlift photocatalytic reactor performed better than the bubbling and stirring photoreactor.

$$BrO_3^- + 6e^- + 6H^+ \rightarrow Br^- + 3H_2O \quad (1)$$

The usage of a single photocatalyst is always accompanied by the problem of low separation and rapid recombination of the photogenerated electron-hole pairs. To overcome this problem electron acceptor agents are usually used during photocatalytic degradation processes. Another potential solution to this problem is the usage of heterojunction photocatalysts in slurry and immobilized photocatalytic reactors (Barzegar et al., 2021; Fakhravar et al., 2020; Parsaei et al., 2023; Sabzehmeidani et al., 2023; Zamani et al., 2022; Zhang et al., 2017).

5.2.5. Nature and concentration of EPs

The ultimate objective of any photocatalytic reactor is the efficient removal of pollutants of emerging concerns, such as pesticides, endocrine-disrupting compounds, personal care products, and pharmaceuticals (Oulton et al., 2010; Sundar and Kanmani, 2020). These pollutants are recalcitrant to traditional methods of wastewater treatment, and their occurrence was associated

with ecotoxicological and human health risks even at a very low concentration. Therefore, the ability of the photocatalytic reactor to eliminate EPs at a nano-gram level should be a must-deal concern in the next-generation photocatalytic reactors.

The concentration of the contaminant is a crucial factor that can affect the photocatalytic reactor's performance. Many studies reported a decrease in the photocatalytic efficiency of the reactor when the initial concentration of the emergent contaminant increased (Fouad et al., 2023). This happens due to the inefficient light penetration throughout the photoreactor to reach the surface of the photocatalyst (Abdellah et al., 2018).

5.3. The photocatalytic degradation kinetic modeling

Photocatalytic degradation kinetic modelling plays a pivotal role in understanding and optimizing the degradation of EPs in wastewater (Colina-Márquez et al., 2019; Khataee et al., 2010). These models are used to predict and evaluate pollutant degradation rates under specific conditions, including light intensity (usually UV or visible), photocatalyst properties, and contaminant concentration (Alvarado-Rolon et al., 2018; Amani-Ghadim and Dorraji, 2015; Ayodele et al., 2021). Various models are employed to describe the kinetics of photocatalytic degradation, with the choice depending on experimental conditions and contaminant characteristics (Colina-Márquez et al., 2019; Olivo Alanís, 2019). Among the most widely used kinetic models in photocatalytic degradation studies are the Langmuir-Hinshelwood (L-H) model (Eckert et al., 2015; Vargas et al., 2020), the Turchi-Ollis model (Franz and Bestetti, 2023; Turchi and Ollis, 1990), and the Direct-Indirect model (Liu and Zhao, 2014; Mills et al., 2015; Vargas et al., 2020). The L-H model is widely used for describing heterogeneous catalytic reactions, relating the initial concentration of the contaminant to its degradation rate based on

surface adsorption. The Turchi-Ollis model focuses on hydroxyl radicals and direct photolysis, accounting for the continuous disruption of adsorption equilibrium due to the reactivity of photo-generated radicals. The Direct-Indirect model distinguishes between direct charge transfer from photogenerated electrons or holes on the catalyst surface and indirect reactions through intermediate species like hydroxyl radicals, which react with the pollutants. The kinetic models used for EPs degradation using photocatalytic processes are summarized in Table 3.

In fact, the photocatalytic degradation kinetics of EPs in suspension (Fouad et al., 2023) and immobilized (Manassero et al., 2017b) photocatalytic reactor is commonly described by the L-H model. In most cases, the rate constant is independent of many operating parameters such as pH, temperature, light intensity, oxygen concentration, and photocatalyst loading, etc (Sacco et al., 2020). This photodegradation kinetic model incorporates the concentration of EPs, photocatalyst loading, and a combination of kinetic and adsorption equilibrium constants. In another attempt to achieve a complete kinetics modeling of the photocatalytic reactor, Khataee et al. (2010) suggested a new models expressing the photocatalytic degradation rate in terms of light intensity and initial dye concentration. This new kinetic model explained well the dependence of kinetic parameters (*i.e.*, apparent adsorption constant K_s, and apparent rate constant K_r) on light intensity. The development of a complete kinetic model that considers the different operating parameters affecting the photocatalytic performances of the reactor is of great importance and should be investigated more deeply as it gives a general guideline for effectively designing new generation photoreactors with small physical footprint and low energy consumption (Sacco et al., 2020).

6. Recent engineering tools for modeling of heterogeneous photocatalytic processes

Machine learning-based models are increasingly being applied in heterogeneous photocatalytic processes to enhance efficiency and optimize reaction conditions (Boutra et al., 2022). By analyzing large datasets generated from experimental results, these models can identify patterns and correlations that traditional methods may overlook. For instance, machine learning algorithms can predict the performance of various photocatalysts under different light conditions, solvent environments, and reactant concentrations, allowing researchers to rapidly screen and select the most effective materials (Vasseghian et al., 2021). Additionally, these models can aid in designing novel photocatalysts by simulating their interactions at the molecular level, ultimately leading to improved energy conversion and pollutant degradation rates in environmental applications (Anandhi and Iyapparaja, 2024). This integration of machine learning not only accelerates the development of photocatalytic technologies but also paves the way for more sustainable and efficient chemical processes (Goodarzi et al., 2023).

6.1.Machine learning based models

Semiconductor photocatalysts are tremendous for effectively removing EPs from water, underscoring the need for advanced modeling techniques to optimize their efficiency. ML techniques have been shown to be quite useful in water treatment processes (Anandhi and Iyapparaja, 2024; Salahshoori et al., 2024). Especially in those where not all the information required by classical models to predict the behavior of the process is available (Bahramian et al., 2023). These ML techniques include adaptive neuro-fuzzy inference system (ANFIS), ANN, fuzzy logic (FN), genetic algorithm (GA) (Mahmoodi et al., 2017), decision trees (DT) (Can and Yildirim, 2019), random forest (RF) and support vector machine (SVM) (Oyehan et al., 2019; Vaez et al., 2015). Among these, the most popular in water treatment and more specifically in

heterogeneous photocatalytic technologies are likely to be ANN-based models (Ayodele et al., 2021; Vasseghian et al., 2021).

Neural network models, inspired by the structure and functioning of the human brain, are computational systems designed to learn and perform tasks by processing data through interconnected nodes or neurons (Anandhi and Iyapparaja, 2024; Salahshoori et al., 2024). An ANN-based model is composed of neurons (nodes), which receive input signals, perform computations, and produce output signals (Hosseini et al., 2022). Neurons are organized into layers, including the input layer (receiving raw data), hidden layers (processing intermediate information), and output layer (producing the final output) (Fig. 9). An ANN learns from data by adjusting the strengths of connections between neurons, represented by weights. Biases, additional parameters, contribute to the flexibility of the model. During training, these weights and biases are optimized to minimize the difference between predicted and actual outcomes. Neurons apply activation functions to their input, introducing non-linearities to the model. Common activation functions include the sigmoid, hyperbolic tangent (tanh) and rectified linear unit (ReLU), enabling the network to capture complex relationships within the data. ANNs are organized into layers, each serving a specific purpose (Ye et al., 2020). The input layer receives raw data, hidden layers process information, and the output layer produces the result. Optimization algorithms, such as stochastic gradient descent, guide the iterative adjustment of weights and biases used to minimize the loss function. These algorithms ensure the model converges towards an optimal configuration (Ward et al., 2020; Zheng et al., 2019). There are different types of ANN-based models; feedforward neural networks (FNN) (Ojha et al., 2017), which have information flowing in one direction—from the input layer to the output layer. Recurrent neural networks (RNNs) that incorporate feedback loops (Grossberg, 2013), allowing

them to capture sequential dependencies in data. Convolutional neural networks (CNNs), which are usually designed for processing grid-like data, etc. The use of ANNs to forecast the dynamics and efficacy of photocatalytic degradation processes for EPs across diverse operational scenarios has been studied by many researchers (Alvarado-Rolon et al., 2018; Mojiri et al., 2019).

Zhou et al. (2020) prepared a porous polymeric carbon nitride using 2, 5-dibromopyrazine and urea as the mixed precursors and applied to the degradation of sulfadiazine (SD) under the simulated light. An ANN-based model was used to optimize the removal of SD. 70 experimental sets were considered for modeling the process. 70% of the experimental data were used for training, 15% of the experimental data is used for testing and the remaining 15% of the data is used for verification. The inputs of the ANN were the degradation reaction time (1-60 min), amount of catalyst (200-2,000 ppm) and EPs concentration (4-20 ppm) being the output the removal efficiency (%). The optimized ANN was formed by 8 neurons in the hidden layer. A R^2 and mean square error (MSE) of 0.9556 and 0.0071 were obtained, respectively. Zulfiqar et al. (2019) studied the photocatalytic degradation of phenol via commercial TiO_2 nanoparticles. They compared ANN and response surface methodology (RSM) for scrutinizing the suitable modeling and optimized condition of the TiO_2 nanoparticles in yielding a profound photocatalytic degradation rate of phenol. The structure of the obtained ANN and data division (70%, 15%, 15%) was similar to that obtained by Zhou et al. (2020), but Zulfiqar et al. (2019) considered one more input (pH). The ranges studied were 2-12 for the pH, between 5 and 710 min for degradation reaction time, 150-3,000 ppm for catalyst and 5-150 ppm for the EPs. An R^2 of 0.9559 and root mean square error (RMSE) of 5.0945 were obtained for the ANN-based model. Oladipo et al. (2018) used an ANN for modeling the degradation of organophosphorus pesticides in a single and binary system. The obtained ANN models were formed by 5 inputs (irradiation

time, composite dosage, interfering ions, pH and EPs concentration), 2 hidden layers with 9 and 4 neurons respectively y 1 output (degradation rate). They used 65% of the experimental data for training, 19% for validation and 16% for testing. An R^2 of 0.988 and MSE of 0.0131 were obtained. An ANN model for the photodegradation of dye over ZnO photocatalyst was proposed by Amani-Ghadim and Dorraji (2015). The optimum ANN was formed by 5 inputs (pH, ZnO concentration, time, power per square meter and AB9 concentration), 1 hidden layer with 9 neurons and 1 output (photodegradation efficiency). The ANN-based model showed a performance in terms of R^2 and RMSE of 0.9883 and 0.0242, respectively. Das et al. (2014) proposed an ANN for predicting the photodegradation of carbamazepine over TiO-ZnO photocatalyst. The proposed ANN showed a good prediction of the carbamazepine with a R^2 of 0.997 and a MSE of about 0.02. The structure of the ANN had 4 inputs (reaction time, pH, carbamazepine concentration and TiO-ZnO concentration), 1 hidden layer with and 1 output (pollutant removal in %). The inputs studied were in a range of 3-12 for the pH, 50-800 ppm for TiO-ZnO concentration, 5-40 ppm for carbamazepine concentration and reaction time between 0 and 150 min.

Gordanshekan et al. (2023) studied the operational effects on photocatalytic degradation of cefixime (CFX) using green Bi_2WO_6/g-C_3N_4 and Bi_2WO_6/TiO_2 as catalysts. 70% of experimental data were used for trining the ANN, 15% for testing and 15% for validation. The inputs of the proposed ANN-based model were the mass Bi_2WO_6/g-C_3N_4, Bi_2WO_6/TiO_2 and Bi_2WO_6 in percentage, reaction time in min, the ratio of EPs concentration to the photocatalyst load (C/L) in $mg.g^{-1}$, initial pH, visible light source in W, UV source in W, concentration of $NaHCO_3$, NaCl and Na_2SO_4 in ppm, TiO_2 mass ratio in Bi_2WO_6/TiO_2 (%), the g-C_3N_4 mass ratio in Bi_2WO_6/g-C_3N_4 (%) and Bi_2WO_6 mass ratio in Bi_2WO_6/g-C_3N_4 or Bi_2WO_6/TiO_2 (%). 1

hidden layer with 18 neurons and 1 output (degradation of CFX). This architecture was proposed for modeling the photodegradation kinetic and isotherm adsorption and total photocatalytic removal kinetic. In general, the ANN-based model showed fitting performance in terms of R^2 above 0.95. CFX removal was also studied by Baaloudj et al. (2022) using $Bi_{12}TiO_{20}$ as photocatalyst. Its efficiency was modelled using ANNs. Concentration range for $Bi_{12}TiO_{20}$ (500-1,500 ppm), CFX concentration (5-15 ppm), pH (4-8), reaction time (15-180 min) were considered as inputs, 1 hidden and output layer. The optimized ANN had 10 neurons in the hidden layer obtaining a performance result in terms of R^2 and MSE of about 0.999 and 1.13, respectively. An ANN-based model proposed by Yang et al. (2022) was used for predicting the crystal violet dye (CV) degradation using chitosan conjugated Mn-magnetic nano-biocomposite (Mn-CCMN). 70% of the experimental data were used for training the ANN, 15% for verification and testing. The proposed ANN had 4 inputs, 2 hidden layers with 15 neurons each and one output (Fig. 10). A R^2 and RSME of 0.9948 and 0.23, respectively were obtained.

Hosseini et al. (2022) studied the photodegradation of tetracycline (TC) antibiotic under different operating conditions in terms of pH, photocatalyst dose, irradiation time and TC concentration (inputs of the proposed ANN-based model). The topology of the ANN obtained had 1 hidden layer with 8 neurons obtaining an R^2 close to 1. The photocatalytic degradation of ofloxacin antibiotic TS-1/ C_3N_4 composite photocatalyst was studied by Shang et al. (2022). They proposed an ANN topology 3:3:1, so 3 inputs (Catalyst dose, TS-1 loading percentage and luminous power density), 1 hidden layer with 3 neurons and 1 output. The ranges studied for the three different inputs were 800-1,600 ppm, 0-100 % and 20-50 $mW.cm^{-2}$. 80% of the experimental data were used for training, and 10% for validation and testing, respectively. The ANN-based model had a performance of 0.9993 and 4.45 10^{-5} in terms of R^2 and MSE,

respectively. Bhattacharya et al. (2022) studied the photodegradation of CBZ by the TiO_2- GO nanocomposite in a photocatalytic reactor and modeled the process using an ANN-based model. The inputs of the model were the pH dose and speed, and the output was the removal. The proposed model got an R^2 = 0.93167. A modeling and optimization study of a solar-driven CPR photocatalytic reactor for decomposition of EPs in wastewater was presented by Ghalamchi et al. (2022). They used an ANN model to assess the impact of operating parameters (flow rate, oxidant, Phenazopyridine concentration, and pH) on the degradation of Phenazopyridine. The best ANN-based model had 8 neurons in the hidden layer and had a RMSE value of 0.9299 for the validation data set. Fig. 11 shows the ANN predictions and experimental data of the mentioned study (Ghalamchi et al., 2022).

Qarajehdaghi et al. (2023) investigated a Quaternary composite of CdS/g-C_3N_4/rGO/CMC as a promising visible-light photocatalyst for efficient ciprofloxacin degradation. Inputs included ciprofloxacin concentration (2-10 ppm), catalyst dosage (100-900 ppm), pH (3-11), and irradiation time (10-50 min). The study compared Response Surface Methodology (RSM) and ANN based on their R^2 performance metrics. The proposed ANN topology was 4:9:1. Fig. 12 shows the MSE value with the number of neurons in the hidden layer and the influence of the operation parameters in percentage. The ANN-based model showed performance in terms of R^2 close to 1.

Finally, ML appears as a versatile tool for process control, for the optimization of continuous heterogeneous photocatalytic processes devoted to EPs removal from wastewater, especially for solar-driven systems which strongly depend on intermittent solar energy supply.

6.2. Computational Fluid Dynamics (CFD)

Computational Fluid Dynamics consist of a wide range of numerical methods capable of simulating the three-dimensional (3D) and time-dependent behavior of fluid flows by solving the fundamental equations of fluid mechanics (Ferziger et al., 2019). Thus, CFD is a transdisciplinary field at the interface of fluid mechanics, applied mathematics, and engineering sciences that has found increasing application in chemical engineering, as general-purpose commercial software packages have become available in the 1980s (Artemov et al., 2009). In fact, CFD can not only predict local hydrodynamics (i.e., pressure and velocity components), but the simulations can also provide access to various physical quantities, such as local temperature, species concentrations, or reaction rates. More recent advances include the modeling of multiphase, two- or three-phase reactors with parallel and consecutive reactions coupled with mass and heat transfer under turbulent flow conditions (Kuipers and van Swaaij, 1998; Yeoh and Tu, 2019).

The major breakthrough underlying the development of CFD came in the 1970s, when specific pressure-velocity coupling algorithms were developed to solve the incompressible Navier-Stokes equations, such as the SIMPLE (Semi-Implicit Pressure Linked Equations) algorithm (Artemov et al., 2009). The extension to turbulent flows with Reynolds-averaged Navier-Stokes (RANS) equations, i.e. turbulent kinetic energy, and turbulent dissipation rate (k and ε), and to heat, mass or electric charge transfer quickly emerged, since these phenomena are governed by a transport equation, also called convection-diffusion equation, which is a first-order partial differential equation (Eq. (2)):

$$\underbrace{\frac{\partial(\rho\phi)}{\partial t}}_{\substack{unsteady\\term}} + \underbrace{div(\rho\mathbf{u}\phi)}_{\substack{convection\\term}} = \underbrace{div\left(\Gamma_\phi \cdot grad(\phi)\right)}_{diffusion\ term} + \underbrace{S_\phi}_{\substack{source\\term}} \tag{2}$$

where, t is time, ρ fluid density, u the velocity vector (vectors are in bold), ϕ can be any scalar, S_ϕ is the source term of ϕ, and Γ_ϕ the (scalar) diffusion coefficient of ϕ; div and $grad$ are divergence and gradient operators. The formulation of common transport equations of CFD is summarized in Table 4. When transport equations are also available for dispersed or separated multiphase flows, so that chemical and electrochemical processes can be simulated.

Typical source terms in the energy balance ($q_{R,C}$ in Table 4) include viscous heating, the enthalpy of chemical or biochemical reactions, diffusion thermo-effect (Duffour effect), or the radiation fluxes between the surfaces in the case of radiatively non-participating fluid. Specific kinetic models for chemical reactions have also been added in various CFD solvers, such as finite-rate kinetics (based on rate constants and reaction orders), combustion kinetics with mixing conditions, or the classical kinetics of heterogeneous catalysis (such as the Langmuir-Hinshelwood model). Heterogeneous photocatalysis applied to water treatment involves multiphase fluid-solid systems, except in wall reactors and microchannels (catalyst coated on the wall) where the flow is single phase. But CFD is also able to simulate multiphase flows with suspended and fixed photocatalysts. For fixed-bed reactors, the single-phase transport equations can simply be modified to account for a local solid volume fraction; the main changes involve the friction terms in the momentum mass balance (Tong et al., 2020). For suspended solids, multiphase simulations in CFD are computationally intensive, so the pseudo-homogeneous assumption can be used. This means that the single-phase transport equations are solved with the physical properties of the slurry (ρ, μ, etc.) using a single-phase flow CFD solver (Turolla et al., 2016), which assumes that the photocatalyst concentration is spatially homogeneous. Conversely, if the solid distribution in the photoreactor is to be investigated, two-phase granular flow CFD simulations must be performed. The conventional assumption is the Euler-Euler

approach, which assumes that both phases form an interpenetrating continuum for which the conservation of mass and momentum equations are solved by introducing a local phase fraction. When three phases are involved, *e.g.*, in pneumatically agitated photocatalytic reactors, the Euler-Euler approach can be extended to three-phase simulations with a dispersed gas phase and a dispersed solid phase, but this is very computationally intensive (Boyjoo et al., 2013).

CFD is therefore an incredibly powerful tool for the design, scale-up or optimization of unit operations and chemical reactors, because it can be tuned into the physics of the system, which reduces the need for experimental investigation, thereby saving development cost and time and providing a deeper understanding of physical phenomena. However, CFD remains computationally expensive, even though the development of parallel solvers able to run CFD simulations in parallel on multicore processors or large computer clusters has drastically reduced the runtime to a few days even for complex flows. It should be noted that although the computational time has decreased, data validation during post-processing remains a time-consuming and expensive process. Another limitation may arise from solvers that do not include all physical models. A hundred commercial CFD solutions are now available, but many of them are limited to specific cases, e.g., to single-phase flows, Newtonian fluids, incompressible flows, isothermal flows, or non-reactive flows, etc. The same limitations apply to public domain codes (more than 50 are already available), some of which are even more restricted, *e.g.*, to two-dimensional (2D) geometries (Mohebbi, 2018). These differences result from the numerical solver which is at the heart of each CFD simulation. CFD methodology requires five main sequential steps: (i) Formulate the flow problem, which consists in defining the geometry, the physical assumptions, the boundary and initial conditions to achieve the objectives of the simulations. Design the geometry and in particular the flow domain using CAD (Computer-

Aided Design) software, (ii) generate the grid using a mesh generator: this consists in dividing the continuous geometry into a discrete number of topological volumes in 3D (usually tetrahedral or hexahedral, but also polygonal, etc.), denoted "cells", (iii) use a numerical solver to solve the discretized form of the governing equations ("processing"), which implies that this solver is compatible with the grid topology and the physical model, and (iv) visualize and critically analyze the results, which is currently referred to as "post-processing." . In fact, commercial CFD solvers usually include a vast set of solvers which can assume alternatively, 2D, 2D-axisymmetric, or 3D flows, steady or transient flows, but also isothermal/non-isothermal flows, laminar/turbulent flows, single-processor/parallel, etc. Commercial software packages typically offer an "all-in-one" solution from pre-processing to post-processing, while public domain solvers often rely on independent free CAD, meshing, and visualization software solutions. However, the choice between all-in-one or specialized codes, as well as between commercial and open-access solvers, is still a subject of controversy (Janczarek and Kowalska, 2021).

While local hydrodynamics in photoreactors can be predicted from the transport equations of Table 4, the application of CFD to heterogeneous photocatalysis requires two additional models (Fig. 13). The first one is the kinetic model of the photodegradation reaction. For example, the degradation rate r_m of species m in a heterogeneous photocatalytic process can usually follow a modified two-parameter Langmuir-Hinshelwood kinetics (k_T is the kinetic constant and K is the binding constant associated with species adsorption on the catalyst) as a function of the molar concentration C_m of species m (M_m is the molar mass of this species), with $n_m = 1$ or $n_m = 0.5$ (Eq. (3)) (Ballari et al., 2019; Boyjoo et al., 2013).

$$-r_m = M_m \cdot k_T \frac{KC_m}{1+KC_m} \cdot \Phi \cdot {L_a}^{n_m} \quad (3)$$

From Eq. (3), it emerges that radiation transport modeling is needed to predict L_a (Fig. 13). Radiative transfer is the complex process of energy transfer. The propagation of radiation through a medium is affected by three main physical phenomena: absorption, emission, and scattering processes (Fig. 14a). Scattering is usually negligible in comparison to absorption in pure liquids, but it cannot be neglected when solid particles are suspended. Unlike conventional transport equations, light transfer models are not included in most of the CFD software solutions except the most advanced ones. Therefore, the local photon absorption rate L_a in Eq. (3) is difficult to predict. This quantity can be estimated at any position $\mathbf{r}$ and time t using the Radiative Transfer Equation (RTE) which describes the spatial and temporal evolution of spectral radiance $I_\lambda(\boldsymbol{r}, \boldsymbol{s}, t)$ (in the direction of vector $\mathbf{s}$, i.e., the propagation direction). The RTE is expressed as follows (Eq. (4)):

$$\underbrace{\frac{1}{c}\cdot\frac{\partial I_\lambda(\mathbf{r},\mathbf{s},t)}{\partial t}}_{unsteady\ term} + \mathbf{s}\cdot\underbrace{\boldsymbol{grad}\left(I_\lambda(\mathbf{r},\mathbf{s},t)\right)}_{spatial\ term} + \underbrace{\left(k_{s,\lambda}+k_{a,\lambda}\right)\cdot I_\lambda(\mathbf{r},\mathbf{s},t)}_{out-scattering+absorption} = \underbrace{j_\lambda}_{emission} + \underbrace{\frac{k_{s,\lambda}}{4\pi}\cdot\int_0^{4\pi} p[\mathbf{s},\mathbf{s}']\cdot I_\lambda(\boldsymbol{r},\boldsymbol{s},t)\,d\Omega'}_{in-scattering\ term} + \underbrace{\frac{1}{c}\cdot S_\lambda(\mathbf{r},\mathbf{s},t)}_{source\ term} \quad (4)$$

Spectral (monochromatic) radiance $I_\lambda(\mathbf{r},\mathbf{s},t)$ is defined as the energy flux per unit normal area dA (m^2), per unit solid angle $d\Omega$, in the time interval t to $t+dt$ (s), and in the wavelength interval λ to $\lambda+d\lambda$ (m). c is the speed of light in the medium (which depends on its refractive index), $k_{s,\lambda}$ the scattering coefficient (m^{-1}), and $k_{a,\lambda}$ the absorption coefficient (m^{-1}). In heterogeneous catalysis $S_\lambda(\mathbf{r},\mathbf{s},t)$ is a source term, and j_λ is the emission term. $p[\mathbf{s},\mathbf{s}']$ is the scattering phase function, representing the probability of light propagating in the direction of vector $\mathbf{s}'$ by scattering in a solid angle $d\Omega'$, such that $\int_{4\pi} p[\mathbf{s},\mathbf{s}']d\Omega' = 4\pi$. As illustrated by Eq. (4), RTE is a complex equation considering on the one hand emission (usually negligible in

photocatalytic processes in water), and on the other hand absorption and scattering which are essential in heterogeneous photocatalysis (Fig. 14a). If $I_\lambda(\mathbf{r},\mathbf{s},t)$ can be estimated locally, the monochromatic irradiance $E_\lambda(\mathbf{r},t)$ and then, $L_a(\mathbf{r},t)$, can be deduced from the following equation (Eq. (5)):

$$E_\lambda(\mathbf{r},t) = \int_0^{4\pi} I_\lambda(\mathbf{r},\mathbf{s},t)\cdot d\Omega \quad \text{and} \quad L_a(\mathbf{r},t) = \int_{\lambda_{min}}^{\lambda_{max}} k_{s,\lambda}\cdot E_\lambda(\mathbf{r},t)\cdot d\lambda \tag{5}$$

where the wavelength interval $[\lambda_{min},\lambda_{max}]$ defines the whole absorbable range of the photocatalyst. Steady conditions may usually be applied, except when solar-driven photocatalytic reactors are studied.

The RTE (Eq. (4)) is an integro-differential equation depending on six variables, i.e., time (t), three spatial coordinates of the vector $\mathbf{r}(x,y,z)$, and two directional variables of the unit vector $\mathbf{s}(\theta,\psi)$ for each wavelength λ (Fig. 14b). This differs from the conventional transport equation of CFD (Eq. (2)) and cannot be easily solved using the standard CFD solvers based on the finite-volume method (FVM) (Ferziger et al., 2019). Two strategies can, therefore, be applied: (i) Uncoupling hydrodynamics and radiation transfer: in this case, conventional CFD methods can be applied to predict only the flow field as a first step. Then, the RTE or simplified analytic solutions of the RTE can be used to predict L_a, so that the local reaction rate can be deduced when coupled to the kinetic model. Monte Carlo (MC) methods constitute the best and the most accurate way to solve the RTE (Modest, 2013), and (ii) solving simultaneously transport equations, RTE, and the kinetic model, which requires specific developments compatible with FVM to solve the RTE. These mainly include the *Spherical Harmonics method* (P_N approximation) and the *Discrete Ordinate method* (DO or S_N approximation) (Modest, 2013).

The development of more efficient solvers for the RTE, faster, or more numerically stable, is still ongoing (Moreno-SanSegundo et al., 2020).

A typical example of the first strategy applied to a photocatalytic reactor can be found Rasul et al. (2023), where the RTE is not solved. In this case, simple solutions approximating RTE can be used. For example, CFD can be used to define illuminated and dark zones (where the light intensity is too low for the reaction to proceed), as shown in Fig. 15a for an internal illumination, using a simple one-dimensional (1D) approach. A typical illustration of this approach with external illumination can be found in Loubière et al. (2016). The common methods to estimate L_a are the Beer-Lambert equation (1D, steady, no emission, no in-scattering), the two-flux model (TFM), which accounts for anisotropic out-scattering, the four-flux model (FFM), and the six-flux model (SFM), as in Fig. 15b (Alvarado-Rolon et al., 2018; Li Puma and Brucato, 2007).

For the second strategy, a simplified version of multi-flux models can be used, assuming that the scattering function is isotropic : this constitutes the Discrete Transfer (DT) model, which tracks a defined number of rays (Qi et al., 2011). Since the assumption of isotropic scattering is usually unrealistic, DO/FVM is the most popular method when CFD solvers are used to solve the RTE, but the P_N/FVM method and in particular the P_1 model constitute possible alternatives. In the DO (or segmented-N, S_N) method, the RTE is solved along a set of discrete directions, *i.e.*, a finite number of discrete solid angles, each associated with a unit vector **s** (Modest, 2013). Thus, the angular space 4π is discretized into $N_\theta \cdot N_\Psi$ solid angles (N_θ and N_Ψ can be different) where θ and Ψ are the polar and azimuthal angles, respectively (Fig. 14b). Quadrature rules are used to estimate the integrals. The RTE is transformed into several transport equations, all of which are similar and can be solved by a CFD solver using FVM. The DO method is mathematically simple, which explains why it is the most popular one for solving the RTE, but it has a high

computational cost, and the numerical solution is subject to false-diffusion error (Ferziger et al., 2019).

In the Spherical Harmonics Method (P_N approximation), the radiance is approximated by a truncated series of spherical harmonics, where N is the order of truncation. The mathematical complexity increases sharply with N, and the model leads to several transport-like equations that can be solved using FVM. The advantage is that the P_N method is often less computationally expensive than the DO method. However, due to the complexity of higher-order P_N models, only the P_1 model has been implemented in most CFD solvers. This considers one isotropic and one anisotropic term, which are proportional. The P_1 model finally reduces to a single additional convection-diffusion transport equation, as scattering appears as a diffusive term. It also eliminates the angular coordinates in the solving process. Therefore, the computational cost of the P_1 model is low, but it constitutes, however, a rough approximation for highly anisotropic scattering media. More detailed comparison between these methods and with the MC method can be found in Barbosa et al. (2023) in the case of photocatalytic reactors.

Solving the RTE also requires the measurement or the estimation of the radiative properties of the photocatalyst, namely, $k_{s,\lambda}$ and $k_{a,\lambda}$ (or of their wavelength-average values) (Boyjoo et al., 2013). The phase scattering function, which is more difficult to measure, must also be defined. Except isotropic scattering, the most common phase scattering function is described by the Henyey–Greenstein distribution model (Eq (6)):

$$p[\mathbf{s}, \boldsymbol{s}'] = p[\omega\,] = \frac{1}{2}\frac{(1-g^2)}{\left(1+g^2-2g\cdot cos(\omega)\right)^{3/2}} \tag{6}$$

This model depends only on the angle ω between $\mathbf{s}$ and $\mathbf{s}'$ (Valadés-Pelayo et al., 2015). The asymmetric parameter g is the single fitting parameter of this model. Other examples of scattering phase functions used in photocatalytic reactors can be found in Wang et al. (2021). Finally, the source term, usually the lamp emission model, must also be defined. Typical lamp emission models in photocatalytic reactors can be found in (Boyjoo et al., 2013; Tong et al., 2020).

Applications of CFD to heterogeneous photocatalytic degradation of organic pollutants in water have been reviewed by several authors in the last years (Barbosa et al., 2023; Tong et al., 2020). These reviews demonstrate that CFD can be applied to all the types of photocatalytic reactors, including annular, flat-plate, tubular or multitube, slurry bubble columns or fluidized beds, and also to microreactors, illuminated by either UV or solar light, and operated under batch or continuous flow conditions.

However, it also appears that not many studies in a CFD environment have addressed the degradation of EPs in even in the recent period, even though some of them can be found in the literature. CFD is often used in the preliminary stages of photoreactor development, when theoretical kinetics can be assumed, or a model molecule can be used for experimental validation. Thus, the pollutant is sometimes not clearly defined, for example in Qi et al. (2011), even though their simulations were compared to data on Congo Red, or sometimes it is used to estimate the optical properties of the photocatalyst (Turolla et al., 2016). The simulation strategies also strongly depend on the type of photocatalytic reactor, such as suspended catalyst, or photocatalyst coated either on a packed bed or on the walls (Fig. 16) and on the objective of the authors (comparison of photocatalysts or photocatalytic reactor designs, optimization of operating conditions, etc.).

For suspended photocatalysts, Turolla et al. (2016) studied the degradation of oxalic acid in an annular UV photoreactor with TiO_2 nanoparticles. Assuming a laminar single-phase flow with a pseudo-homogeneous slurry phase and a complex photodegradation kinetic model extracted from the literature, the RTE was solved using the DO method. The commercial code Ansys Fluent was used. Only a 2D domain was simulated because the authors' objective was to estimate the optical properties of the nanoparticles, including the best model for the phase function, by fitting experimental scattering data. The degradation of oxalic acid was investigated more recently by Gao et al. (2023) in a continuous cylindrical photocatalytic reactor equipped with four lamps. The same commercial code was used, and the same assumptions were made except on the flow regime which was turbulent. Therefore, the RNG $k-\varepsilon$ was applied. The authors's objective was to optimize the operating conditions and the simulations predicted a maximum degradation yield of 27% when the photocatalyst concentration was 20 $mg.L^{-1}$. The comparison between these two previous works (Gao et al., 2023; Turolla et al., 2016) highlights the above-mentioned versatility of CFD. Contrary to these studies, Qi et al. (2011) investigated the mineralization of organic pollutants, focusing on multiphase hydrodynamics. The authors assumed a simpler pseudo-first order photocatalytic degradation rate versus concentration, which corresponds to dilute organic compounds (which is the case of emerging micropollutants: $KC_m \ll 1$), in an annular bubble column photocatalytic reactor with suspended particles of TiO_2 P25. A turbulent $k-\varepsilon$ multiphase Euler-Euler flow model was assumed to describe the three-phase flow using the Ansys CFX commercial package. Batch conditions were assumed for the liquid and the solid phases. The photocatalytic degradation rate was assumed to be proportional to L_a and the simple Discrete Transfer model was applied to solve the RTE to counterbalance the high computational cost of three-phase CFD simulations. The simulations were used to define

the gas flow rate necessary to homogenize the local catalyst concentration and to define the global catalyst concentration necessary to mineralize the pollutant in about 4 h of treatment. The radial gradient of organic pollutant, due to the radial profile of radiation intensity was estimated. The results highlight that CFD may better elucidate the coupling between hydrodynamics and light intensity distribution and provide better guidance for scale-up processes from a methodological point of view. A similar approach was applied more recently by Luo et al. (2017) using the commercial software package Ansys Fluent, who focused on the three-phase hydrodynamics (gas flow rate, draft tube geometry) of an internal-loop airlift photocatalytic reactor to optimize the spatial distribution of the photocatalyst, but without solving the RTE. Boyjoo et al. (2013) also used a three-phase slurry reactor irradiated by 1, 2, or 4 UV lamps. They used the DO method to solve the RTE with the Ansys Fluent code. A zero-order with respect to pollutant concentration was assumed, but a two-regime model was proposed for the order of L_a: the reaction rate was proportional to L_a when the local incident radiation intensity was less than 225 W.m^{-2} and proportional to ${L_a}^{1/2}$ otherwise. This divided the photocatalytic reactor into two zones with different degradation kinetic models: where the first-order kinetics predominated, the volumetric reaction rate was between 12 and 20 times that of the other regions. The use of several less powerful lamps could, therefore, increase the volume of the zones where first-order kinetics prevailed: compared to a single lamp in the center of the reactor, the maximum increase in overall degradation rate was 56% and 123% for optimal placement with 2 and 4 lamps, respectively.

Contrary to suspended solid photocatalytic reactors, packed bed photocatalytic reactors have been far less studied in a CFD environment. The main strategies accounting for the effect of the packed bed on the flow field have been summarized by (Tong et al., 2020). A typical example

was provided by Denny et al. (2009), who investigated the photocatalytic degradation of oxalic acid, as already described (Gao et al., 2023; Turolla et al., 2016). A packed bed of TiO_2-coated glass beads was used as the photocatalyst irradiated by end-emitting optical fibers or side-emitting optical fibers. A laminar flow coupled to the DO model for solving the RTE was chosen. The photodegradation kinetics of oxalic acid was modeled using a Langmuir-Hinshelwood rate law and the reaction rate was first order with respect to L_a when $L_a < 250$ W.m^{-2} and half order above this value. A batch treatment was applied. The results demonstrated that under light transfer limitation, both optical fiber bundles provided nearly the same photodegradation yields *vs* time; conversely, the simulations emphasized that at high power inputs, faster degradation rates could be achieved with side-emitting optical fibers due to a more uniform light distribution, which minimized the volume of the regions where reaction rate was proportional to ${L_a}^{1/2}$. Thus, CFD proved to be a useful tool to improve the fiber bundle design and to determine the optimum power input.

For immobilized photocatalysts on reactor walls, Duran et al. (2011) investigated immobilized photocatalytic reactors using a composite sol-gel TiO_2 coating under continuous flow conditions. The authors compared several hydrodynamic models as a function of flow conditions (laminar, transitional, and turbulent flows) using the Ansys Fluent commercial code with the DO method and studied the mineralization of benzoic acid using a first-order kinetic with respect to the pollutant concentration and L_a. They emphasized that the degradation rate of benzoic acid was limited by the rate of mass transport, especially the external mass transfer, highlighting that the hydrodynamic model was the key point. The same conclusion was drawn by Corbel et al. (2012) in a microchannel reactor. The authors investigated the degradation of salicylic acid in a microchannel photocatalytic reactor (which imposes a laminar flow regime) with an immobilized

catalyst. The commercial code COMSOL Multiphysics was used to simulate the photodegradation flow in a 2D domain using a Langmuir-Hinshelwood degradation kinetic coupled with a surface diffusion model. It should be noted that this code uses the Finite Element Method (FEM) to solve the transport equations: FEM is more accurate than FVM, but it is more computationally expensive and therefore less popular in CFD. A good agreement between experiments and simulations was reported. Radiative transfer was not limited due to the size of the microchannel (1 mm^2), while the flow rate was the key parameter to prevent diffusion limitation. A similar study was driven by Kumar and Bansal (2016) with similar conclusions using Rhodamine B in an annular photocatalytic reactor coated with an immobilized TiO_2 catalyst and the Ansys Fluent code: increasing Reynolds number (*i.e.*, flow rate) improved the photocatalytic pollutant degradation rate in the continuous flow reactor because it reduced mass transfer limitation. The same authors developed an interesting optimization procedure to optimize the degradation yield of Rhodamine B as a function of flow rate and pollutant concentration by combining CFD with design of experiments methodology (Kumar and Bansal, 2013). Leblebici et al. (2015a) have also investigated the performance of TiO_2 coating on the degradation of phenol in a circular flat plate photoreactor under UV-LED light. COMSOL Multiphysics was used to simulate the laminar flow, while a first-order degradation rate was assumed with respect to both the pollutant concentration and L_a. The originality is that the catalyst coating was rated as a porous medium. The authors could estimate the photonic efficiency of the reaction as a function power input and obtain a good agreement with experimental data.

Systems coupling membrane process and heterogeneous photocatalysis were also studied. Chakachaka et al. (2023) used a CFD-assisted process to optimize an integrated photocatalytic

membrane system for water treatment. $CoFe_2O_4$-PES membranes were used in a batch photoreactor. The commercial software Simscale, based on free OpenFOAM solvers, was used to simulate the flow field and solve the RTE. The degradation of Naproxen, a non-steroidal anti-inflammatory drug, was studied. pH, flow rate, fluid, and light intensity were optimized. Under optimum conditions, the degradation rate of naxprofen reached 4.93 10^{11} $mol.J^{-1}$. A removal yield of 99% could be reached in the hybrid photocatalytic-membrane process, which superseded the photocatalytic process (81%) and the membrane process (83%). This result was explained by the enhanced hydrodynamic and mass transfer conditions. A good agreement between simulations and experiments was reported.

An advantage of microreactors is that they can be used more easily than other photocatalytic reactors to estimate the kinetic parameters of degradation (Visan et al., 2019). Yusuf et al. (2020) and Yusuf and Palmisano (2021) simulated the degradation of 4-nitrophenol under a simulated solar source in a continuous flow microreactor using 2D and 3D CFD calculations, respectively. They used COMSOL Multiphysics to fit the adsorption parameters and the kinetic constant from experimental data. The fitted parameters derived from 2D and 3D simulations were in good agreement, and the 3D simulations could be used to assess the respective effects of flow rate and microchannel geometry (height, length) on the conversion of 4-nitrophenol. A similar approach was developed by Balestrin et al. (2024) to study the degradation of salicylic acid using a single-phase turbulent model with the Ansys Fluent commercial package, but the RTE was reduced to the Beer-Lambert law.

In conclusion, CFD is clearly an interesting, flexible, and efficient tool to simulate the degradation of EPs in water by heterogeneous photocatalytic processes to improve the design of photoreactors, improve light distribution and optimize the operating conditions. CFD can also be

used to determine the kinetic model or to validate the optical parameters of the photocatalyst. The review of the literature has shown that models can vary widely not only as a function of reactor type, but also on the same reactor type between different works. This shows that no single approach has yet gained general acceptance. However, the success of a CFD strategy depends on one key point: CFD applied to heterogeneous photocatalytic reactors requires a synergy between chemists, chemical engineers and CFD specialists to *(i)* define adequate and realistic physical models that can effectively represent the experimental trends, *(ii)* critically evaluate the simulated data, distinguishing numerical errors from model limitations. Regarding the physical phenomena to focus on in a CFD strategy as a function of reactor type, some guidelines are summarized in Table 5. In addition, the development of new approaches able to integrate ML in a design strategy by coupling ML to CFD, as recently illustrated by Sun et al. (2024), seems promising but still to be applied to photo-processes dedicated to EPs removal.

7. Challenges and recommendations for future research

The study of semiconductors as photocatalysts unveils their pivotal role in pollutant degradation, owing to electron-hole pair generation, light absorption and surface reactivity TiO_2 modification strategies, such as metallic and non-metallic doping, and semiconductor coupling, have been shown to be effective in improving photocatalytic performance, but semiconductors such as CdS, $Zn_xCd_{1-x}S$ and silver-based semiconductors are unadvisable due to their toxicity, onerous cost, and poor stability. Various studies have demonstrated the rising efficiency of integrated processes for improving EPs rejection, such as electrocoagulation with UV/TiO_2, ultrasound with photo-Fenton and hybrid systems such as $Bi_{12}TiO_{20}$-polyaniline. Despite these developments in the field of materials science, there are still many challenges to be overcome to optimize operational parameters, minimize costs, and ensure scalability.

In addition, the different types of photocatalytic reactors and the main factors influencing their design and efficiency are examined. Suspended systems exhibit higher photocatalytic performance because of the increased surface area available for reactions. Nevertheless, the need for separation processes and the fouling risk requires design improvements. Immobilized systems, however, are more practical for continuous operation, particularly with innovations such as fiber-optic reactors and microreactors. Regarding CFD, it is a powerful tool for simulating EPs degradation in heterogeneous photocatalytic processes. It offers interesting possibilities for improving reactor performance and design, and kinetic modeling. To ensure the successful application of CFD, engineers and CFD specialists need to collaborate to develop accurate models and critically evaluate the simulated data.

In summary, although substantial progress has been made, there remain important gaps in the development of more efficient, cost-effective and scalable photocatalytic systems. Future research should be directed on integrating advanced materials, innovative reactor designs and computational tools to mitigate existing challenges and unleash the true promise of heterogeneous photocatalysis. Future directions and recommendations to fill gaps in the literature and overcome the remaining challenges are presented below:

- There is a lack of in-depth studies on structural optimization of photocatalysts for self-stability, durability, and efficiency. For instance, we recommend combining the high photocatalytic activity materials, such as TiO_2, with the high electron-transport properties of carbon nanostructures like GO, so that the stability of photocatalysts could be improved.

- The literature has mainly focused on solar energy recovery or photocatalytic degradation independently, though few research studies have investigated their synergistic integration. Using a combination of perovskite-based materials and traditional solar panels, for example, maximizes the synergy between photocatalysis and energy recovery resulting in sustainable solutions considering environmental aspects.

- Computational (such as density functional theory) and spectroscopic studies are still insufficient to fully understand photocatalytic mechanisms and photo-corrosion, which are essential for improving materials design. These strategies can help shed light on the electronic structure and surface reactions of photocatalysts, allowing the design of more efficient materials.

- Whilst CFD is a useful tool for reactor design, its application to photoreactor design, particularly for solar processes, is still in its infancy for photobioreactors. In addition, CFD advances for process intensification in photocatalytic applications, like optimizing light distribution and flow dynamics, are still insufficient. It would be valuable to examine multi-criteria optimization strategies considering both economic and environmental aspects of photoreactors. Coupling ML and CFD also appears as a potential way to develop a systematic approach to improve photoreactor design that has not been tested up to now.

- ML also emerges as an attractive method for photocatalytic process control, especially when intermittent solar light is used.

Term	Definition

Technical terminology

Heterogeneous photocatalysis	Heterogeneous photocatalysis is a process where a solid material (the photocatalyst) facilitates a chemical reaction upon exposure to light, with enough radiation to promote an electron from the valence band (V_B) to the conduction band (C_B).
Semiconductor photocatalyst	A semiconductor photocatalyst is a material that absorbs photons from light sources (usually artificial light or natural sunlight) to excite electrons from the valence band to the conduction band, creating electron-hole pairs. These charge carriers participate in redox reactions by either reducing or oxidizing the substances present on the surface of the catalyst.
Photoreactor	A photoreactor (photocatalytic reactor) is a device designed to performs the process of photocatalysis reaction, allowing the interaction between light, photocatalyst, and reactants to induce chemical transformations.
Advanced oxidation processes (AOPs)	Advanced Oxidation Processes (AOPs) are a set of chemical treatment procedures designed to remove organic (and sometimes inorganic) pollutants from water and air by oxidation through reactions with highly reactive species, primarily hydroxyl radicals ($^{\bullet}OH$).
Photolysis	Photolysis is a chemical process in which a chemical compound is broken down or separated by the action of light.
Reactive oxygen species	Reactive Oxygen Species are highly reactive chemicals derived from diatomic oxygen (O_2), water, and hydrogen peroxide. They include free radicals (molecules with unpaired electrons) and non-radical species, which can easily react with other molecules.
Energy band gap	The energy band gap (E_g) is the energy level between the top of the valence band (where electrons are bound to atoms) and the bottom of the conduction band (where electrons are free to move and conduct electricity) in a material, typically a semiconductor.
Electron/hole pairs	Electron/hole pairs refer to the pairs of charge carriers generated in the semiconductor when an electron is excited from the valence band to the conduction band, leaving behind a positively charged hole.
Electron/hole recombination	Electron/hole recombination is a process in the semiconductor where an excited electron from the conduction band falls back into the empty state in the valence band, resulting in the release of energy.
Valence band	The valence band is the highest energy band in the semiconductor material that is fully occupied by electrons at absolute zero temperature.
Conduction band	The conduction band is the energy band in the semiconductor material that is associated with free electrons capable of conducting electricity.
Computational	Computational Fluid Dynamics (CFD) is a branch of fluid mechanics that uses

Fluid Dynamics (CFD)	numerical methods and algorithms to predict liquid and gas flows based on the governing equations of conservation of mass, momentum, and energy.
Artificial Neutral Network (ANN)	Artificial Neural Network (ANN) is a collection of simple interconnected algorithms that process information in response to external input. The ANN model is organized in layers, each one made up of interconnected nodes.

References

Abd Rahman, N., Choong, C.E., Pichiah, S., Nah, I.W., Kim, J.R., Oh, S.-E., Yoon, Y., Choi, E.H., Jang, M., 2023. Recent advances in the TiO2 based photoreactors for removing

contaminants of emerging concern in water. Separation and Purification Technology 304, 122294. https://doi.org/10.1016/j.seppur.2022.122294

Abdellah, M.H., Nosier, S.A., El-Shazly, A.H., Mubarak, A.A., 2018. Photocatalytic decolorization of methylene blue using TiO2/UV system enhanced by air sparging. Alexandria Engineering Journal 57, 3727–3735. https://doi.org/10.1016/j.aej.2018.07.018

Abdel-Maksoud, Y., Imam, E., Ramadan, A., 2016. TiO2 Solar Photocatalytic Reactor Systems: Selection of Reactor Design for Scale-up and Commercialization—Analytical Review. Catalysts 6, 138. https://doi.org/10.3390/catal6090138

Abromaitis, V., Oghenetejiro, O.A.M.A., Sulciute, A., Urniezaite, I., Sinkeviciute, D., Zmuidzinaviciene, N., Jankunaite, D., Dzingeleviciene, R., Baranauskis, K., Martuzevicius, D., 2024. TiO2 nanotube arrays photocatalytic ozonation for the removal of antibiotic ciprofloxacin from the effluent of a domestic wastewater treatment plant: Towards the process upscaling. Journal of Water Process Engineering 63, 105457. https://doi.org/10.1016/j.jwpe.2024.105457

Ahmad, I., Zou, Y., Yan, J., Liu, Y., Shukrullah, S., Naz, M.Y., Hussain, H., Khan, W.Q., Khalid, N.R., 2023. Semiconductor photocatalysts: A critical review highlighting the various strategies to boost the photocatalytic performances for diverse applications. Advances in Colloid and Interface Science 311, 102830. https://doi.org/10.1016/j.cis.2022.102830

Ahuja, T., Brighu, U., Saxena, K., 2023. Recent advances in photocatalytic materials and their applications for treatment of wastewater: A review. Journal of Water Process Engineering 53, 103759. https://doi.org/10.1016/j.jwpe.2023.103759

Alvarado-Rolon, O., Natividad, R., Romero, R., Hurtado, L., Ramírez-Serrano, A., 2018. Modelling and Simulation of the Radiant Field in an Annular Heterogeneous Photoreactor Using a Four-Flux Model. International Journal of Photoenergy 2018, 1678385. https://doi.org/10.1155/2018/1678385

Amani-Ghadim, A.R., Dorraji, M.S.S., 2015. Modeling of photocatalyatic process on synthesized ZnO nanoparticles: Kinetic model development and artificial neural networks. Applied Catalysis B: Environmental 163, 539–546. https://doi.org/10.1016/j.apcatb.2014.08.020

An, H., Du, Y., Wang, T., Wang, C., Hao, W., Zhang, J., 2008. Photocatalytic properties of BiOX (X = Cl, Br, and I). Rare Metals 27, 243–250. https://doi.org/10.1016/S1001-0521(08)60123-0

Anandhi, G., Iyapparaja, M., 2024. Photocatalytic degradation of drugs and dyes using a maching learning approach. RSC Adv. 14, 9003–9019. https://doi.org/10.1039/D4RA00711E

Aoudj, S., Drouiche, N., Khelifa, A., 2019. Chapter 9 - Emerging contaminants remediation by heterogeneous photocatalysis, in: Mishra, A.K., Anawar, H.M.D., Drouiche, Nadjib (Eds.), Emerging and Nanomaterial Contaminants in Wastewater. Elsevier, pp. 245–275. https://doi.org/10.1016/B978-0-12-814673-6.00009-7

Artemov, V., Beale, S.B., de Vahl Davis, G., Escudier, M.P., Fueyo, N., Launder, B.E., Leonardi, E., Malin, M.R., Minkowycz, W.J., Patankar, S. V., Pollard, A., Rodi, W., Runchal, A., Vanka, S.P., 2009. A tribute to D.B. Spalding and his contributions in science and engineering. International Journal of Heat and Mass Transfer, Special Issue Honoring Professor D. Brian Spalding 52, 3884–3905. https://doi.org/10.1016/j.ijheatmasstransfer.2009.03.038

Askari, N., Jamalzadeh, M., Askari, A., Liu, N., Samali, B., Sillanpaa, M., Sheppard, L., Li, H., Dewil, R., 2025. Unveiling the photocatalytic marvels: Recent advances in solar heterojunctions for environmental remediation and energy harvesting. Journal of Environmental Sciences (China) 148, 283–297. https://doi.org/10.1016/j.jes.2024.01.006

Ayodele, B.V., Alsaffar, M.A., Mustapa, S.I., Cheng, C.K., Witoon, T., 2021. Modeling the effect of process parameters on the photocatalytic degradation of organic pollutants using artificial neural networks. Process Safety and Environmental Protection 145, 120–132. https://doi.org/10.1016/j.psep.2020.07.053

Baaloudj, O., Nasrallah, N., Bouallouche, R., Kenfoud, H., Khezami, L., Assadi, A.A., 2022. High efficient Cefixime removal from water by the sillenite Bi12TiO20: Photocatalytic mechanism and degradation pathway. Journal of Cleaner Production 330, 129934. https://doi.org/10.1016/j.jclepro.2021.129934

Baaloudj, O., Nasrallah, N., Kenfoud, H., Bourkeb, K.W., Badawi, A.K., 2023. Polyaniline/Bi12TiO20 Hybrid System for Cefixime Removal by Combining Adsorption and Photocatalytic Degradation. ChemEngineering 7, 4. https://doi.org/10.3390/chemengineering7010004

Bahramian, M., Dereli, R.K., Zhao, W., Giberti, M., Casey, E., 2023. Data to intelligence: The role of data-driven models in wastewater treatment. Expert Systems with Applications 217, 119453. https://doi.org/10.1016/j.eswa.2022.119453

Balestrin, E., de Souza, S.M.A.G.U., Valle, J.A.B., da Silva, A., 2024. Intrinsic kinetic model with variable light intensity of the emerging pollutants degradation in a photocatalytic differential reactor with immobilized TIO2: Experiments and CFD. The Canadian Journal of Chemical Engineering 102, 2277–2293. https://doi.org/10.1002/cjce.25197

Ballari, M. de los M., Satuf, M., Alfano, O., 2019. Photocatalytic Reactor Modeling: Application to Advanced Oxidation Processes for Chemical Pollution Abatement. Topics in Current Chemistry 377. https://doi.org/10.1007/s41061-019-0247-2

Bampos, G., Petala, A., Frontistis, Z., 2021. Recent Trends in Pharmaceuticals Removal from Water Using Electrochemical Oxidation Processes. Environments 8, 85. https://doi.org/10.3390/environments8080085

Bandala, E.R., Arancibia-Bulnes, C.A., Orozco, S.L., Estrada, C.A., 2004. Solar photoreactors comparison based on oxalic acid photocatalytic degradation. Solar Energy, Photocatalysis 77, 503–512. https://doi.org/10.1016/j.solener.2004.03.021

Barbosa, I.S.O., Santos, R.J., Dias, M.M., Faria, J.L., Silva, C.G., 2023. Radiation Models for Computational Fluid Dynamics Simulations of Photocatalytic Reactors. Chemical Engineering & Technology 46, 1059–1077. https://doi.org/10.1002/ceat.202200551

Barzegar, M.H., Sabzehmeidani, M.M., Ghaedi, M., Avargani, V.M., Moradi, Z., Roy, V.A.L., Heidari, H., 2021. S-scheme heterojunction g-C3N4/TiO2 with enhanced photocatalytic activity for degradation of a binary mixture of cationic dyes using solar parabolic trough reactor. Chemical Engineering Research and Design 174, 307–318. https://doi.org/10.1016/j.cherd.2021.08.015

Bhattacharya, S., Das, P., Bhowal, A., Majumder, S.K., 2022. Metal-oxide coated Graphene oxide nano-composite for the treatment of pharmaceutical compound in photocatalytic reactor: Batch, Kinetics and Mathematical Modeling using Response Surface Methodology and Artificial Neural Network. Environmental Science and Pollution Research 29, 61938–61953. https://doi.org/10.1007/s11356-021-18227-2

Bibi, S., Shah, S.S., Muhammad, F., Siddiq, M., Kiran, L., Aldossari, S.A., Sheikh Saleh Mushab, M., Sarwar, S., 2023. Cu-doped mesoporous TiO2 photocatalyst for efficient degradation of organic dye via visible light photocatalysis. Chemosphere 339, 139583. https://doi.org/10.1016/j.chemosphere.2023.139583

Bilal, M., Adeel, M., Rasheed, T., Zhao, Y., Iqbal, H.M.N., 2019. Emerging contaminants of high concern and their enzyme-assisted biodegradation - A review. Environ Int 124, 336–353. https://doi.org/10.1016/j.envint.2019.01.011

Binjhade, R., Mondal, R., Mondal, S., 2022. Continuous photocatalytic reactor: Critical review on the design and performance. Journal of Environmental Chemical Engineering 10, 107746. https://doi.org/10.1016/j.jece.2022.107746

Bonet-San-Emeterio, M., Felipe Montiel, N., del Valle, M., 2021. Graphene for the Building of Electroanalytical Enzyme-Based Biosensors. Application to the Inhibitory Detection of Emerging Pollutants. Nanomaterials 11, 2094. https://doi.org/10.3390/nano11082094

Boutra, B., Sebti, A., Trari, M., 2022. Response surface methodology and artificial neural network for optimization and modeling the photodegradation of organic pollutants in water. International Journal of Environmental Science and Technology 19. https://doi.org/10.1007/s13762-021-03875-1

Boyjoo, Y., Ang, M., Pareek, V., 2013. Some aspects of photocatalytic reactor modeling using computational fluid dynamics. Chemical Engineering Science 101, 764–784. https://doi.org/10.1016/j.ces.2013.06.035

Braham, R., Harris, A., 2009. Review of Major Design and Scale-up Considerations for Solar Photocatalytic Reactors. Industrial & Engineering Chemistry Research - IND ENG CHEM RES 48. https://doi.org/10.1021/ie900859z

Byrne, C., Subramanian, G., Pillai, S.C., 2018. Recent advances in photocatalysis for environmental applications. Journal of Environmental Chemical Engineering 6, 3531–3555. https://doi.org/10.1016/j.jece.2017.07.080

Can, E., Yildirim, R., 2019. Data mining in photocatalytic water splitting over perovskites literature for higher hydrogen production. Applied Catalysis B: Environmental 242, 267–283. https://doi.org/10.1016/j.apcatb.2018.09.104

Chakachaka, V.M., Tshangana, C.S., Mamba, B.B., Muleja, A.A., 2023. CFD-Assisted Process Optimization of an Integrated Photocatalytic Membrane System for Water Treatment. Membranes 13, 827. https://doi.org/10.3390/membranes13100827

Chandrabose, G., Dey, A., Gaur, S.S., Pitchaimuthu, S., Jagadeesan, H., Braithwaite, N.S.J., Selvaraj, V., Kumar, V., Krishnamurthy, S., 2021. Removal and degradation of mixed dye pollutants by integrated adsorption-photocatalysis technique using 2-D MoS2/TiO2 nanocomposite. Chemosphere 279, 130467. https://doi.org/10.1016/j.chemosphere.2021.130467

Chaudhuri, A., Zondag, S.D.A., Schuurmans, J.H.A., van der Schaaf, J., Noël, T., 2022. Scale-Up of a Heterogeneous Photocatalytic Degradation Using a Photochemical Rotor–Stator Spinning Disk Reactor. Organic Process Research & Development 26, 1279–1288. https://doi.org/10.1021/acs.oprd.2c00012

Chen, D., Cheng, Y., Zhou, N., Chen, P., Wang, Y., Li, K., Huo, S., Cheng, P., Peng, P., Zhang, R., Wang, L., Liu, H., Liu, Y., Ruan, R., 2020. Photocatalytic degradation of organic pollutants using TiO2-based photocatalysts: A review. Journal of Cleaner Production 268, 121725. https://doi.org/10.1016/j.jclepro.2020.121725

Chen, D.H., Ye, X., Li, K., 2005. Oxidation of PCE with a UV LED Photocatalytic Reactor. Chemical Engineering & Technology 28, 95–97. https://doi.org/10.1002/ceat.200407012

Chen, X., Kuo, D.-H., Lu, D., 2017. Visible light response and superior dispersed S-doped TiO2 nanoparticles synthesized via ionic liquid. Advanced Powder Technology 28, 1213–1220. https://doi.org/10.1016/j.apt.2017.02.007

Colina-Márquez, J., Guerra, M., Perez, R., 2019. Modeling of a Solar Heterogeneous Photocatalytic Reactor with TiO2 for Treatment of Wastewater Contaminated By Albendazole. INGENIERÍA Y COMPETITIVIDAD 21, 1–10. https://doi.org/10.25100/iyc.v21i2.8105

Corbel, S., Charles, G., Becheikh, N., Roques-Carmes, T., Zahraa, O., 2012. Modelling and design of microchannel reactor for photocatalysis: Here, the freedom of design and accuracy of the stereolithography technique were exploited to study the photolytic degradation of salicylic acid as a model water pollutant in stereolithograp. Virtual and Physical Prototyping 7, 203–209. https://doi.org/10.1080/17452759.2012.708837

Danion, A., Disdier, J., Guillard, C., Jaffrezic-Renault, N., 2007. Malic acid photocatalytic degradation using a TiO2-coated optical fiber reactor. Journal of Photochemistry and Photobiology A: Chemistry 190, 135–140. https://doi.org/10.1016/j.jphotochem.2007.03.022

Das, L., Maity, U., Basu, J.K., 2014. The photocatalytic degradation of carbamazepine and prediction by artificial neural networks. Process Safety and Environmental Protection 92, 888–895. https://doi.org/10.1016/j.psep.2013.10.001

Deblonde, T., Cossu-Leguille, C., Hartemann, P., 2011. Emerging pollutants in wastewater: A review of the literature. International Journal of Hygiene and Environmental Health, The second European PhD students workshop: Water and health ? Cannes 2010 214, 442–448. https://doi.org/10.1016/j.ijheh.2011.08.002

Denny, F., scott, jason, Pareek, V., Peng, G.-D., Amal, R., 2009. CFD modelling for a TiO2-coated glass-bead photoreactor irradiated by optical fibres: Photocatalytic degradation of oxalic acid. Chemical Engineering Science 64, 1695–1706. https://doi.org/10.1016/j.ces.2008.12.021

Díez, A.M., Licciardello, N., Kolen´ko, Y.V., 2023. Photocatalytic processes as a potential solution for plastic waste management. Polymer Degradation and Stability 215, 110459. https://doi.org/10.1016/j.polymdegradstab.2023.110459

Divya, G., Jaishree, G., Sivarao, T., Divya Lakshmi, K.V., 2023. Microwave assisted sol–gel approach for Zr doped TiO 2 as a benign photocatalyst for bismark brown red dye pollutant. RSC Advances 13, 8692–8705. https://doi.org/10.1039/D3RA00328K

Duran, J.E., Mohseni, M., Taghipour, F., 2011. Computational fluid dynamics modeling of immobilized photocatalytic reactors for water treatment. AIChE Journal 57, 1860–1872. https://doi.org/10.1002/aic.12399

Eckert, H., Bobeth, M., Teixeira, S., Kühn, K., Cuniberti, G., 2015. Modeling of photocatalytic degradation of organic components in water by nanoparticle suspension. Chemical Engineering Journal, Photocatalysis for disinfection and removal of contaminants of emerging concern 261, 67–75. https://doi.org/10.1016/j.cej.2014.05.147

Eggen, T., Moeder, M., Arukwe, A., 2010. Municipal landfill leachates: A significant source for new and emerging pollutants. Science of The Total Environment 408, 5147–5157. https://doi.org/10.1016/j.scitotenv.2010.07.049

Ehrampoush, M.H., Moussavi, Gh.R., Ghaneian, M.T., Rahimi, S., Ahmadian, M., 2011. Removal of methylene blue dye from textile simulated sample using tubular reactor and TiO[2]/UV-C photocatalytic process. Iranian Journal of Environmental Health Science and Engineering 8, 35–40.

El-Kalliny, A.S., Ahmed, S.F., Rietveld, L.C., Appel, P.W., 2014. Immobilized photocatalyst on stainless steel woven meshes assuring efficient light distribution in a solar reactor. Drinking Water Engineering and Science 7, 41–52. https://doi.org/10.5194/dwes-7-41-2014

European Commission, 2024. Water Framework Directive - European Commission [WWW Document].

Fageria, P., Gangopadhyay, S., Pande, S., 2014. Synthesis of ZnO/Au and ZnO/Ag nanoparticles and their photocatalytic application using UV and visible light. RSC Advances 4, 24962–24972. https://doi.org/10.1039/C4RA03158J

Fakhravar, S., Farhadian, M., Tangestaninejad, S., 2020. Metronidazole degradation by Z-scheme Ag2S/BiVO4@α-Al2O3 heterojunction in continuous photo-reactor: response surface methodology optimization, reaction mechanism and the effect of water matrix.

Journal of Environmental Chemical Engineering 8, 104136. https://doi.org/10.1016/j.jece.2020.104136

Fernandes, A., Makoś, P., Wang, Z., Boczkaj, G., 2020. Synergistic effect of TiO2 photocatalytic advanced oxidation processes in the treatment of refinery effluents. Chemical Engineering Journal 391, 123488. https://doi.org/10.1016/j.cej.2019.123488

Ferziger, J.H., Perić, M., Street, R.L., 2019. Computational Methods for Fluid Dynamics. Springer.

Fouad, S.M., El-Shazly, Y.M.S., Alyoubi, M.A., Nosier, S.A., Abdel-Aziz, M.H., 2023. Enhanced photocatalytic degradation of cationic dyes using slurry of anatase titania in a falling film reactor. Case Studies in Chemical and Environmental Engineering 8, 100518. https://doi.org/10.1016/j.cscee.2023.100518

Franz, S., Bestetti, M., 2023. 5 - Kinetic models in photoelectrocatalysis, in: Palmisano, L., Yurdakal, S. (Eds.), Photoelectrocatalysis. Elsevier, pp. 217–263. https://doi.org/10.1016/B978-0-12-823989-6.00009-6

Fujishima, A., Zhang, X., Tryk, D.A., 2008. TiO2 photocatalysis and related surface phenomena. Surface Science Reports 63, 515–582. https://doi.org/10.1016/j.surfrep.2008.10.001

Gao, L., Jiang, Y., Ye, K., Deng, B., 2023. A Study on the Effects of Operating Parameters on the Degradation of Oxalic Acid in a Photocatalytic Reactor using Computational Fluid Dynamics. Pollution 9, 579–590. https://doi.org/10.22059/poll.2022.347830.1598

García-Galán, M.J., Garrido, T., Fraile, J., Ginebreda, A., Díaz-Cruz, M.S., Barceló, D., 2010. Simultaneous occurrence of nitrates and sulfonamide antibiotics in two ground water bodies of Catalonia (Spain). Journal of Hydrology, Water Quality and Assessment under Scarcity. Prospects and challenges in Mediterranean watersheds 383, 93–101. https://doi.org/10.1016/j.jhydrol.2009.06.042

Ge, J., Zhang, Y., Heo, Y.-J., Park, S.-J., 2019. Advanced Design and Synthesis of Composite Photocatalysts for the Remediation of Wastewater: A Review. Catalysts 9, 122. https://doi.org/10.3390/catal9020122

Geissen, V., Mol, H., Klumpp, E., Umlauf, G., Nadal, M., Van Der Ploeg, M., Van De Zee, S.E.A.T.M., Ritsema, C.J., 2015. Emerging pollutants in the environment: A challenge for water resource management. International Soil and Water Conservation Research 3, 57–65. https://doi.org/10.1016/j.iswcr.2015.03.002

George, A., Raj, D.M.A., Raj, A.D., Nguyen, B.-S., Phan, T.-P., Pazhanivel, T., Sivashanmugan, K., Josephine, R.L., Irudayaraj, A.A., Arumugam, J., Nguyen, V.-H., 2020. Morphologically tailored CuO nanostructures toward visible-light-driven photocatalysis. Materials Letters 281, 128603. https://doi.org/10.1016/j.matlet.2020.128603

Ghalamchi, L., Rasoulifard, M.H., Mohammadi, Z., Dorraji, M.S.S., Sehati, N., Eskandarian, M.R., 2022. A solar-driven CPC photoreactor for decomposition of emerging contaminants in wastewater: Modeling and optimization. Chemical Engineering Research and Design 182, 580–591. https://doi.org/10.1016/j.cherd.2022.04.032

Goodarzi, N., Ashrafi-Peyman, Z., Khani, E., Moshfegh, A.Z., 2023. Recent Progress on Semiconductor Heterogeneous Photocatalysts in Clean Energy Production and Environmental Remediation. Catalysts 13, 1102. https://doi.org/10.3390/catal13071102

Gordanshekan, A., Arabian, S., Solaimany Nazar, A.R., Farhadian, M., Tangestaninejad, S., 2023. A comprehensive comparison of green Bi2WO6/g-C3N4 and Bi2WO6/TiO2 S-scheme heterojunctions for photocatalytic adsorption/degradation of Cefixime: Artificial neural network, degradation pathway, and toxicity estimation. Chemical Engineering Journal 451, 139067. https://doi.org/10.1016/j.cej.2022.139067

Gorges, R., Meyer, S., Kreisel, G., 2004. Photocatalysis in microreactors. Journal of Photochemistry and Photobiology A: Chemistry 167, 95–99. https://doi.org/10.1016/j.jphotochem.2004.04.004

Grossberg, S., 2013. Recurrent Neural Networks. Scholarpedia 8, 1888. https://doi.org/10.4249/scholarpedia.1888

Guettaï, N., Ait Amar, H., 2005. Photocatalytic oxidation of methyl orange in presence of titanium dioxide in aqueous suspension. Part I: Parametric study. Desalination, Desalination and the Environment 185, 427–437. https://doi.org/10.1016/j.desal.2005.04.048

Gupta, G., Kaur, M., Kansal, S.K., Umar, A., Ibrahim, A.A., 2022. α-Bi2O3 nanosheets: An efficient material for sunlight-driven photocatalytic degradation of Rhodamine B. Ceramics International 48, 29580–29588. https://doi.org/10.1016/j.ceramint.2022.06.210

He, J., Kumar, A., Khan, M., Lo, I.M.C., 2021. Critical review of photocatalytic disinfection of bacteria: from noble metals- and carbon nanomaterials-TiO2 composites to challenges of water characteristics and strategic solutions. Science of The Total Environment 758, 143953. https://doi.org/10.1016/j.scitotenv.2020.143953

Hkiri, K., Mohamed, H.E.A., Harrisankar, N., Gibaud, A., van Steen, E., Maaza, M., 2024. Environmental water treatment with green synthesized WO3 nanoflakes for cationic and anionic dyes removal: Photocatalytic studies. Catalysis Communications 187, 106851. https://doi.org/10.1016/j.catcom.2024.106851

Hodes, G., Kamat, P. V., 2015. Understanding the Implication of Carrier Diffusion Length in Photovoltaic Cells. The Journal of Physical Chemistry Letters 6, 4090–4092. https://doi.org/10.1021/acs.jpclett.5b02052

Hofstadler, K., Bauer, R., Novalic, S., Heisler, G., 1994. New Reactor Design for Photocatalytic Wastewater Treatment with TiO2 Immobilized on Fused-Silica Glass Fibers: Photomineralization of 4-Chlorophenol. Environ. Sci. Technol. 28, 670–674. https://doi.org/10.1021/es00053a021

Hosseini, O., Zare-Shahabadi, V., Ghaedi, M., Azqhandi, M.H.A., 2022. Experimental design, RSM and ANN modeling of tetracycline photocatalytic degradation using LDH@CN. Journal of Environmental Chemical Engineering 10, 108345. https://doi.org/10.1016/j.jece.2022.108345

Jabbar, Z.H., Graimed, B.H., Ammar, S.H., Sabit, D.A., Najim, A.A., Radeef, A.Y., Taher, A.G., 2024. The latest progress in the design and application of semiconductor photocatalysis systems for degradation of environmental pollutants in wastewater: Mechanism insight and theoretical calculations. Materials Science in Semiconductor Processing 173, 108153. https://doi.org/10.1016/j.mssp.2024.108153

Janczarek, M., Kowalska, E., 2021. Computer Simulations of Photocatalytic Reactors. Catalysts 11, 198. https://doi.org/10.3390/catal11020198

Janssens, R., Hainaut, R., Gillard, J., Dailly, H., Luis, P., 2021. Performance of a Slurry Photocatalytic Membrane Reactor for the Treatment of Real Secondary Wastewater Effluent Polluted by Anticancer Drugs. Industrial & Engineering Chemistry Research 60, 2223–2231. https://doi.org/10.1021/acs.iecr.0c04846

Jari, Y., Roche, N., Necibi, M.C., El Hajjaji, S., Dhiba, D., Chehbouni, A., 2022. Emerging Pollutants in Moroccan Wastewater: Occurrence, Impact, and Removal Technologies. Journal of Chemistry 2022. https://doi.org/10.1155/2022/9727857

Jo, W.-K., Tayade, R.J., 2014. New Generation Energy-Efficient Light Source for Photocatalysis: LEDs for Environmental Applications. Industrial & Engineering Chemistry Research 53, 2073–2084. https://doi.org/10.1021/ie404176g

Jones-Lepp, T.L., Alvarez, D.A., 2010. Sampling and analysis of emerging pollutants.

Jorfi, S., Barzegar, G., Ahmadi, M., Darvishi Cheshmeh Soltani, R., alah Jafarzadeh Haghighifard, N., Takdastan, A., Saeedi, R., Abtahi, M., 2016. Enhanced coagulation-photocatalytic treatment of Acid red 73 dye and real textile wastewater using UVA/synthesized MgO nanoparticles. Journal of Environmental Management 177, 111–118. https://doi.org/10.1016/j.jenvman.2016.04.005

Khan, J.A., Sayed, M., Shah, N.S., Khan, S., Khan, A.A., Sultan, M., Tighezza, A.M., Iqbal, J., Boczkaj, G., 2023. Synthesis of N-doped TiO2 nanoparticles with enhanced photocatalytic activity for 2,4-dichlorophenol degradation and H2 production. Journal of Environmental Chemical Engineering 11, 111308. https://doi.org/10.1016/j.jece.2023.111308

Khan, S., Jain, M., Pant, K., Ziora, Z., Blaskovich, M., 2024. Photocatalytic degradation of parabens: A comprehensive meta-analysis investigating the environmental remediation potential of emerging pollutant. The Science of the total environment 920, 171020. https://doi.org/10.1016/j.scitotenv.2024.171020

Khan, S., Naushad, M., Govarthanan, M., Iqbal, J., Alfadul, S.M., 2022. Emerging contaminants of high concern for the environment: Current trends and future research. Environ Res 207, 112609. https://doi.org/10.1016/j.envres.2021.112609

Khasawneh, O.F.S., Palaniandy, P., Ahmadipour, M., Mohammadi, H., Bin Hamdan, M.R., 2021. Removal of acetaminophen using Fe2O3-TiO2 nanocomposites by photocatalysis under simulated solar irradiation: Optimization study. Journal of Environmental Chemical Engineering 9, 104921. https://doi.org/10.1016/j.jece.2020.104921

Khataee, A.R., Fathinia, M., Aber, S., 2010. Kinetic Modeling of Liquid Phase Photocatalysis on Supported TiO2 Nanoparticles in a Rectangular Flat-Plate Photoreactor. Ind. Eng. Chem. Res. 49, 12358–12364. https://doi.org/10.1021/ie101997u

Kuipers, J.A.M., van Swaaij, W.P.M., 1998. Computational Fluid Dynamics Applied To Chemical Reaction Engineering, in: Wei, J. (Ed.), Advances in Chemical Engineering. Academic Press, pp. 227–328.

Kumar, J., Bansal, A., 2016. CFD simulations of immobilized-titanium dioxide based annular photocatalytic reactor: Model development and experimental validation. Indian Journal of Chemical Technology (IJCT) 22, 95–104. https://doi.org/10.56042/ijct.v22i3-4.3145

Kumar, J., Bansal, A., 2013. Photocatalytic degradation in annular reactor: Modelization and optimization using computational fluid dynamics (CFD) and response surface methodology (RSM). Journal of Environmental Chemical Engineering 1, 398–405. https://doi.org/10.1016/j.jece.2013.06.002

Kumari, P., Bahadur, N., Kong, L., O'Dell, L.A., Merenda, A., Dumée, L.F., 2022. Engineering Schottky-like and heterojunction materials for enhanced photocatalysis performance - A review. Materials Advances 3, 2309–2323. https://doi.org/10.1039/d1ma01062j

Lavudya, P., Pant, H., Srikanth, V.V.S.S., Ammanabrolu, R., 2023. Mesoporous and phase pure anatase TiO2 nanospheres for enhanced photocatalysis. Inorganic Chemistry Communications 152, 110699. https://doi.org/10.1016/j.inoche.2023.110699

Leblebici, M.E., Rongé, J., Martens, J., Stefanidis, G., Van Gerven, T., 2015a. Computational modelling of a photocatalytic UV-LED reactor with internal mass and photon transfer consideration. Chemical Engineering Journal 264, 962–970. https://doi.org/10.1016/j.cej.2014.12.013

Leblebici, M.E., Stefanidis, G.D., Van Gerven, T., 2015b. Comparison of photocatalytic space-time yields of 12 reactor designs for wastewater treatment. Chemical Engineering and Processing: Process Intensification 97, 106–111. https://doi.org/10.1016/j.cep.2015.09.009

Lee, C.M., Palaniandy, P., Dahlan, I., 2017. Pharmaceutical residues in aquatic environment and water remediation by TiO2 heterogeneous photocatalysis: a review. Environmental Earth Sciences 76, 611. https://doi.org/10.1007/s12665-017-6924-y

Leong, S., Razmjou, A., Wang, K., Hapgood, K., Zhang, X., Wang, H., 2014. TiO2 based photocatalytic membranes: A review. Journal of Membrane Science 472, 167–184. https://doi.org/10.1016/j.memsci.2014.08.016

Li, D., Xiong, K., Li, W., Yang, Z., Liu, C., Feng, X., Lu, X., 2010. Comparative Study in Liquid-Phase Heterogeneous Photocatalysis: Model for Photoreactor Scale-Up. Industrial & Engineering Chemistry Research 49, 8397–8405. https://doi.org/10.1021/ie100277g

Li, F., Fang, Z., Xu, Z., Xiang, Q., 2024. The confusion about S-scheme electron transfer: critical understanding and a new perspective. Energy & Environmental Science 17, 497–509. https://doi.org/10.1039/D3EE03282E

Li, P., Zhao, T., Zhao, Z., Tang, H., Feng, W., Zhang, Z., 2023. Biochar Derived from Chinese Herb Medicine Residues for Rhodamine B Dye Adsorption. ACS Omega 8, 4813–4825. https://doi.org/10.1021/acsomega.2c06968

Li Puma, G., Brucato, A., 2007. Dimensionless analysis of slurry photocatalytic reactors using two-flux and six-flux radiation absorption–scattering models. Catalysis Today, Materials, Applications and Processes in Photocatalysis 122, 78–90. https://doi.org/10.1016/j.cattod.2007.01.027

Li Puma, G., Machuca-Martínez, F., Mueses, M., Colina-Márquez, J., Bustillo-Lecompte, C., 2020. Scale-Up and Optimization for Slurry Photoreactors., in: Advanced Oxidation Processes - Applications, Trends, and Prospects. IntechOpen. https://doi.org/10.5772/intechopen.91920

Li, Q., Jia, R., Shao, J., He, Y., 2019. Photocatalytic degradation of amoxicillin via TiO2 nanoparticle coupling with a novel submerged porous ceramic membrane reactor. Journal of Cleaner Production 209, 755–761. https://doi.org/10.1016/j.jclepro.2018.10.183

Li, W., Liao, G., Duan, W., Gao, F., Wang, Y., Cui, R., Wang, X., Wang, C., 2024. Synergistically electronic interacted PVDF/CdS/TiO2 organic-inorganic photocatalytic membrane for multi-field driven panel wastewater purification. Applied Catalysis B: Environment and Energy 354, 124108. https://doi.org/10.1016/j.apcatb.2024.124108

Lin, M., Chen, H., Zhang, Z., Wang, X., 2023. Engineering interface structures for heterojunction photocatalysts. Physical Chemistry Chemical Physics 25, 4388–4407. https://doi.org/10.1039/D2CP05281D

Ling, C.M., Mohamed, A.R., Bhatia, S., 2004. Performance of photocatalytic reactors using immobilized TiO2 film for the degradation of phenol and methylene blue dye present in water stream. Chemosphere 57, 547–554. https://doi.org/10.1016/j.chemosphere.2004.07.011

Liu, B., Zhao, X., 2014. Kinetic study of the heterogeneous photocatalysis of porous nanocrystalline TiO2 assemblies using a continuous random walk simulation. Phys. Chem. Chem. Phys. 16, 22343–22351. https://doi.org/10.1039/C4CP02243B

Liu, J., Yang, L., Li, C., Chen, Y., Zhang, Z., 2022. Optimal monolayer WO3 nanosheets/TiO2 heterostructure and its photocatalytic performance under solar light. Chemical Physics Letters 804, 139861. https://doi.org/10.1016/j.cplett.2022.139861

Loeb, S.K., Alvarez, P.J.J., Brame, J.A., Cates, E.L., Choi, W., Crittenden, J., Dionysiou, D.D., Li, Q., Li-Puma, G., Quan, X., Sedlak, D.L., David Waite, T., Westerhoff, P., Kim, J.-H., 2019. The Technology Horizon for Photocatalytic Water Treatment: Sunrise or Sunset? Environmental Science & Technology 53, 2937–2947. https://doi.org/10.1021/acs.est.8b05041

Loubière, K., Oelgemöller, M., Aillet, T., Dechy-Cabaret, O., Prat, L., 2016. Continuous-flow photochemistry: A need for chemical engineering. Chemical Engineering and Processing: Process Intensification 104, 120–132. https://doi.org/10.1016/j.cep.2016.02.008

Low, J., Yu, J., Jaroniec, M., Wageh, S., Al-Ghamdi, A.A., 2017. Heterojunction Photocatalysts. Advanced Materials 29, 1601694. https://doi.org/10.1002/adma.201601694

Luo, M., Chen, Q., Jeong, T., Chen, J., 2017. Numerical modelling of a three-phase internal air-lift circulating photocatalytic reactor. Water Science and Technology 76, 3044–3053. https://doi.org/10.2166/wst.2017.477

Ma, F., Wan, Y., Yuan, G., Meng, L., Dong, Z., Hu, J., 2012. Occurrence and Source of Nitrosamines and Secondary Amines in Groundwater and its Adjacent Jialu River Basin, China. Environmental Science & Technology 46, 3236–3243. https://doi.org/10.1021/es204520b

Mahmoodi, N.M., Keshavarzi, S., Ghezelbash, M., 2017. Synthesis of nanoparticle and modelling of its photocatalytic dye degradation ability from colored wastewater. Journal of Environmental Chemical Engineering 5, 3684–3689. https://doi.org/10.1016/j.jece.2017.07.010

Manassero, A., Satuf, M.L., Alfano, O.M., 2017a. Photocatalytic reactors with suspended and immobilized TiO2: Comparative efficiency evaluation. Chemical Engineering Journal 326, 29–36. https://doi.org/10.1016/j.cej.2017.05.087

Manassero, A., Satuf, M.L., Alfano, O.M., 2017b. Photocatalytic degradation of an emerging pollutant by TiO2-coated glass rings: a kinetic study. Environ Sci Pollut Res 24, 6031–6039. https://doi.org/10.1007/s11356-016-6855-2

Martín-Sómer, M., Pablos, C., van Grieken, R., Marugán, J., 2017. Influence of light distribution on the performance of photocatalytic reactors: LED vs mercury lamps. Applied Catalysis B: Environmental 215, 1–7. https://doi.org/10.1016/j.apcatb.2017.05.048

Matamoros, V., Arias, C., Brix, H., Bayona, J.M., 2009. Preliminary screening of small-scale domestic wastewater treatment systems for removal of pharmaceutical and personal care products. Water Research 43, 55–62. https://doi.org/10.1016/j.watres.2008.10.005

Mehrotra, K., Yablonsky, G.S., Ray, A.K., 2003. Kinetic Studies of Photocatalytic Degradation in a TiO2 Slurry System: Distinguishing Working Regimes and Determining Rate Dependences. Industrial & Engineering Chemistry Research 42, 2273–2281. https://doi.org/10.1021/ie0209881

Méndez-Arriaga, F., Torres-Palma, R.A., Pétrier, C., Esplugas, S., Gimenez, J., Pulgarin, C., 2009. Mineralization enhancement of a recalcitrant pharmaceutical pollutant in water by advanced oxidation hybrid processes. Water Research, AOPs for Effluent Treatment 43, 3984–3991. https://doi.org/10.1016/j.watres.2009.06.059

Mills, A., O'Rourke, C., Moore, K., 2015. Powder semiconductor photocatalysis in aqueous solution: An overview of kinetics-based reaction mechanisms. Journal of Photochemistry and Photobiology A: Chemistry 310, 66–105. https://doi.org/10.1016/j.jphotochem.2015.04.011

Mishra, R.K., Mentha, S.S., Misra, Y., Dwivedi, N., 2023. Emerging pollutants of severe environmental concern in water and wastewater: A comprehensive review on current

developments and future research. Water-Energy Nexus 6, 74–95. https://doi.org/10.1016/j.wen.2023.08.002

Mishra, S., Sundaram, B., 2023. A review of the photocatalysis process used for wastewater treatment. Materials Today: Proceedings. https://doi.org/10.1016/j.matpr.2023.07.147

Modest, M.F., 2013. Radiative Heat Transfer. Academic Press.

Mohd Nasir, S.N.F., Mohamed, N.A., Arzaee, N.A., Mat Teridi, M.A., 2023. Chapter 3 - Engineering of graphitic carbon nitride-based heterojunction photocatalysts, in: Thomas, S., Anas, S., Joy, J. (Eds.), Synthesis, Characterization, and Applications of Graphitic Carbon Nitride. Elsevier, pp. 43–57.

Mohebbi, F., 2018. FOILcom: A fast and robust program for solving two dimensional subsonic (subcritical) inviscid steady compressible flows over isolated airfoils. Unpublished. https://doi.org/10.13140/RG.2.2.36459.64801/1

Mojiri, A., Andasht Kazeroon, R., Gholami, A., 2019. Cross-Linked Magnetic Chitosan/Activated Biochar for Removal of Emerging Micropollutants from Water: Optimization by the Artificial Neural Network. Water 11, 551. https://doi.org/10.3390/w11030551

Molinari, R., Pirillo, F., Falco, M., Loddo, V., Palmisano, L., 2004. Photocatalytic degradation of dyes by using a membrane reactor. Chemical Engineering and Processing: Process Intensification, Special Issue on Membrane Reactors 43, 1103–1114. https://doi.org/10.1016/j.cep.2004.01.008

Monllor-Satoca, D., Gómez, R., González-Hidalgo, M., Salvador, P., 2007. The "Direct–Indirect" model: An alternative kinetic approach in heterogeneous photocatalysis based on the degree of interaction of dissolved pollutant species with the semiconductor surface. Catalysis Today, Selected Contributions of the 4th European Meeting on Solar Chemistry and Photocatalysis: Environmental Applications (SPEA 4) 129, 247–255. https://doi.org/10.1016/j.cattod.2007.08.002

Montenegro-Ayo, R., Pérez, T., Lanza, M.R.V., Brillas, E., Garcia-Segura, S., dos Santos, A.J., 2023. New electrochemical reactor design for emergent pollutants removal by electrochemical oxidation. Electrochimica Acta 458. https://doi.org/10.1016/j.electacta.2023.142551

Moreno-SanSegundo, J., Casado, C., Marugán, J., 2020. Enhanced numerical simulation of photocatalytic reactors with an improved solver for the radiative transfer equation. Chemical Engineering Journal 388, 124183. https://doi.org/10.1016/j.cej.2020.124183

Mozia, S., 2010. Photocatalytic membrane reactors (PMRs) in water and wastewater treatment. A review. Separation and Purification Technology 73, 71–91. https://doi.org/10.1016/j.seppur.2010.03.021

Murali, A., Sarswat, P.K., Free, M.L., 2020. Minimizing electron-hole pair recombination through band-gap engineering in novel ZnO-CeO2-rGO ternary nanocomposite for photoelectrochemical and photocatalytic applications. Environmental Science and Pollution Research 27, 25042–25056. https://doi.org/10.1007/s11356-020-08990-z

Murillo-Sierra, J.C., Hernández-Ramírez, A., Zhao, Z.-Y., Martínez-Hernández, A., Gracia-Pinilla, M.A., 2021. Construction of direct Z-scheme WO3/ZnS heterojunction to enhance the photocatalytic degradation of tetracycline antibiotic. Journal of Environmental Chemical Engineering 9, 105111. https://doi.org/10.1016/j.jece.2021.105111

Navidpour, A.H., Abbasi, S., Li, D., Mojiri, A., Zhou, J.L., 2023. Investigation of Advanced Oxidation Process in the Presence of TiO2 Semiconductor as Photocatalyst: Property, Principle, Kinetic Analysis, and Photocatalytic Activity. Catalysts 13, 232. https://doi.org/10.3390/catal13020232

Nguyen, T.-K.-T., Nguyen, T.-B., Chen, W.-H., Chen, C.-W., Kumar Patel, A., Bui, X.-T., Chen, L., Singhania, R.R., Dong, C.-D., 2023. Phosphoric acid-activated biochar derived from sunflower seed husk: Selective antibiotic adsorption behavior and mechanism. Bioresource Technology 371, 128593. https://doi.org/10.1016/j.biortech.2023.128593

Ojha, V.K., Abraham, A., Snášel, V., 2017. Metaheuristic design of feedforward neural networks: A review of two decades of research. Engineering Applications of Artificial Intelligence 60, 97–116. https://doi.org/10.1016/j.engappai.2017.01.013

Okpara, E.C., Olatunde, O.C., Wojuola, O.B., Onwudiwe, D.C., 2023. Applications of Transition Metal Oxides and Chalcogenides and their Composites in Water Treatment: a review. Environmental Advances 11, 100341. https://doi.org/10.1016/j.envadv.2023.100341

Oladipo, A.A., Vaziri, R., Abureesh, M.A., 2018. Highly robust AgIO3/MIL-53 (Fe) nanohybrid composites for degradation of organophosphorus pesticides in single and binary systems: Application of artificial neural networks modelling. Journal of the Taiwan Institute of Chemical Engineers 83, 133–142. https://doi.org/10.1016/j.jtice.2017.12.013

Olivo Alanís, D.S., 2019. Modeling of the photocatalytic reactor for blue wastewater degradation by a composite based on zinc oxide, green pigments, and phenolic resins. (phd). Universidad Autónoma de Nuevo León.

O'Neal Tugaoen, H., Garcia-Segura, S., Hristovski, K., Westerhoff, P., 2018. Compact light-emitting diode optical fiber immobilized TiO2 reactor for photocatalytic water treatment. Science of The Total Environment 613–614, 1331–1338. https://doi.org/10.1016/j.scitotenv.2017.09.242

Oulton, R.L., Kohn, T., Cwiertny, D.M., 2010. Pharmaceuticals and personal care products in effluent matrices: A survey of transformation and removal during wastewater treatment and implications for wastewater management. Journal of Environmental Monitoring 12, 1956–1978. https://doi.org/10.1039/C0EM00068J

Oyehan, T.A., Liadi, M.A., Alade, I.O., 2019. Modeling the efficiency of TiO2 photocatalytic degradation of MTBE in contaminated water: a support vector regression approach. SN Applied Sciences 1, 386. https://doi.org/10.1007/s42452-019-0417-4

Parsaei, S., Rashid, M., Ghoorchian, A., Dashtian, K., Mowla, D., 2023. Bi-metal-organic framework-derived S-scheme InP/CuO-C heterostructure for robust photocatalytic

degradation of ciprofloxacin in a microfluidic photoreactor. Chemical Engineering Journal 475, 146448. https://doi.org/10.1016/j.cej.2023.146448

Patricia Tcaciuc, A., Borrelli, R., M. Zaninetta, L., M. Gschwend, P., 2018. Passive sampling of DDT, DDE and DDD in sediments: accounting for degradation processes with reaction–diffusion modeling. Environmental Science: Processes & Impacts 20, 220–231. https://doi.org/10.1039/C7EM00501F

Peng, X., Ou, W., Wang, C., Wang, Z., Huang, Q., Jin, J., Tan, J., 2014. Occurrence and ecological potential of pharmaceuticals and personal care products in groundwater and reservoirs in the vicinity of municipal landfills in China. Science of The Total Environment 490, 889–898. https://doi.org/10.1016/j.scitotenv.2014.05.068

Poblete, R., Cortes, E., Pérez, N., Rodríguez, C.A., Luna-Galiano, Y., 2024. Treatment of landfill leachate by combined use of ultrasound and photocatalytic process using fly ash as catalyst. Journal of Environmental Management 349, 119552. https://doi.org/10.1016/j.jenvman.2023.119552

Qarajehdaghi, M., Mehrizad, A., Gharbani, P., Shahverdizadeh, G.H., 2023. Quaternary composite of CdS/g-C3N4/rGO/CMC as a susceptible visible-light photocatalyst for effective abatement of ciprofloxacin: Optimization and modeling of the process by RSM and ANN. Process Safety and Environmental Protection 169, 352–362. https://doi.org/10.1016/j.psep.2022.11.030

Qi, N., Zhang, H., Jin, B., Zhang, K., 2011. CFD modelling of hydrodynamics and degradation kinetics in an annular slurry photocatalytic reactor for wastewater treatment. Chemical Engineering Journal 172, 84–95. https://doi.org/10.1016/j.cej.2011.05.068

Qureshi, W.A., Ali, R.N., Haider, S.N.-U.-Z., Ahmad, N., Khan, M.U., Wang, L., Cheng, C., Rao, S., Ali, A., Liu, Q.Q., Yang, J., 2024. Construction of B doped g-C3N4/Ni-MOF-74 porous heterojunction with boosted carrier separation for photocatalytic H2 generation. Materials Today Sustainability 25, 100679. https://doi.org/10.1016/j.mtsust.2024.100679

Rajabi, S., Derakhshan, Z., Nasiri, A., Feilizadeh, M., Mohammadpour, A., Salmani, M., Kochaki, S.H., Shouhanian, H., Hashemi, H., 2024. Synergistic degradation of metronidazole and penicillin G in aqueous solutions using AgZnFe2O4@chitosan nano-photocatalyst under UV/persulfate activation. Environmental Technology & Innovation 35, 103724. https://doi.org/10.1016/j.eti.2024.103724

Rasul, M.G., Ahmed, S., Sattar, M.A., Jahirul, M.I., 2023. Hydrodynamic performance assessment of photocatalytic reactor with baffles and roughness in the flow path: A modelling approach with experimental validation. Heliyon 9, e19623. https://doi.org/10.1016/j.heliyon.2023.e19623

Rathi, B.S., Kumar, P.S., 2021. Application of adsorption process for effective removal of emerging contaminants from water and wastewater. Environ Pollut 280, 116995. https://doi.org/10.1016/j.envpol.2021.116995

Ratshiedana, R., Fakayode, O.J., Mishra, A.K., Kuvarega, A.T., 2021. Visible-light photocatalytic degradation of tartrazine using hydrothermal synthesized Ag-doped TiO2

nanoparticles. Journal of Water Process Engineering 44, 102372. https://doi.org/10.1016/j.jwpe.2021.102372

Reddy, P.A.K., Reddy, P.V.L., Kwon, E., Kim, K.-H., Akter, T., Kalagara, S., 2016. Recent advances in photocatalytic treatment of pollutants in aqueous media. Environment International 91, 94–103. https://doi.org/10.1016/j.envint.2016.02.012

Rengifo-Herrera, J.A., Pulgarin, C., 2023. Why five decades of massive research on heterogeneous photocatalysis, especially on TiO2, has not yet driven to water disinfection and detoxification applications? Critical review of drawbacks and challenges. Chemical Engineering Journal 477, 146875. https://doi.org/10.1016/j.cej.2023.146875

Richardson, S.D., Ternes, T.A., 2014. Water Analysis: Emerging Contaminants and Current Issues. Anal. Chem. 86, 2813–2848. https://doi.org/10.1021/ac500508t

Rueda-Marquez, J.J., Levchuk, I., Fernández Ibañez, P., Sillanpää, M., 2020. A critical review on application of photocatalysis for toxicity reduction of real wastewaters. Journal of Cleaner Production 258, 120694. https://doi.org/10.1016/j.jclepro.2020.120694

Sabzehmeidani, M.M., Karimi, H., Ghaedi, M., 2023. Degradation of binary mixtures of dyes by step-scheme quaternary photocatalyst in continuous flow-loop ultrasound assisted micro-photoreactor. Journal of Molecular Liquids 388, 122830. https://doi.org/10.1016/j.molliq.2023.122830

Sacco, O., Sannino, D., Vaiano, V., 2019. Packed Bed Photoreactor for the Removal of Water Pollutants Using Visible Light Emitting Diodes. Applied Sciences 9, 472. https://doi.org/10.3390/app9030472

Sacco, O., Vaiano, V., Sannino, D., 2020. Main parameters influencing the design of photocatalytic reactors for wastewater treatment: a mini review. Journal of Chemical Technology & Biotechnology 95, 2608–2618. https://doi.org/10.1002/jctb.6488

Saeed, M., Muneer, M., Haq, A. ul, Akram, N., 2022. Photocatalysis: an effective tool for photodegradation of dyes—a review. Environmental Science and Pollution Research 29, 293–311. https://doi.org/10.1007/s11356-021-16389-7

Sahay, P., Mohite, D., Arya, S., Dalmia, K., Khan, Z., Kumar, A., 2023. Removal of the emergent pollutants (hormones and antibiotics) from wastewater using different kinds of biosorbent—a review. emergent mater. 6, 373–404. https://doi.org/10.1007/s42247-023-00460-9

Salahshoori, I., Yazdanbakhsh, A., Baghban, A., 2024. Machine learning-powered estimation of malachite green photocatalytic degradation with NML-BiFeO3 composites. Sci Rep 14, 8676. https://doi.org/10.1038/s41598-024-58976-x

Salmanzadeh-Jamadi, Z., Habibi-Yangjeh, A., Feizpoor, S., Pourbasheer, E., Chand, H., Krishnan, V., Wang, C., Xie, J., Zhong, Y., 2022. Novel visible-light TiO2/Bi3O4Br photocatalysts with n-n heterojunction: Highly impressive performance for elimination of tetracycline and dye contaminants. Optical Materials 123, 111831. https://doi.org/10.1016/j.optmat.2021.111831

San, N., Hatipoğlu, A., Koçtürk, G., Çınar, Z., 2001. Prediction of primary intermediates and the photodegradation kinetics of 3-aminophenol in aqueous TiO2 suspensions. Journal of Photochemistry and Photobiology A: Chemistry 139, 225–232. https://doi.org/10.1016/S1010-6030(01)00368-9

Saroha, J., Rani, E., Devi, M., Pathi, P., Kumar, M., Sharma, S.N., 2023. Plasmon-assisted photocatalysis of organic pollutants by Au/Ag–TiO2 nanocomposites: a comparative study. Materials Today Sustainability 23, 100466. https://doi.org/10.1016/j.mtsust.2023.100466

Sellappan, R., Nielsen, M.G., González-Posada, F., Vesborg, P.C.K., Chorkendorff, I., Chakarov, D., 2013. Effects of plasmon excitation on photocatalytic activity of Ag/TiO2 and Au/TiO2 nanocomposites. Journal of Catalysis 307, 214–221. https://doi.org/10.1016/j.jcat.2013.07.024

Sewnet, A., Abebe, M., Asaithambi, P., Alemayehu, E., 2022. Visible-Light-Driven g-C3N4/TiO2 Based Heterojunction Nanocomposites for Photocatalytic Degradation of Organic Dyes in Wastewater: A Review. Air, Soil and Water Research 15, 11786221221117266. https://doi.org/10.1177/11786221221117266

Shang, Q., Liu, X., Zhang, M., Zhang, P., Ling, Y., Cui, G., Liu, W., Shi, X., Yue, J., Tang, B., 2022. Photocatalytic degradation of ofloxacin antibiotic wastewater using TS-1/C3N4 composite photocatalyst: Reaction performance optimisation and estimation of wastewater component synergistic effect by artificial neural network and genetic algorithm. Chemical Engineering Journal 443, 136354. https://doi.org/10.1016/j.cej.2022.136354

Sun, X., Cao, W., Shan, X., Liu, Y., Zhang, W., 2024. A generalized framework for integrating machine learning into computational fluid dynamics. Journal of Computational Science 82, 102404. https://doi.org/10.1016/j.jocs.2024.102404

Sundar, K.P., Kanmani, S., 2020. Progression of Photocatalytic reactors and it's comparison: A Review. Chemical Engineering Research and Design 154, 135–150. https://doi.org/10.1016/j.cherd.2019.11.035

Szymański, K., Grzechulska-Damszel, J., Mozia, S., 2024. Application of a submerged photocatalytic membrane reactor with ultrafiltration membrane for ketoprofen removal during long term process: Impact of feed matrix. Journal of Water Process Engineering 59, 104953. https://doi.org/10.1016/j.jwpe.2024.104953

Taheran, M., Naghdi, M., Brar, S.K., Verma, M., Surampalli, R.Y., 2018. Emerging contaminants: Here today, there tomorrow! Environmental Nanotechnology, Monitoring & Management 10, 122–126. https://doi.org/10.1016/j.enmm.2018.05.010

Tahir, M., Tasleem, S., Tahir, B., 2020. Recent development in band engineering of binary semiconductor materials for solar driven photocatalytic hydrogen production. International Journal of Hydrogen Energy 45, 15985–16038. https://doi.org/10.1016/j.ijhydene.2020.04.071

Tanos, F., Makhoul, E., Nada, A.A., Bekheet, M.F., Riedel, W., Kawrani, S., Belaid, H., Petit, E., Viter, R., Fedorenko, V., Ramanavicius, A., Boulos, M., Cornu, D., Razzouk, A., Lesage, G., Cretin, M., Bechelany, M., 2024. Graphene oxide-induced CuO reduction in TiO2/CaTiO3/Cu2O/Cu composites for photocatalytic degradation of drugs via peroxymonosulfate activation. Applied Surface Science 656, 159698. https://doi.org/10.1016/j.apsusc.2024.159698

Tong, H., Ouyang, S., Bi, Y., Umezawa, N., Oshikiri, M., Ye, J., 2012. Nano-photocatalytic Materials: Possibilities and Challenges. Advanced Materials 24, 229–251. https://doi.org/10.1002/adma.201102752

Tong, K., Yang, L., Du, X., Yang, Y., 2020. Review of modeling and simulation strategies for unstructured packing bed photoreactors with CFD method. Renewable and Sustainable Energy Reviews 131, 109986. https://doi.org/10.1016/j.rser.2020.109986

Tseng, D.-H., Juang, L.-C., Huang, H.-H., 2012. Effect of Oxygen and Hydrogen Peroxide on the Photocatalytic Degradation of Monochlorobenzene in TiO2 Aqueous Suspension. International Journal of Photoenergy 2012, e328526. https://doi.org/10.1155/2012/328526

Turchi, C.S., Ollis, D.F., 1990. Photocatalytic degradation of organic water contaminants: Mechanisms involving hydroxyl radical attack. Journal of Catalysis 122, 178–192. https://doi.org/10.1016/0021-9517(90)90269-P

Turolla, A., Santoro, D., de Bruyn, J.R., Crapulli, F., Antonelli, M., 2016. Nanoparticle scattering characterization and mechanistic modelling of UV–TiO2 photocatalytic reactors using computational fluid dynamics. Water Research 88, 117–126. https://doi.org/10.1016/j.watres.2015.09.039

US EPA, O., 2014. Drinking Water Contaminant Candidate List (CCL) and Regulatory Determination [WWW Document].

Vaez, M., Omidkhah, M., Alijani, S., Zarringhalam Moghaddam, A., Sadrameli, M., Gholipour Zanjani, N., 2015. Evaluation of photocatalytic activity of immobilized titania nanoparticles by support vector machine and artificial neural network. The Canadian Journal of Chemical Engineering 93, 1009–1016. https://doi.org/10.1002/cjce.22171

Valadés-Pelayo, P.J., Guayaquil Sosa, F., Serrano, B., de Lasa, H., 2015. Photocatalytic reactor under different external irradiance conditions: Validation of a fully predictive radiation absorption model. Chemical Engineering Science 126, 42–54. https://doi.org/10.1016/j.ces.2014.12.003

Vargas, R., Carvajal, D., Madriz, L., Scharifker, B.R., 2020. Chemical kinetics in solar to chemical energy conversion: The photoelectrochemical oxygen transfer reaction. Energy Reports 6, 2–12. https://doi.org/10.1016/j.egyr.2019.10.004

Vasilachi, I.C., Asiminicesei, D.M., Fertu, D.I., Gavrilescu, M., 2021. Occurrence and Fate of Emerging Pollutants in Water Environment and Options for Their Removal. Water 13, 181. https://doi.org/10.3390/w13020181

Vasseghian, Y., Berkani, M., Almomani, F., Dragoi, E.-N., 2021. Data mining for pesticide decontamination using heterogeneous photocatalytic processes. Chemosphere 270, 129449. https://doi.org/10.1016/j.chemosphere.2020.129449

Verlicchi, P., Galletti, A., Petrovic, M., Barceló, D., 2010. Hospital effluents as a source of emerging pollutants: An overview of micropollutants and sustainable treatment options. Journal of Hydrology 389, 416–428. https://doi.org/10.1016/j.jhydrol.2010.06.005

Visan, A., van Ommen, J.R., Kreutzer, M.T., Lammertink, R.G.H., 2019. Photocatalytic Reactor Design: Guidelines for Kinetic Investigation. Ind. Eng. Chem. Res. 58, 5349–5357. https://doi.org/10.1021/acs.iecr.9b00381

Wang, D., Mueses, M.A., Márquez, J.A.C., Machuca-Martínez, F., Grčić, I., Peralta Muniz Moreira, R., Li Puma, G., 2021. Engineering and modeling perspectives on photocatalytic reactors for water treatment. Water Research 202, 117421. https://doi.org/10.1016/j.watres.2021.117421

Wang, D., Ren, B., Chen, S., Liu, S., Feng, W., Sun, Y., 2023. Novel BiVO4/TiO2 composites with Z-scheme heterojunction for photocatalytic degradation. Materials Letters 330, 133229. https://doi.org/10.1016/j.matlet.2022.133229

Wang, H., Li, X., Zhao, X., Li, C., Song, X., Zhang, P., Huo, P., Li, X., 2022. A review on heterogeneous photocatalysis for environmental remediation: From semiconductors to modification strategies. Chinese Journal of Catalysis 43, 178–214. https://doi.org/10.1016/S1872-2067(21)63910-4

Wang, H., Zhang, N., Cheng, G., Guo, H., Shen, Z., Yang, L., Zhao, Y., Alsaedi, A., Hayat, T., Wang, X., 2020. Preparing a photocatalytic Fe doped TiO2/rGO for enhanced bisphenol A and its analogues degradation in water sample. Applied Surface Science 505, 144640. https://doi.org/10.1016/j.apsusc.2019.144640

Wang, L., Zhang, J., Cheng, D., Guo, W., Cao, X., Xue, J., Haris, M., Ye, Y., Ngo, H.H., 2024. Biochar-based functional materials for the abatement of emerging pollutants from aquatic matrices. Environ Res 252, 119052. https://doi.org/10.1016/j.envres.2024.119052

Ward, R., Wu, X., Bottou, L., 2020. AdaGrad stepsizes: Sharp convergence over nonconvex landscapes. Journal of Machine Learning Research 21, 1–30.

Weerathunga, H., Tang, C., Brock, A.J., Sarina, S., Wang, T., Liu, Q., Zhu, H.-Y., Du, A., Waclawik, E.R., 2022. Nanostructure Shape-Effects in ZnO heterogeneous photocatalysis. Journal of Colloid and Interface Science 606, 588–599. https://doi.org/10.1016/j.jcis.2021.08.052

WHO, 2011. World health statistics. WHO.

Wu, H., Meng, S., Zhang, J., Zheng, X., Wang, Y., Chen, S., Qi, G., Fu, X., 2020. Construction of two-dimensionally relative p-n heterojunction for efficient photocatalytic redox reactions under visible light. Applied Surface Science 505, 144638. https://doi.org/10.1016/j.apsusc.2019.144638

Xinchen, W., Masakazu, A., Xianzhi, F., 2020. Current Developments in Photocatalysis and Photocatalytic Materials. New Horizons in Photocatalysis, Elesevier. ed.

Xu, H., Li, M., Wang, J.K., 2012. Photocatalytic Degradation of Methylene Blue Using Nano-ZnO at Air Lift Circulating Reactor. Advanced Materials Research 476–478, 1910–1914. https://doi.org/10.4028/www.scientific.net/AMR.476-478.1910

Yang, Y., Khan, Hamayun, Gao, S., Khalil, A.K., Ali, N., Khan, A., Show, P.L., Bilal, M., Khan, Hammad, 2022. Fabrication, characterization, and photocatalytic degradation potential of chitosan-conjugated manganese magnetic nano-biocomposite for emerging dye pollutants. Chemosphere 306, 135647. https://doi.org/10.1016/j.chemosphere.2022.135647

Yang, Y., Yang, X., Jia, Q., Zheng, S., Lin, Z., Qin, Z., 2023. Enhanced photocatalytic performance of (N, F) co-doped TiO2 loaded on coal-based hierarchical porous carbon foam under simulated sunlight. Vacuum 207, 111577. https://doi.org/10.1016/j.vacuum.2022.111577

Ye, Z., Yang, J., Zhong, N., Tu, X., Jia, J., Wang, J., 2020. Tackling environmental challenges in pollution controls using artificial intelligence: A review. Science of The Total Environment 699, 134279. https://doi.org/10.1016/j.scitotenv.2019.134279

Yeoh, G.H., Tu, J., 2019. Computational Techniques for Multiphase Flows. Elsevier Science.

Yu, Y., Wang, Z., Yao, B., Zhou, Y., 2024. Occurrence, bioaccumulation, fate, and risk assessment of emerging pollutants in aquatic environments: A review. Science of The Total Environment 923, 171388. https://doi.org/10.1016/j.scitotenv.2024.171388

Yuan, L., Yan, P., Wang, P., Li, L., Xiao, X., Xie, Y., 2024. Constructing stable type-II NaLiTi3O7/La2S3 heterojunctions for efficient photocatalytic charge separation and hydrogen production. International Journal of Hydrogen Energy 64, 958–964. https://doi.org/10.1016/j.ijhydene.2024.03.300

Yusuf, A., Oladipo, H., Yildiz Ozer, L., Garlisi, C., Loddo, V., Abu-Zahra, M.R.M., Palmisano, G., 2020. Modelling of a recirculating photocatalytic microreactor implementing mesoporous N-TiO2 modified with graphene. Chemical Engineering Journal 391, 123574. https://doi.org/10.1016/j.cej.2019.123574

Yusuf, A., Palmisano, G., 2021. Three-dimensional CFD modelling of a photocatalytic parallel-channel microreactor. Chemical Engineering Science 229, 116051. https://doi.org/10.1016/j.ces.2020.116051

Zamani, S., Rahimi, M.R., Ghaedi, M., 2022. Spinning disc photoreactor based visible-light-driven Ag/Ag2O/TiO2 heterojunction photocatalyst film toward the degradation of amoxicillin. Journal of Environmental Management 303, 114216. https://doi.org/10.1016/j.jenvman.2021.114216

Zhang, C., Li, Y., Shen, H., Shuai, D., 2021. Simultaneous coupling of photocatalytic and biological processes: A promising synergistic alternative for enhancing decontamination of recalcitrant compounds in water. Chemical Engineering Journal 403, 126365. https://doi.org/10.1016/j.cej.2020.126365

Zhang, H., Wan, Y., Luo, J., Darling, S.B., 2021. Drawing on Membrane Photocatalysis for Fouling Mitigation. ACS Applied Materials & Interfaces 13, 14844–14865. https://doi.org/10.1021/acsami.1c01131

Zhang, L., Qin, M., Yu, W., Zhang, Q., Xie, H., Sun, Z., Shao, Q., Guo, X., Hao, L., Zheng, Y., Guo, Z., 2017. Heterostructured TiO2/WO3 Nanocomposites for Photocatalytic Degradation of Toluene under Visible Light. Journal of The Electrochemical Society 164, H1086. https://doi.org/10.1149/2.0881714jes

Zhang, Y., Zhao, Y.-G., Maqbool, F., Hu, Y., 2022. Removal of antibiotics pollutants in wastewater by UV-based advanced oxidation processes: Influence of water matrix components, processes optimization and application: A review. Journal of Water Process Engineering 45, 102496. https://doi.org/10.1016/j.jwpe.2021.102496

Zhang, Z., Anderson, W.A., Moo-Young, M., 2004. Experimental analysis of a corrugated plate photocatalytic reactor. Chemical Engineering Journal 99, 145–152. https://doi.org/10.1016/j.cej.2004.01.001

Zhao, D., Zhou, W., Shen, L., Li, B., Sun, H., Qianqian, Z., Tang, C., Lin, H., Chung, T.-S., 2024. New directions on membranes for removal and degradation of emerging pollutants in aqueous systems. Water Res. 251, 121111. https://doi.org/10.1016/j.watres.2024.121111

Zhao, L., Deng, J., Sun, P., Liu, J., Ji, Y., Nakada, N., Qiao, Z., Tanaka, H., Yang, Y., 2018. Nanomaterials for treating emerging contaminants in water by adsorption and photocatalysis: Systematic review and bibliometric analysis. Science of the Total Environment 627, 1253–1263. https://doi.org/10.1016/j.scitotenv.2018.02.006

Zhao, W., Feng, Y., Huang, H., Zhou, P., Li, J., Zhang, L., Dai, B., Xu, J., Zhu, F., Sheng, N., Leung, D.Y.C., 2019. A novel Z-scheme Ag3VO4/BiVO4 heterojunction photocatalyst: Study on the excellent photocatalytic performance and photocatalytic mechanism. Applied Catalysis B: Environmental 245, 448–458. https://doi.org/10.1016/j.apcatb.2019.01.001

Zhao, Y., Zhang, S., Shi, R., Waterhouse, G.I.N., Tang, J., Zhang, T., 2020. Two-dimensional photocatalyst design: A critical review of recent experimental and computational advances. Materials Today 34, 78–91. https://doi.org/10.1016/j.mattod.2019.10.022

Zheng, Q., Aiello, A., Choi, Y.S., Tarr, K., Shen, H., Durkin, D.P., Shuai, D., 2020. 3D printed photoreactor with immobilized graphitic carbon nitride: A sustainable platform for solar water purification. Journal of Hazardous Materials 399, 123097. https://doi.org/10.1016/j.jhazmat.2020.123097

Zheng, Q., Tian, X., Jiang, N., Yang, M., 2019. Layer-wise learning based stochastic gradient descent method for the optimization of deep convolutional neural network. Journal of Intelligent & Fuzzy Systems 37, 5641–5654. https://doi.org/10.3233/JIFS-190861

Zhou, Chengzhuang, Wang, Q., Zhou, Chengyun, 2020. Photocatalytic degradation of antibiotics by molecular assembly porous carbon nitride: Activity studies and artificial neural

networks modeling. Chemical Physics Letters 750, 137479. https://doi.org/10.1016/j.cplett.2020.137479

Zhu, R., Che, S., Liu, X., Lin, S., Xu, G., Ouyang, F., 2014. A novel fluidized-bed-optical-fibers photocatalytic reactor (FBOFPR) and its performance. Applied Catalysis A: General 471, 136–141. https://doi.org/10.1016/j.apcata.2013.11.044

Zulfiqar, M., Samsudin, M.F.R., Sufian, S., 2019. Modelling and optimization of photocatalytic degradation of phenol via TiO2 nanoparticles: An insight into response surface methodology and artificial neural network. Journal of Photochemistry and Photobiology A: Chemistry 384, 112039. https://doi.org/10.1016/j.jphotochem.2019.112039

List of figures

bed photocatalytic reactor; (d) parallel-plate disk photoreactor; (e) flat-plate photoreactor; and (f) flat-plate photocatalytic reactor filled with structured catalyst (Sacco et al., 2020).

Fig. 9. Typical structure of an ANN.

Fig. 10. Optimized ANN topology obtained by Yang et al. (2022).

Fig. 11. ANN model prediction versus experimental values for train, test, and validation data sets (Ghalamchi et al., 2022).

Fig. 12. MSE of the designed networks as a function of the number of hidden neurons (a) and the relative importance of operational parameters on the CIP removal efficiency (b).

Fig. 13. Schematic description of the modeling of heterogeneous photocatalytic reactions in a CFD environment.

Fig. 14. (a) Schematic description of the physical processes involved in light transfer. (b) Geometrical description of the RTE parameters.

Fig. 15. (a) Schematic light distribution in an internal illumination reactor based on a 1D model. (b) Principle of the two-flux (TFM), four-flux (FFM), and six-flux (SFM) models.

Fig. 16. Examples of photoreactors designs: (a) internal-loop airlift reactor with a draft tube and a suspended photocatalyst; immobilized photocatalyst in parallel plate (b), annular with external irradiation (c), and annular with internal irradiation (d) photoreactors.

List of tables

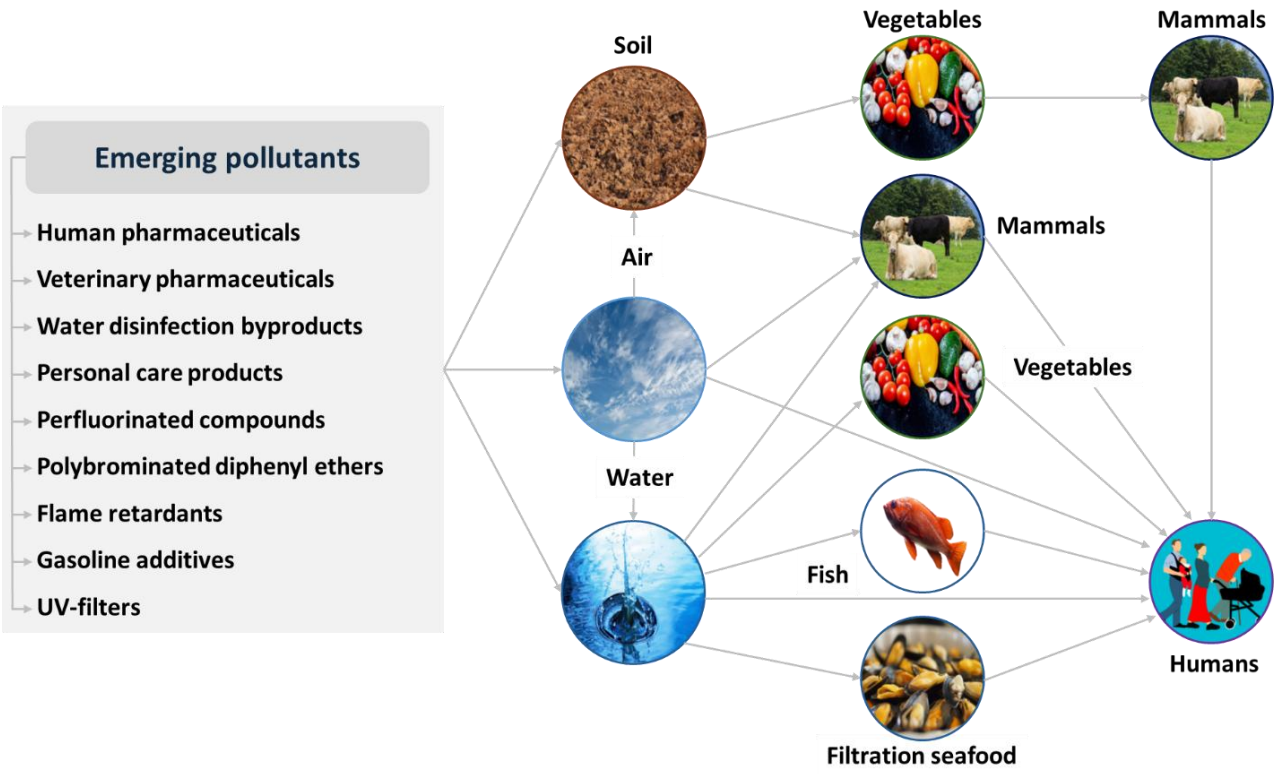

Fig. 1. Illustrative diagram of the fate of EPs along the food chain (adapted from (Díez et al. (2023)).

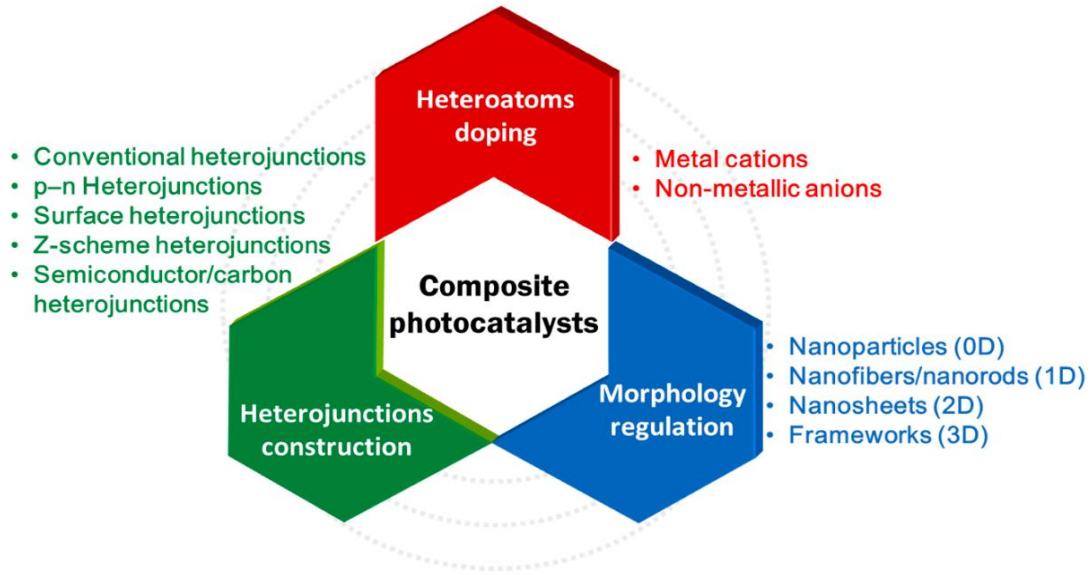

Fig. 2. The design and synthesis techniques for composite photocatalysts (Ge et al., 2019).

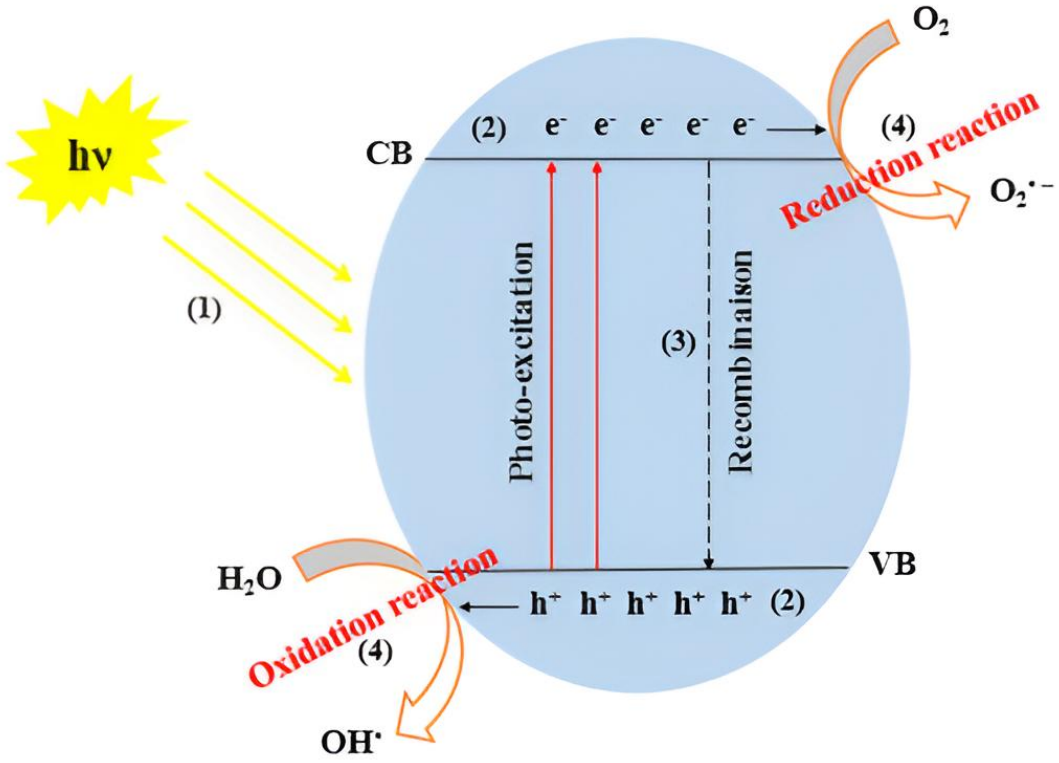

Fig. 3. Schematic illustration of the mechanism of a semiconductor photocatalytic process.

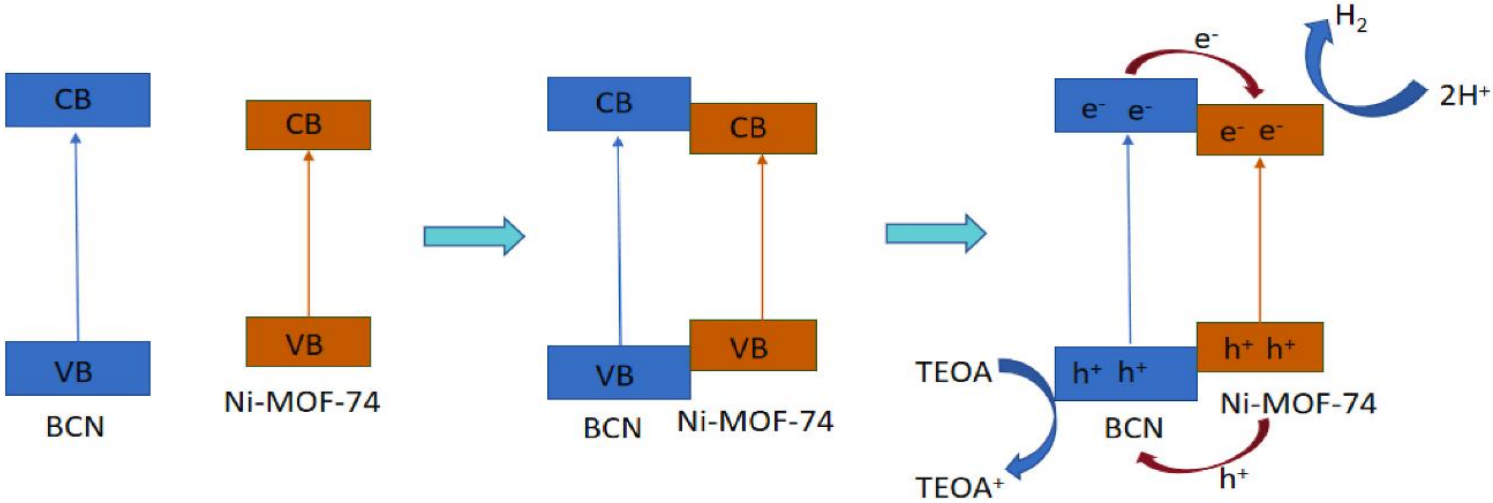

BCN: Boron-doped g-C_3N_4 composite.
MOF: Metal-organic frameworks.
TEOA: Triethanolamine

Fig. 4. Type-I heterojunction mechanism over BCN-NM-3 composite (Qureshi et al., 2024).

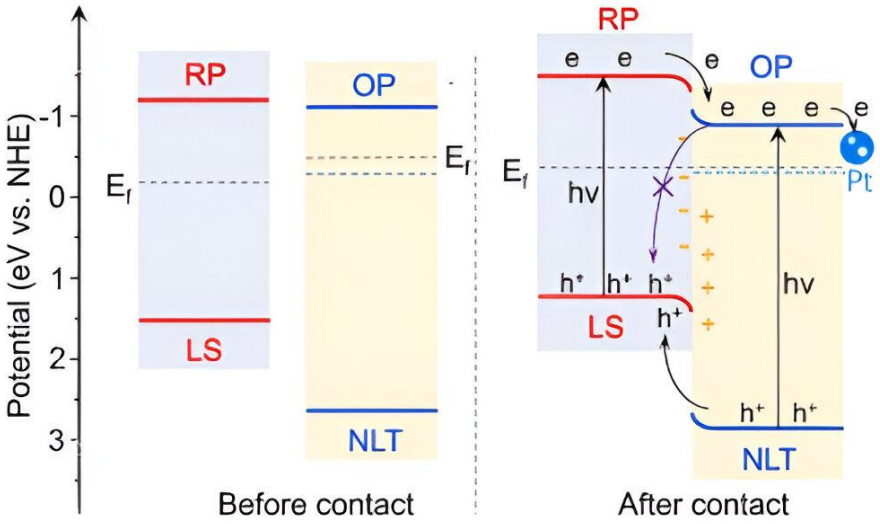

RP: The reductive photocatalyst
OP: Oxidative photocatalyst
LS: La_2S_3 semiconductors
NLT: $NaLiTi_3O_7$

Fig. 5. Charge transfer mechanisms. RP and OP represent the reductive photocatalyst and oxidative photocatalyst (Yuan et al., 2024).

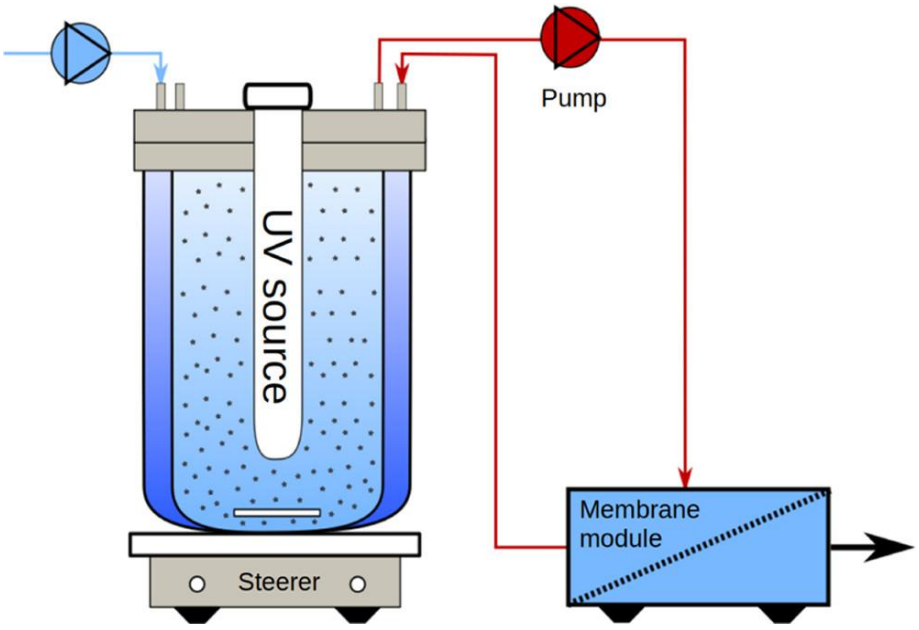

Fig. 6. Slurry photoreactor with membrane module (Janssens et al., 2021).

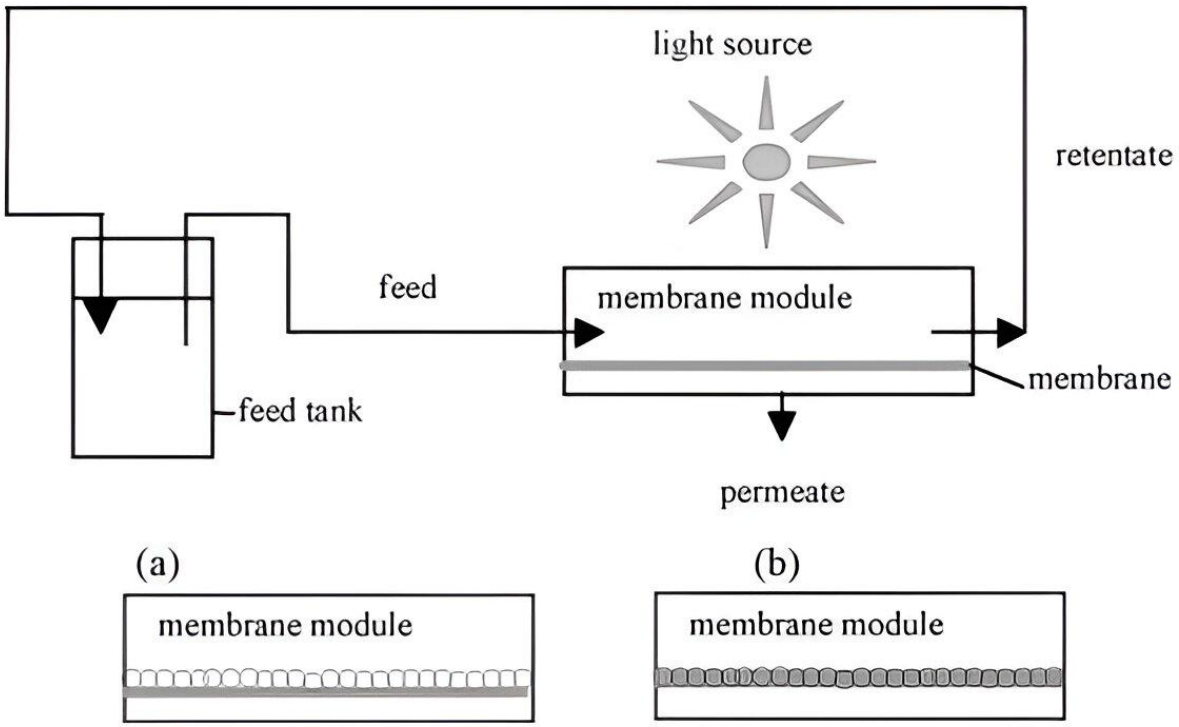

Fig. 7. Photocatalytic membrane reactor with immobilized photocatalyst (a) on membrane and (b) within a membrane structure (Mozia, 2010).

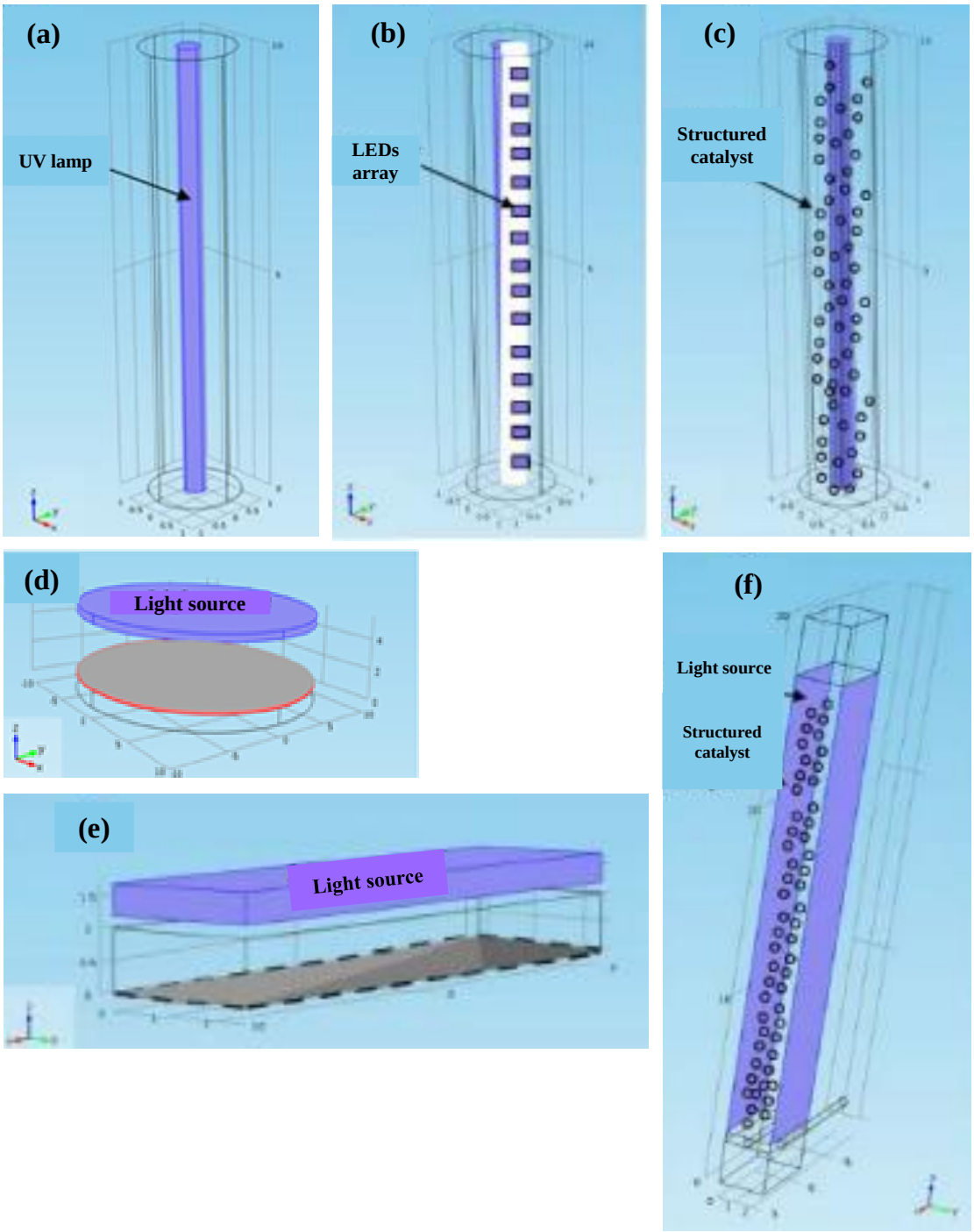

Fig. 8. Different photoreactor geometries: (a) annular geometry irradiated using a central lamp; (b) annular geometry irradiated using central light emitting diodes (LEDs); (c) annular packed-bed photocatalytic reactor; (d) parallel-plate disk photoreactor; (e) flat-plate photoreactor; and (f) flat-plate photocatalytic reactor filled with structured catalyst (Sacco et al., 2020).

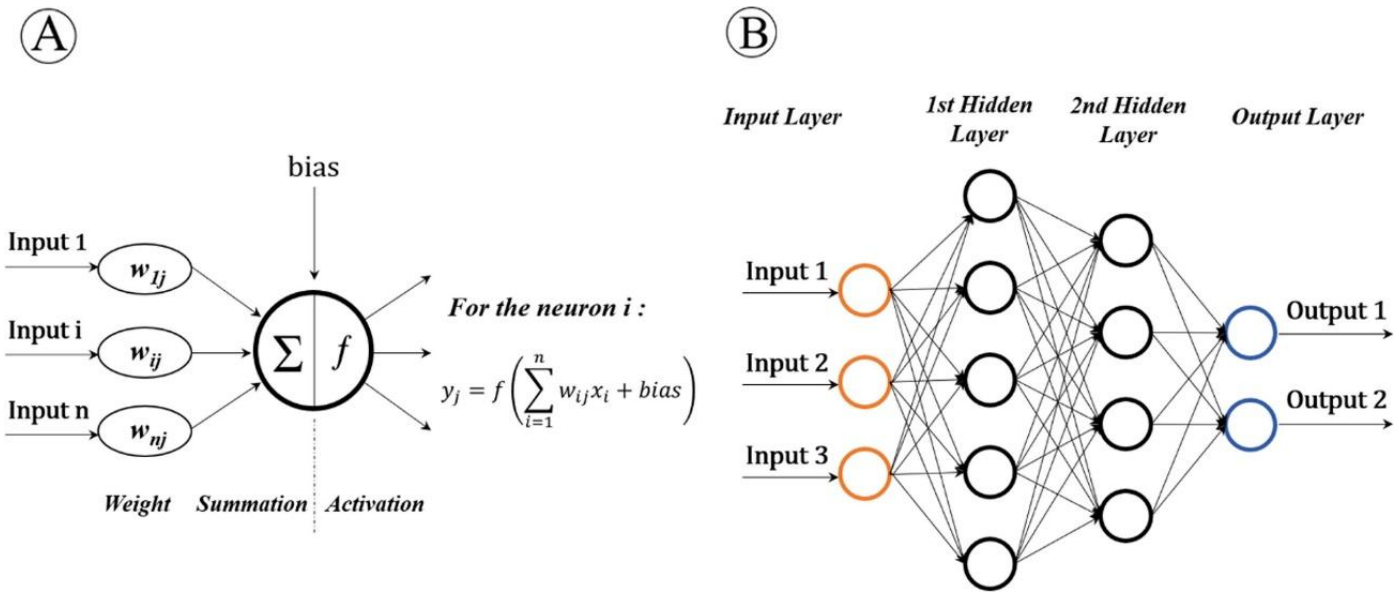

Fig. 9. Typical structure of an ANN *(Ye et al., 2020)*.

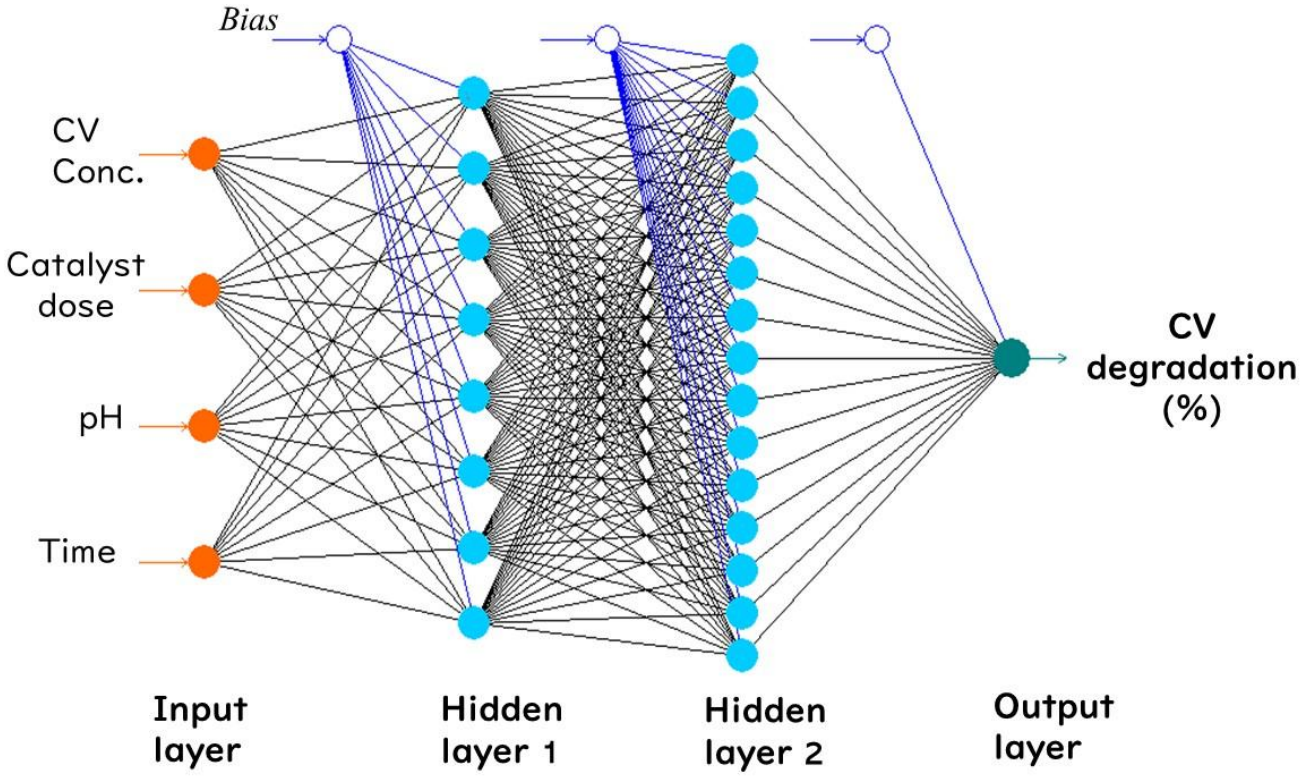

Fig. 10. Optimized ANN topology obtained by Yang et al. (Yang et al., 2022).

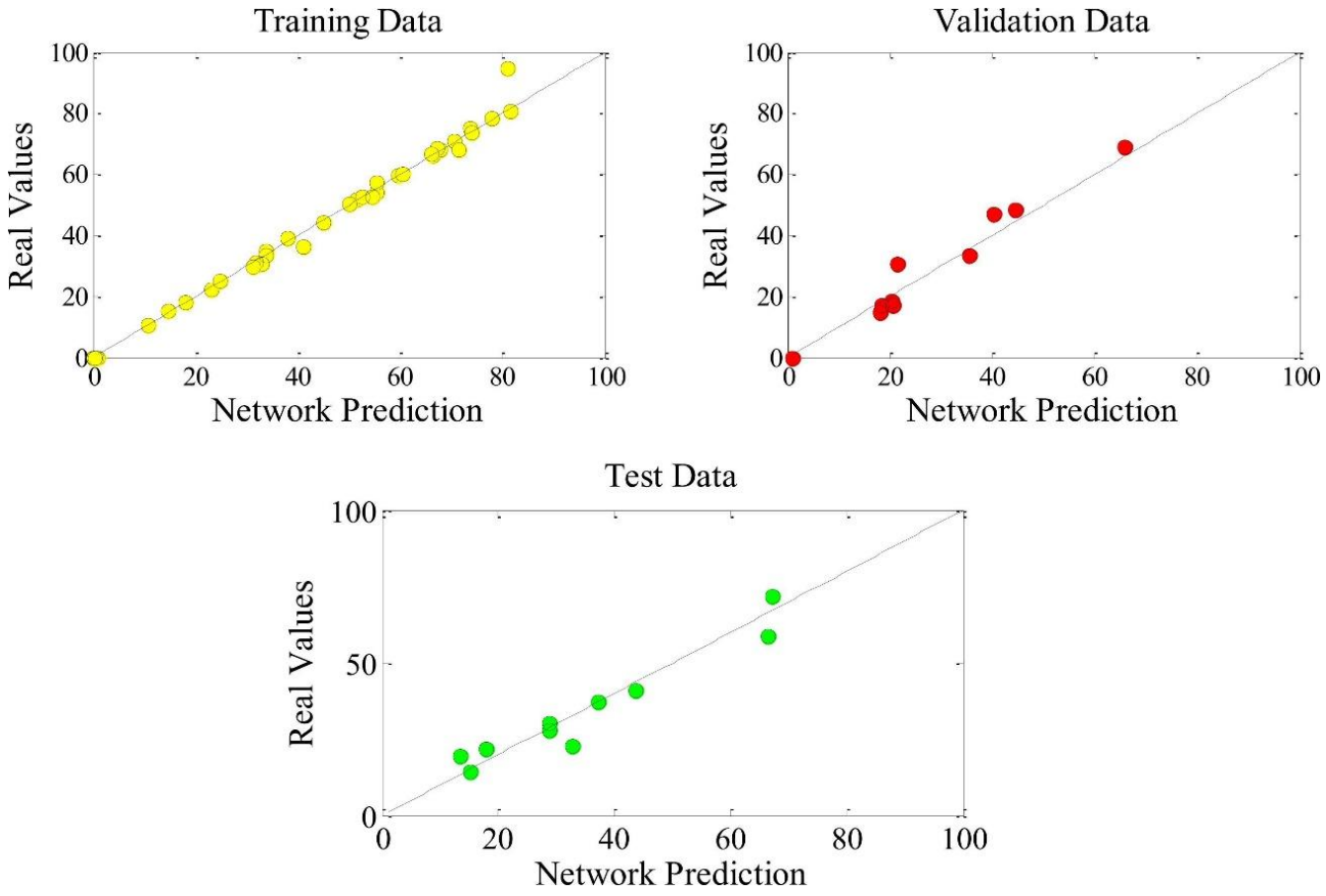

Fig. 11. ANN model prediction versus experimental values for train, test, and validation data sets (Ghalamchi et al., 2022).

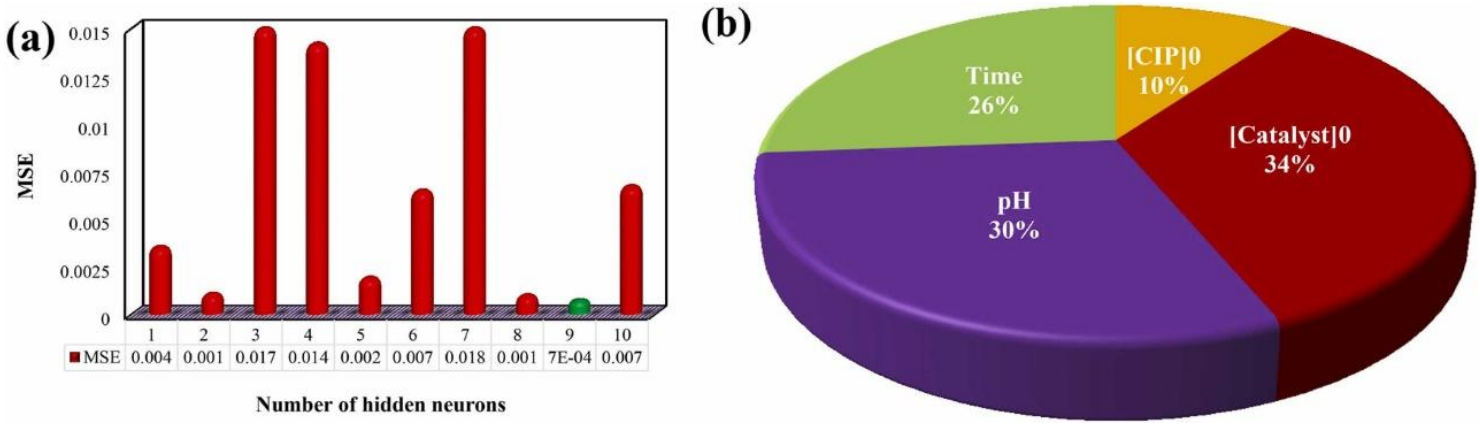

Fig. 12. MSE of the designed networks as a function of the number of hidden neurons (a) and the relative importance of operational parameters on the CIP removal efficiency (b).

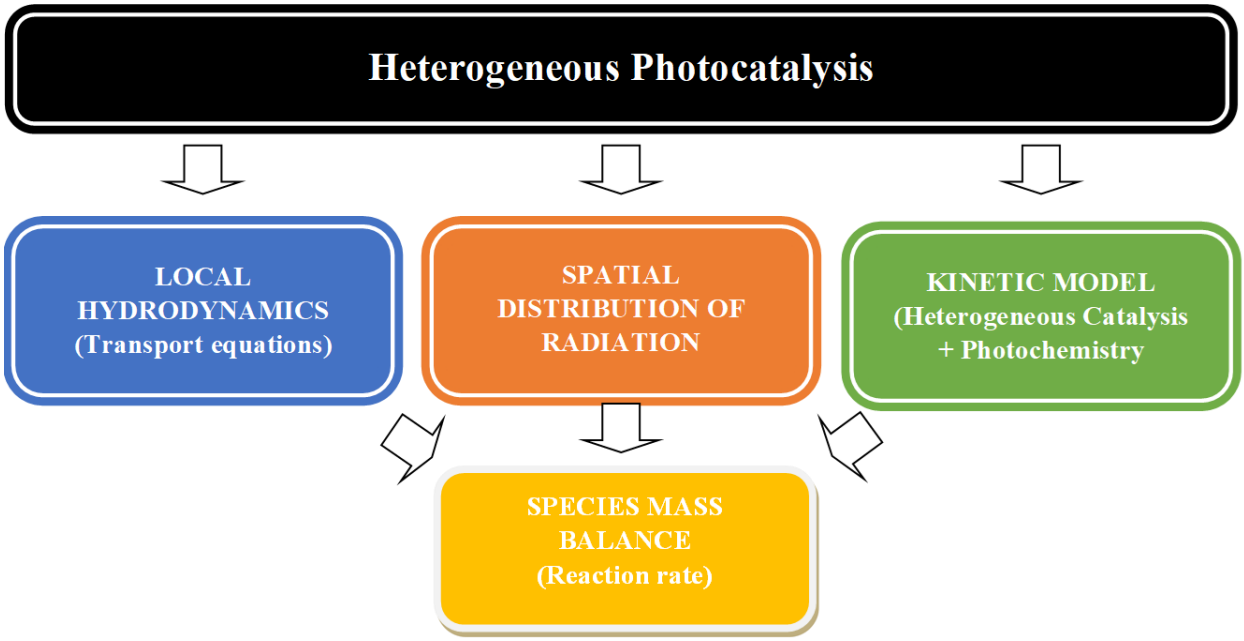

Fig. 13. Schematic description of the modeling of heterogeneous photocatalytic reactions in a CFD environment.

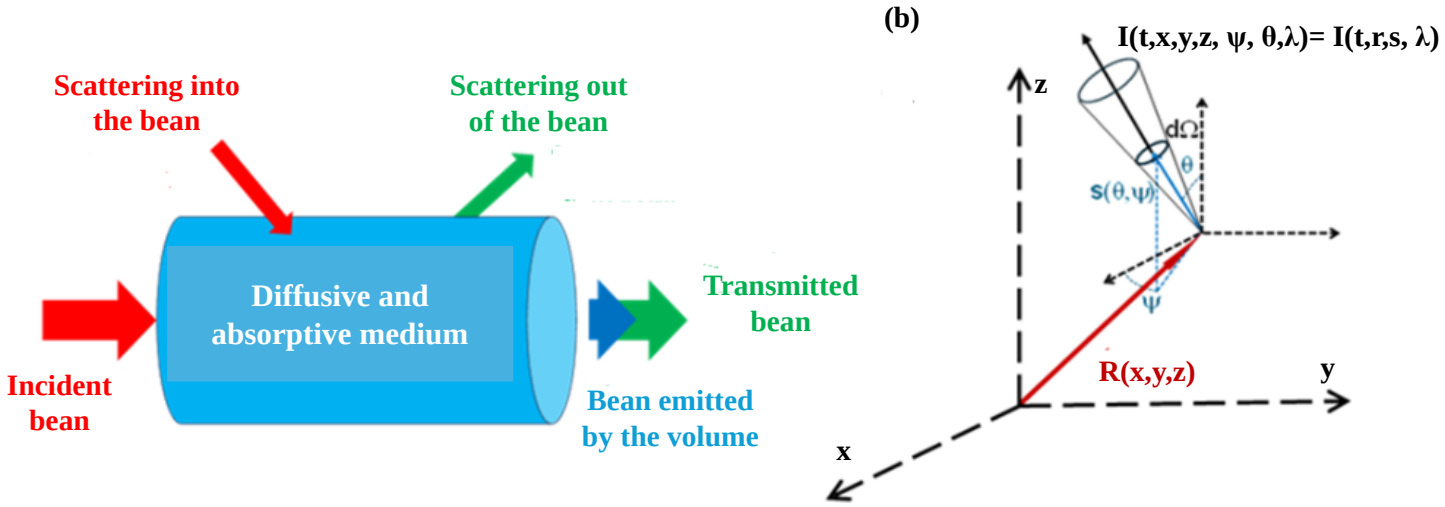

Fig. 14. (a) Schematic description of the physical processes involved in light transfer. (b) Geometrical description of the RTE parameters.

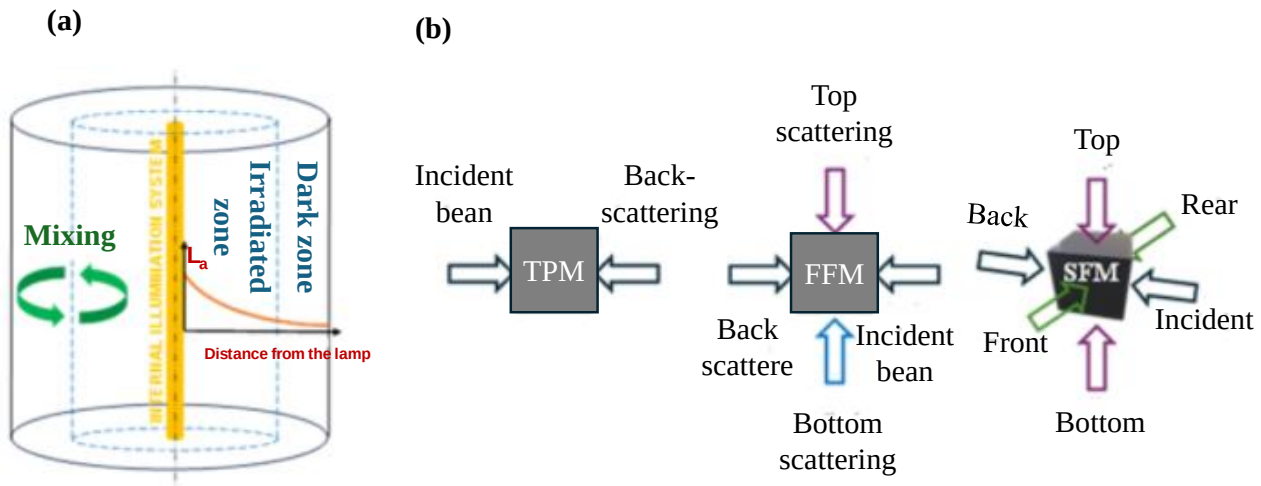

Fig. 15. (a) Schematic light distribution in an internal illumination reactor based on a 1D model. (b) Principle of the two-flux (TFM), four-flux (FFM), and six-flux (SFM) models.

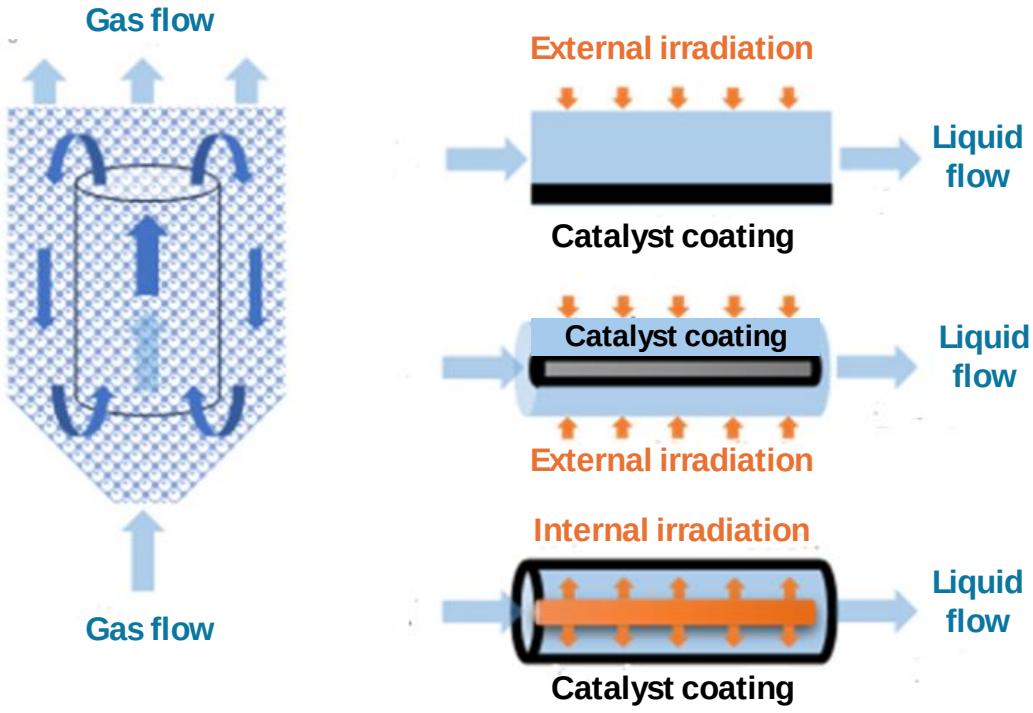

Fig. 16. Examples of photoreactors designs: (a) internal-loop airlift reactor with a draft tube and a suspended photocatalyst; immobilized photocatalyst in parallel plate (b), annular with external irradiation (c), and annular with internal irradiation (d) photoreactors.

Table 1 Summary of the Performance comparison of TiO_2 based composite photocatalytic materials for aqueous EPs removal.

Photocatalyst	**Pollutant**	**Light source**	**Removal efficiency**	**Key results**	**Ref.**
Cu−TiO_2	Congo red	Visible light	99%	3w% Cu−TiO_2 prepared via solvothermal method, 50 min irradiation.	Bibi et al. (2023)
Ag−TiO_2	Tartrazine	Visible light	87%	0.21% Ag−TiO_2 prepared by hydrothermal method. 180 min irradiation time, cycles: 5 times.	Ratshiedana et al. (2021)
Fe−TiO_2	Bisphenol A (BPA)	Visible light	99.9%	Fe doped TiO_2 synthesized by one-step hydrothermal deposition method, 95 $mg.L^{-1}$ of BPA, 120 irradiation time.	Wang et al. (2020)
Zr−TiO_2	Bismark Brown Red (BBR)	Metal halide lamp	99%	Cycles: 4 times.	Divya et al. (2023)
(N, F) −TiO_2	Phenol	Visible light	−	(N, F) co-doped TiO_2 prepared by solvothermal method, specific surface area of 301.8 $m^2.g^{-1}$.	Yang et al. (2023)
N−TiO_2	2,4-dichlorophenol	Visible light	77.6%	Sol gel preparation method, 153.4 µM 2,4-DCP, 1 $g.L^{-1}$ photocatalyst dosage, pH 5.6, and 240 min irradiation.	Khan et al. (2023)
S−TiO_2	Phenol	Visible light	84%	S^{6+}−doped TiO_2 prepared via ionic liquid method, 80 min irradiation.	Chen et al. (2017)
Bi_3O_4Br/TiO_2	Rhodamine B	Visible light	99%	TiO_2/BiOBr (30%) prepared via hydrothermal method, 90 min irradiation.	Salmanzadeh-Jamadi et al. (2022)
WO_3/TiO_2	Methylene blue	Sunlight	98%	WO_3/TiO_2 Catalyst prepared via a space-constrained method, 10 min irradiation, cycle: 5 times.	Liu et al. (2022)

$BiVO_4/TiO_2$	Rhodamine B	Sunlight	96.7%	$BiVO_4/TiO_2$ (30 wt%) fabricated by hydrothermal method, 60 min irradiation.	Wang et al. (2024)
Fe_2O_3/TiO_2	Acetaminophen	Sunlight	95.8%	Fe_2O_3−TiO_2 synthesized via the sol-gel method, [Catalyst] = 1.25 $g.L^{-1}$, [ACT] = 30 mg/L, pH= 11.	Khasawneh et al. (2021)
$GO/TiO_2/CaTiO_3/Cu_2O/Cu$	Paracetamol	150 W linear halogen lamp	96%	$TiO_2/CaTiO_3/Cu_2O/Cu$ with 3 % GO prepared by Solid state synthesis method, 0.5 mM peroxymonosulfate, 10 ppm paracetamol, and 180 min irradiation time, Cycles: 5 times.	Tanos et al. (2024)

Table 2 Main steps in the photocatalysis process.

Role of Semiconductors	Description
Adsorption	Adsorption is the crucial initial step in heterogeneous photocatalysis, where target substrates are attracted to the surface of the photocatalyst, facilitating the photocatalytic reaction. This process can involve various mechanisms, such as van der Waals forces, electrostatic interactions, hydrogen bonding, or chemical bonding (Chen et al., 2020). Factors influencing adsorption include the photocatalyst's properties (surface area, chemistry, and morphology), the target molecules' characteristics (size, shape, and chemical composition), and environmental conditions (temperature, pressure, and pH) (Saeed et al., 2022). Once adsorbed, the target molecules are positioned to undergo subsequent reactions when exposed to light energy, initiating a series of processes that include photon absorption, electron-hole pair generation, charge carrier migration, and redox reactions.
Light Absorption and Generation of Electron-Hole Pairs	Semiconductors possess an impressive capability to absorb light energy efficiently, which is essential for their function in heterogeneous photocatalysis. Their effectiveness stems from a unique electronic configuration optimized for photon interaction. Upon illumination, semiconductors absorb photons, transferring energy to their electrons, which then transition from the valence band to the conduction band, creating electron-hole pairs. The excited electrons, now in the conduction band, seek out reducing agents to donate their excess energy, while the positively charged holes attract oxidizing agents, facilitating oxidation reactions of nearby molecules (Navidpour et al., 2023). This dynamic interaction of electron-hole pairs on the semiconductor's surface emphasizes their dual role as catalysts and initiators of chemical transformations. Ultimately, the light absorption by semiconductors underpins their photocatalytic activity, initiating a series of reactions that lead to significant chemical transformations characteristic of heterogeneous photocatalysis.
Migration and Redox Reactions	During the migration and redox reactions in heterogeneous photocatalysis, photogenerated electrons and holes travel to the surface of the photocatalyst, where they participate in reactions with adsorbed molecules (Rengifo-Herrera and Pulgarin, 2023). This stage is critical as the efficiency of pollutant degradation depends on the successful migration of these charge carriers, with recombination potentially reducing their effectiveness. Photoexcited electrons can reduce oxygen to form superoxide radicals (O_2 •-) or hydroxyl radicals (•OH), while holes can oxidize water or hydroxide ions to generate •OH. These highly reactive species possess strong oxidative potential and are pivotal in breaking down organic pollutants by cleaving chemical bonds and transforming complex molecules into simpler, less harmful byproducts (Wu et al., 2020). The intricate interplay of these redox processes highlights the effectiveness of photocatalysis as a sustainable method for mitigating environmental pollution.

Table 3 Summary of the various kinetic models used for EPs degradation using photocatalytic processes.

Kinetic model	Degradation Equation	Nomenclature	Ref.
Langmuir-Hinshelwood (L-H) model	$r = \frac{kKC}{1+KC}$	r ($mg.L^{-1}\cdot min^{-1}$): is the reaction rate. k ($mg.L^{-1}\cdot min^{-1}$): is the rate constant of the surface reaction. K ($L.mg^{-1}$): is the adsorption equilibrium constant. C ($mg.L^{-1}$): is the reactive concentration of the pollutant at time t.	Eckert et al. (2015)
Turchi-Ollis model	$r = K_{OH}\,[OH^*] + K_{direct}\,C$	r ($mg.L^{-1}\cdot min^{-1}$): is the reaction rate. K_{OH} ($L.mg^{-1}.min^{-1}$): is the rate constant for hydroxyl radical-driven reactions. [OH^*] ($mg.L^{-1}$): is the concentration of surface-bound hydroxyl radicals. K_{direct} (min^{-1}): is the rate constant for direct photolysis of the contaminant, C ($mg.L^{-1}$): is the concentration of the contaminant.	Franz and Bestetti (2023)
Direct-Indirect model	$r = r_{direct} + r_{indirect}$	r ($mg.L^{-1}\cdot min^{-1}$): is the reaction rate. r_{direct} ($mg.L^{-1}\cdot min^{-1}$): is the rate of the direct reaction with the surface charge carriers. $r_{indirect}$ ($mg.L^{-1}\cdot min^{-1}$): is the rate of the reaction with intermediate reactive species.	Monllor-Satoca et al. (2007)
Michaelis-Menten model	$r = \frac{V_{max}C}{K_m + C}$	r ($mg.L^{-1}\cdot min^{-1}$): is the reaction rate. V_{max} ($mg.L^{-1}\cdot min^{-1}$): is the maximum reaction rate. C ($mg.L^{-1}$): is the reactive concentration of the pollutant. K_m ($mg.L^{-1}$): is the Michaelis constant.	Bonet-San-Emeterio et al. (2021)
Reaction-Diffusion model	$\frac{\partial C}{\partial t} = D\frac{\partial^2 C}{\partial x^2} - r(C)$	D ($m^2.s^{-1}$) : is the diffusion coefficient. C ($mg.L^{-1}$) : is the pollutant concentration. x (m) : is the distance within the reactor. r ($mg.L^{-1}\cdot min^{-1}$): is the reaction rate.	Patricia Tcaciuc et al. (2018)

Table 4 Variables ϕ, coefficients of the diffusion term Γ_ϕ, and source terms S_ϕ of the standard transport equations in CFD in the case of an incompressible fluid flow described by the RANS equations.

	$\boldsymbol{\phi}$	$\boldsymbol{\Gamma_\phi}$	$\boldsymbol{S_\phi}$	**Abbreviations**
Continuity equation	1	0	0	P is the pressure, μ the dynamic viscosity, and $\mu_t = \rho C_\mu (k^2/\varepsilon)$ the turbulent viscosity.
Velocity component i	u_i	$\mu + \mu_t$	$-\frac{\partial}{\partial x_i}\left(P + \frac{2}{3}\rho k\right) + \rho g_i$	Pr, Pr_t, Sc and Sc_t: Prandtl, turbulent Prandtl, Schmidt and turbulent Schmidt dimensionless number, respectively.
Specific enthalpy	h	$\mu/Pr + \mu_t/Pr_t$	$\frac{\partial P}{\partial t} - div(\mathbf{q}_{R,C})$	
Mass fraction of species m	w_m	$\mu/Sc + \mu_t/Sc_t$	r_m	g_i: the component of the acceleration of gravity in the direction of u_i.
Turbulent kinetic energy	k	$\mu + \mu_t/\sigma_k$	$P_k - \rho\varepsilon$	$\mathbf{q}_{R,C}$: a heat flux due to chemical reaction, radiation, or thermophoretic effects.
Turbulent dissipation rate	ε	$\mu + \mu_t/\sigma_\varepsilon$	$C_{1\varepsilon}\frac{\varepsilon}{k}P_k - \rho C_{2\varepsilon}\frac{\varepsilon^2}{k}$	r_k: net production by chemical reaction of species m.
				$C_{1\varepsilon}$, $C_{2\varepsilon}$, C_μ, σ_k, and σ_ε: parameters of the $k-\varepsilon$ RANS model.

Table 5 CFD simulation guidelines as a function of reactor type and study objectives.

Photocatalyst	**CFD simulation guidelines on model**				**Objectives**
	Hydrodynamics	*Mass transfer*	*Light Transfer*	*Reaction kinetics*	
Suspended	+++	+	+++	++	design, optimization, optical parameters
Packed	+++	+	+++	++	design, optimization
Wall	++	+++	+	++	design, optimization, kinetic study, optical parameters

+++ critical ++ important + not critical